Microencapsulated human albumin nanoparticles for drug delivery to the lungs

Patel, Ayasha Vali

Awarding institution:
King's College London

Microencapsulated human albumin nanoparticles for drug delivery to the lungs

Ayasha Vali Patel

In fulfilment of the requirement

for the degree of Doctor of Philosophy (PhD)

School of Cancer and Pharmaceutical Sciences

King's College London

2019

Acknowledgements

I would like to express my gratitude to my supervisors Professor Ben Forbes and Professor Lea Ann Dailey for their continuous guidance and support. I am extremely grateful for their encouragement and advice throughout the past four years.

I am grateful to Nick Childerhouse and Dr Gemma Keegan for their exemplary supervision and guidance, and to everyone else at Vectura Group plc who assisted with this project. Many thanks to Dr Adrian Richter, Professor Peter Imming, Dr Natalja Redinger and Professor Ulrich Schaible for all their help. I would also like to thank everyone in the Drug Delivery group at King's, particularly Dr Arcadia Woods and Wachirun Terakosolphan for their time and assistance in the laboratory.

A special thank you to my fellow PhD students for being like my second family for the past few years- in particular, Laura, Dona, Parastoo and Makiko. I am so grateful for my friends Zainab and Hamida for being the sisters I never had, lifting me and restoring my sanity through the tough times. A big thank you to my family for their endless love and support, especially my mother without whom none of this would have been possible. Finally, thank you to Muhammed for putting up with my craziness, making me smile when it seemed impossible and for being my unit and my source of peace.

To my mother and father

"Verily, with every hardship comes ease"

Abstract

Albumin nanoparticles are attractive candidates for optimising drug delivery to the lungs by modifying local biodistribution. However, there has been little exploration of the loading of therapeutic agents into albumin-based nanoformulations for inhaled delivery. The aim of this work was to develop respirable microparticles containing albumin nanoparticles for drug delivery to the lungs. Human serum albumin (HSA) nanoparticle suspensions were developed using a modified desolvation method. The solubility of four anti-tuberculosis benzothiazinone (BTZ) drug candidates (IR 20, IF 274, FG 2, AR 112; 0.38-134 μg/mL) was enhanced 2 to 140-fold by 50 mg/mL (1 mL) albumin. Tryptophan 213 residue quenching studies indicated moderate drug binding strength to Sudlow's site I. Nanoparticle manufacture was optimised to provide 37-60% drug encapsulation efficiency in HSA particles (169 nm, zeta potential –31 mV). Drug release was <8% over 48 h in aqueous medium, but 66-88% was released by 48 h after the addition of proteases at concentrations representative of the enzyme levels found in lung lining fluid. Dissolution profiles reflected Logistic release kinetics for IR 20 and Weibull release kinetics for FG 2 (R^2= 0.988 and 0.975, respectively) and antimycobacterial activity in an *M. tuberculosis* infected macrophage model was enhanced compared to delivery in DMSO or albumin solution. Pilot spray-drying studies demonstrated that incorporation of albumin nanoparticles into respirable carrier particles was possible. The spray-dried powders developed in this work were suitably sized for lung deposition (~4 μm) and albumin nanoparticles were recoverable after the spray-drying process with good re-dispersibility and size uniformity. An albumin nanoparticle content in the spray-dried mannitol formulation of 40% was selected as the most promising. HSA nanoparticles containing roflumilast, a selective phosphodiesterase 4 inhibitor, were incorporated in the dry powder formulation with little effect on the aerodynamic properties of the powders produced. Roflumilast release from the spray-dried microcarriers was found to be the same as from the suspension form (<20% at 48 hours without the presence of trypsin, and a rapid release rate for the first 4 hours with the presence of trypsin, followed by a slower

rate for the remaining 48 hours (total ~80% drug release). Dose deposition in human lungs was modelled using the PreciseInhale® system, indicating that aerosol administration of a single capsule containing 10 mg of the dry powder formulation would deliver roughly 6 μg roflumilast. This work demonstrates opportunities for developing human serum albumin nanoparticle-based microcarriers as a platform for inhaled drug delivery.

List of publications

Journal articles

Ayasha Patel, Natalja Redinger, Adrian Richter, Arcadia Woods, Gemma Keegan, Nick Childerhouse, Peter Imming, Ulrich E. Schaible, Ben Forbes and Lea Ann Dailey. Antimycobacterial activity of benzothiazinone-loaded human serum albumin nanocarriers designed for inhalation. *Journal of controlled release*, under revision.

Arcadia Woods, Teodora Andrian, Gemma Sharp, Elif Melis Bicer, **Ayasha Patel**, Ian Mudway, Lea Ann Dailey and Ben Forbes. Development of in vitro models of lung protease activity for investigating biopharmaceutical stability in healthy and inflamed lungs. Intended journal submission: *European Journal of Pharmaceutics and Biopharmaceutics*, in preparation.

Conference talks and presentations

Ayasha Patel, Arcadia Woods, Peter Imming, Adrian Richter, Lea Ann Dailey & Ben Forbes. Formulation of Benzothiazinones in Bovine Serum Albumin Nanoparticles. Drug Delivery to the Lungs, 2015. Edinburgh, UK.

Ayasha Patel, Arcadia Woods, Peter Imming, Adrian Richter, Lea Ann Dailey, Ben Forbes. Albumin Nanoparticles as Carriers for Hydrophobic Benzothiazinones Developed for anti-Tuberculosis Therapy. BioBarriers, 2016, Saarbrücken, Germany.

Ayasha Patel, Arcadia Woods, Peter Imming, Adrian Richter, Nick Childerhouse, Lea Ann Dailey and Ben Forbes. Drug loading of Human Albumin Nanocarriers for inhaled Anti-Tuberculosis Therapy. Drug Delivery to the Lungs, 2016, Edinburgh, UK.

Ayasha Patel, Arcadia Woods, Adrian Richter, Peter Imming, Gemma Keegan, Nick Childerhouse, Ben Forbes and Lea Ann Dailey. Human albumin nanocarriers for therapeutic application in the lung. International Symposium on Microencapsulation, 2017, Faro, Portugal.

Ayasha Patel, Natalja Redinger, Adrian Richter, Arcadia Woods, Peter Imming, Ulrich E. Schaible, Nick Childerhouse, Ben Forbes and Lea Ann Dailey. Loading, release and activity

of inhalable benzothiazinone-loaded human albumin nanocarriers for anti-tuberculosis therapy, Drug Delivery to the Lungs, 2017. Edinburgh, UK.

Awards

Best academic poster for *Drug loading of Human Albumin Nanocarriers for inhaled Anti-Tuberculosis Therapy* at Drug Delivery to the Lungs, 2016, Edinburgh, UK.

The Pat Burnell New Investigator award for *Loading, release and activity of inhalable benzothiazinone-loaded human albumin nanocarriers for anti-tuberculosis therapy* at Drug Delivery to the Lungs, 2017, Edinburgh, UK.

Table of Contents

Table of Figures

Table of Tables

List of abbreviations

ANOVA	Analysis of variance
API	Active pharmaceutical ingredient
AZT	Azidothymidine
BAL	Bronchoalveolar lavage
BPM	Breaths per minute
BSA	Bovine serum albumin
BTZ	8-nitro-Benzothiazinone
CFU	Colony-forming unit
CLSM	Confocal laser scanning microscopy
COPD	Chronic pulmonary obstructive disease
DLS	Dynamic light scattering
DMEM	Dulbecco's Modified Eagle Medium
DMSO	Dimethylsulfoxide
DPA	Decaprenylphosphoryl-β-D-arabinose
DPI	Dry powder inhaler
DPR	Decaprenylphosphoryl-β-D-ribose
DprE1	Decaprenylphosphoryl-beta-D-ribose 2-epimerase
DSC	Differential scanning colorimetry
ED	Emitted dose
FBS	Foetal bovine serum
FDA	Food and Drugs Administration
FPF	Fine particle fraction
FSI	Fast screen impactor
FTIR	Fourier-transform infrared spectroscopy

GRAS	Generally regarded as safe
HFA	Hydrofluoroalkane
HPLC	High-performance liquid chromatography
HAS	Human serum albumin
KCPS	Kilo counts per second
LOD	Limit of detection
LOQ	Limit of quantification
MIC	Minimum inhibitory concentration
MOI	Multiplicity of infection
MPPD	Model of particle dosimetry
MW	Molecular weight
MWCO	Molecular weight cut-off
NGI	Next generation impactor
NMR	Nuclear magnetic resonance
NP	Nanoparticle
PBS	Phosphate-buffered saline
PDE-4	Phosphodiesterase 4
PDI	Polydispersity index
PEG	Poly (ethylene glycol)
PLGA	Poly (lactic-co-glycolic acid)
pMDI	Pressurised metered dose inhaler
ROS	Reactive oxygen species
RPM	Revolutions per minute
RSD	Relative standard deviation
SEM	Scanning electron microscopy
SEM-EDX	Scanning electron microscopy- energy dispersive X-ray
SFD	Spray-freeze drying

TB	Tuberculosis
TEM	Transmission electron microscopy
TNF	Tumour necrosis factor

Chapter 1 Introduction

1.1 General introduction

The overall aim of this thesis was to develop a respirable microparticle formulation containing drug-loaded albumin nanoparticles for delivery to the lungs. In this chapter, important background to the topic of aerosolised medicine delivery to the lungs will be discussed, including inhaled nanoparticle delivery and aerosol formulation. This chapter will also provide an introduction to albumin; namely its structure, drug-binding properties, nanoparticle formation and the biological fate of albumin nanoparticles, i.e. their retention and degradation in the lungs. Finally, the specific objectives addressed in this thesis are defined.

1.2 Nanoparticle-based aerosol medicine

The definition of nanoparticle most commonly specifies particles in the size range 1 – 1000 nm, however in terms of drug delivery the size range 1 – 200 nm is usually inferred (Kreuter 1991). Nanoparticles have been recognised as having potential for providing controlled drug delivery to the lung for some years (Paranjpe & Müller-Goymann 2014). Their versatility and ability to address some of the problems encountered in inhaled drug delivery, e.g. loss of dose, make them an exciting and promising area of research. The extensive research into nanoparticle formulations has provided extensive knowledge and understanding of such systems and a wide range of techniques to manufacture nanoparticles enabling a high degree of control over particle properties. There is however a need to perfect pulmonary nanoparticle drug formulations in order to overcome barriers to their applications therapeutically, which include safety concerns, physiological barriers to delivery of the drug payload, limitations in drug-nanoparticle compatibility which is related to low drug-loading efficiencies and scale up issues (Bailey & Berkland 2009).

With the development of new active pharmaceutical ingredients (APIs) that are hydrophobic and hence difficult to formulate and manufacture using aqueous systems, the application of nanoparticle-based drug delivery systems is increasingly important. For

drug delivery to the lungs, the ability of nanoparticles to increase solubilisation of these compounds, control the rate of drug liberation, confer protection from degradation and retard or promote drug absorption at the mucosal surface offers many opportunities. The development of respirable nanoparticle-based medicines not only requires an understanding of aerosol science, but also requires understanding of drug-nanocarrier behaviour, particularly for drug compounds with poor aqueous solubility that have difficulty being formulated for other delivery routes.

1.3 Aerosolised particle delivery to the lung

The anatomical structure of the lungs is advantageous for drug delivery due to a very large surface area, dense vasculature, lower protease activity (compared to the ganstrointestinal tract) and the thin alveolar epithelium making the lungs highly permeable to drugs (Scheuch et al. 2006; Bailey & Berkland 2009). The lungs are suitable for both local and systemic drug delivery. From a therapeutic standpoint, the potential advantages of lung delivery for systemic diseases include a non-invasive delivery system, bypassing hepatic metabolism (as per oral formulations) and reproducible absorption kinetics as pulmonary delivery is independent of diet and interpatient metabolic differences (Patton 1996; Byron & Patton 1994; Labiris & Dolovich 2003). In the treatment of respiratory diseases the pulmonary route offers the advantages of delivering drug directly to the site of the disease, minimising the risk of systemic side effects and potentially offering a rapid response (Labiris & Dolovich 2003). In delivery of particles to the lungs, deposition takes place through impaction, sedimentation or diffusion depending on factors such as the particle size, density, airflow, breathing rate, respiratory volume and the health of the individual (Smola et al. 2008). The region where particles deposit is determined by their aerodynamic diameter (D_a) (defined as the diameter of a sphere of density 1 g/cm^3 with a settling velocity that is the same as the particle of interest) which is defined by Equation 1.1 where ρ is the mass density of the particle, ρ_a is the unit density and D_g is the geometric diameter.

Equation 1.1

$$D_a = \sqrt{\frac{\rho}{\rho_a} D_g}$$

Impaction typically occurs with large particles (>10 μm) as they do not change their path and are typically impacted on the surface of the larger airways at sites where the direction of airflow changes, e.g. bifurcations. Particles of 1-10 μm are predominately deposited by sedimentation (particles settling under the influence of gravity) in the bronchiolar region of the lung. The transport of particles <1 μm in size tends to be driven by diffusion which is time dependant and if not deposited particles of this size are likely to be exhaled. Diffusion in this context is the transport of particles from a higher to lower concentration and typically occurs in areas of low airflow such as the alveoli (Smyth & Hickey 2011). It is generally accepted that particles sized between 1 and 5 μm are well able to reach and are deposited in the respirable airways (Bailey & Berkland 2009).

1.4 Nanoparticles for drug delivery to the lung

Nanoparticles can be formed of the drug itself or can be formed from excipients and used as drug carriers either by encapsulation, dissolving or entrapping the active substance or drug, adsorbing it to the surface of the particle or by chemically attaching the drug (Sung et al. 2007). Nanoparticles have a large surface area to volume ratio, favouring them for drug delivery as the increase in surface area leads to an increase in dissolution rate, as described by the Noyes-Whitney equation (Equation 1.2):

Equation 1.2

$$\frac{dM}{dt} = \frac{DS}{h}(Cs - Cb)$$

Where M is the amount of drug dissolved in time t, D is the diffusion coefficient of the drug, S is the surface area of drug, h is thickness of diffusion layer, Cs = saturation solubility of drug and Cb is the concentration of the drug in bulk medium. Additionally, particles smaller than 1 μm show higher saturation solubility, increasing as the particle size

decreases, thus enhancing mass transfer from the nanoparticles to the surrounding medium (Muller, R.H., Jacobs, C., Kayser 2001). In addition to these properties, the ability of nanoparticles to target delivery and protect drug from degradation make them especially suited for drug delivery (Kunda et al. 2013).

In terms of targeting the lungs, the deposition of nanoparticles upon inhalation is driven by diffusion due to their small size, which means it is likely they will be exhaled and therefore not deposited in the alveolar region of the lung (Kunda et al. 2013). Long term storage of nanoparticles also leads to the formation of poorly respirable aggregates due to their high particle interaction (Kunda et al. 2013; Sung et al. 2007). Hence nanoparticles are often formulated into respirable microparticles (sized within the range 1 – 5 μm) which can reach the desired region of the lungs and deliver a payload of nanoparticles (Chang et al. 2003; Tsapis et al. 2002; Sugiyama et al. 2006; Tsapis et al. 2005).

Pandey et al. investigated poly(lactic-co-glycolic acid) (PLGA) nanoparticles loaded with anti-tuberculosis drugs for aerosolised drug delivery in guinea pigs and demonstrated that a single inhalation resulted in therapeutic levels for up to six days (Pandey et al. 2003). This is an example where inhaled delivery of nanoparticles could improve drug bioavailability and reduce frequency of dosing. Another example of adopting nanoparticles as a means to sustain release of a drug comes from a study by Kawashima et al. where PLGA nanoparticles were loaded with insulin, nebulised and administered to guinea pigs (Kawashima et al. 1999). They compared the hypoglycaemic effect of the nanoparticulate formulation with nebulised insulin solution and found a prolonged period of hypoglycaemia (48 hours) for the nanoparticle formulation compared to 6 hours for the insulin solution, suggesting a sustained release property of the PLGA nanoparticles. A similar study by Zahoor et al. reported that antitubercular drugs were more effective when they were encapsulated in alginate nanoparticles and administered via inhalation to guinea pigs compared to their free oral delivery (Zahoor et al. 2005).

Aside from polymers, other materials have also been studied for nanoparticulate drug delivery to the lung. Dames et al. (Dames et al. 2007) described the ability to direct inhaled, magnetically charged iron oxide nanoparticles to specific areas of the lungs in mice without adversely affecting respiratory mechanics, demonstrating that targeted nanoparticulate aerosol delivery to the lungs is achievable and could prove to be beneficial in the treatment of localised lung infections or tumours by using a targeting approach. Lipid-based nanoparticles have also been studied for drug delivery to the lung although most published data refer to the identification and evaluation of the desired physicochemical parameters of the formulation. However, Pastor et al. developed sodium colistimethate loaded lipid nanoparticles for antimicrobial therapy for cystic fibrosis and found that they demonstrated a sustained release profile *in vitro* (Pastor et al. 2014).

Sham et al. introduced the idea of incorporating nanoparticles in a larger microparticle matrix with spray-drying two nanoparticle systems (gelatin and iso-butyl cyanoacrylate) (Sham et al. 2004). This study proved the concept of delivering nanoparticles to the lungs in larger carrier particles. Tsapis et al. developed large porous particles which dissociated in physiological conditions to produce polymeric nanoparticles, providing the advantages of nanoparticle delivery while also having the convenience of a geometrically large porous system with a low aerodynamic diameter that deposited deep in the lung (Tsapis et al. 2002).

1.5 Formulations, manufacture and delivery devices

There is a plethora of techniques and processes that have been developed to produce respirable microparticles. Nebulisation is one such example. Air-jet nebulisers work by generating high velocity air from compressed jets to shear a solution or suspension into a film that collapses to form aerosolised droplets (Tiano & Dalby 1996). Ultrasonic nebulisers work by vibrating a piezoelectric crystal at high frequencies to generate a mist

(Tiano & Dalby 1996). There are also nebulisers that utilise vibrating mesh technology to generate a mist. These utilise a mesh or membrane with thousands of holes that vibrate at the top of a liquid stock solution/suspension to form a mist of fine droplets through the holes (Ghazanfari et al. 2007). Dailey et al. studied the effect of air-jet and ultrasonic nebulisation on polymeric nanoparticle suspensions and found the nanoparticles were particularly susceptible to aggregation with jet nebulisation, while aggregation was reduced with the use of ultrasonic nebulisers (Dailey et al. 2003). Patlolla et al. postulated their celecoxib-loaded nanostructured lipid carriers would have greater stability against the shear forces generated by nebulisation and upon jet nebulisation found no significant changes in stability or drug content (Patlolla et al. 2010).

The most commonly used type of inhaler is pressurised metered dose inhalers (pMDIs). These are pressurised cannisters that contain drug either in solution or suspended in a liquid propellant. Historically chlorofluorocarbons (CFCs) were used, however due to their adverse effect on the ozone layer these are no longer used and hydrofluoroalkanes are now typically used (Siddiqui & Plosker 2005). Although nanoparticle-based pMDIs do not exist on the market currently, some studies involving nanosized formulations for use with pMDIs have been carried out. Chitosan-based nanoparticles were formulated into pMDIs to demonstrate their potential as a drug delivery carrier (Sharma et al. 2012), while insulin-containing nanoparticles formulated into a pMDI was found to have increased stability (due to the use of essential oil excipients) and higher predicted lung deposition compared to typical pMDI formulations (Nyambura et al. 2009).

The powder formulations used in dry powder inhalers (DPIs) can be engineered to contain nanoparticles. Spray-freeze drying (SFD) is a technique that has been used for particle engineering purposes whereby a drug solution is sprayed into a vessel that contains a cryogenic liquid such as nitrogen, causing the droplets to freeze instantly. The resulting

droplets are then collected and lyophilised to obtain porous dry powder particles (Pilcer & Amighi 2010). Although this technique has the advantage of having the ability to produce different sized particles, it can cause irreversible damage to proteins owing to unfolding and aggregation, causing instability upon reconstitution of the powders (Shoyele & Cawthorne 2006).

Development of microparticulate aerosolised systems often involve spray-drying. Spray-drying is a process in which dry powders are produced by forcing a fluid phase containing dissolved or suspended drug through high pressure nozzles (Bailey & Berkland 2009). In brief, a liquid feed stock is prepared and atomised to form droplets, these droplets come into contact with a hot gas, resulting in the rapid formation of particles by evaporation. A cyclone then separates the dry particles from the hot gas (Pilcer & Amighi 2010). Nanoparticles are typically prepared separately and then formulated as a dispersion where they will essentially be part of a larger microparticle, but still retain their favourable properties such as targeting or enhanced solubility (Vehring 2008) as described in earlier sections of this chapter. Spray-drying is a popular avenue due to its simplicity, ease of scale-up and applicability for a wide range of drugs making it industrially relevant (Bailey & Berkland 2009). A disadvantage of spray-drying is the inclusion of large amounts of excipient to maintain powder properties.

1.6 Protein-based nanoparticle systems

The increased use of engineered nanoparticles in consumer products in recent years has raised concerns about their effect on human health (Luyts et al. 2013; Brown et al. 2001). It has been reported that long term respiratory exposure to some types of nanoparticles may cause serious damage to health such as pulmonary fibrosis, granulomas, hypoxaemia and pleural effusion (Bakand et al. 2012; Song et al. 2009; Oberdörster et al. 2005). Additionally, it has also been reported that inhaled nanoparticles may pass into the systemic circulation and accumulate in secondary organs such as the brain and organs of

the digestive system (Hougaard et al. 2015; Geiser & Kreyling 2010). A possible mechanism for this involves complex formation of nanoparticles with the lung lining proteins to form a ferry boat like transport mechanism. Such an effect has not been reported for microparticles due to their larger size (Geiser & Kreyling 2010).

Pulmonary toxicity of nanoparticles has been attributed to factors such as particle size (Valavanidis et al. 2008), surface charge and reactivity (Brown et al. 2001; Warheit et al. 2009; Zhang 2012), high aspect ratio (Tran et al. 2011) and hydrophobicity (Jones et al. 2014). Several possible mechanisms of nanoparticle toxicity have been suggested, ranging from immediate reactions to long term effects (Bakand et al. 2012). Nanoparticles may cross cell membranes, enter different compartments of the cell and be a direct cause of cell injury owing to their small size (Song et al. 2009; Gojova et al. 2007). The unique surface characteristics of nanoparticles may induce reactive oxygen species (ROS) generation- leading to free radical formation which promotes tissue inflammation and damage to cells, protein and DNA (Zhang et al. 2011). Furthermore, the defence mechanisms of the body may not be able to cope with nano-sized material and macrophage function may be impaired (Mühlfeld et al. 2008). A study reported high numbers of "vacuolated macrophages" i.e. enlarged macrophages with either finely or coarsely vacuolated cytoplasms following treatment with polymeric nanoparticles (Jones et al. 2014). These macrophage responses did not appear to be linked to hydrophobicity or pro-inflammatory potential but may be a sign of autophagy- a process increasingly associated with exposure to nanoparticles (Stern et al. 2012).

The complicated mechanisms of nanotoxicity make it hugely important to gain a better understanding of the fate of nanoparticles in the lungs including their biological interactions and potential nanotoxicity in order for any drug nanocarrier to be considered for clinical development for pulmonary drug delivery purposes. This means that as well as being retained in the lung for the duration required in order to deliver the therapeutic

payload, it has to be demonstrated that particles (and by-products) are also effectively cleared from the lungs and have no or little associated toxicity i.e. are biodegradable and biocompatible.

Protein-based nanoparticulate systems are of particular interest as they have been shown to be non-toxic, reproducible and demonstrate ease of manufacture in terms of scale up (Farokhzad & Langer 2006). Clearance by natural barriers and defence mechanisms in the body such as the blood brain barrier and mucociliary clearance in the lung are major challenges that have to be overcome by nanoparticle-based drug delivery systems. Proteins tackle this problem due to their ability to modify the biological response to nanoparticles (Tezcaner et al. 2016). Plasma lipoprotein, fibrin and fibrinogen have all been investigated for this purpose (Vedakumari et al. 2013; Goszczyński et al. 2013; Rejinold et al. 2011; Huntosova et al. 2012), however albumin is better suited because of its biocompatibility, biodegradability and ability to bind drugs which makes it particularly attractive for drug delivery.

Albumin nanoparticulate formulations have been studied for intravenous and intravitreal administration and one such formulation (Abraxane®) is commercially available. It is indicated for the treatment of metastatic breast cancer in adult patients who have failed first-line treatment for metastatic disease. Abraxane® appears to be well-tolerated in patients with cancer (Fader & Rose 2009). Abraxane® delivers the drug paclitaxel as a suspension of albumin nanoparticles in saline, eliminating the need for a lipid-based or solvent vehicle that caused hypersensitivity in patients upon injection (Fader & Rose 2009). Abraxane® also increases the solubility and circulation time of the drug. In addition to alleviating previous concerns with toxicity, Abraxane® was also found to have higher intratumoural concentrations in preclinical studies (Gradishar et al. 2005; Nyman et al. 2005).

1.7 Albumin

Albumin is the most abundant protein found in human plasma. Physiologically, albumin regulates the plasma osmotic pressure, neutralises any free radicals present in the blood and binds and transports several compounds like fatty acids, vitamins, hormones and drugs (Hawkins et al. 2008). It is this affinity for several drug compounds that makes albumin a popular avenue for drug delivery research (Fujiwara & Amisaki 2013).

Albumin is different to other proteins in terms of superior robustness in stability over a wide pH range (pH 5-9) and at high temperatures (albumin can be heated for up to ten hours at 60°C without causing any structural changes (Kratz 2008). This illustrates the ease of manufacture and handling of albumin that makes it a potentially viable candidate as a protein-based drug delivery vehicle. Furthermore, as albumin is an endogenous protein, metabolic and homeostatic processes already exist which can be utilised that affect drug release from albumin nanoparticles and biodistribution of drug and carrier (Bhushan et al. 2017).

1.8 Ligand binding to HSA

Human serum albumin (HSA) is a monomer of 66 kDa, composed of 585 amino acids. It contains three helical domains, each one subdivided into two subdomains; A and B (Fujiwara & Amisaki 2013).

The affinity of certain ligands to HSA is an important factor with regard to the distribution and the effective concentration of drugs in the blood. The specificity of drug binding to albumin can be altered due to overlap with the binding sites of physiologically occurring fatty acids, (Figure 1.1) (Fujiwara & Amisaki 2013). It should be noted that the literature reports different nomenclatures for fatty acid and drug binding sites. For example, as presented in the albumin map, Figure 1.2, the fatty acid-binding site 7 is commonly known as drug-binding site 1 (subdomain IIA), while fatty acid-binding sites 3 and 4 overlap with

drug site 2 (subdomain IIIA). The fatty acid binding sites 2,5 and 6 do not generally overlap with drug binding sites (Ghuman et al. 2005; Fujiwara & Amisaki 2013). A brief overview of the two most important drug-binding sites are presented since they are the major candidates for ligand binding.

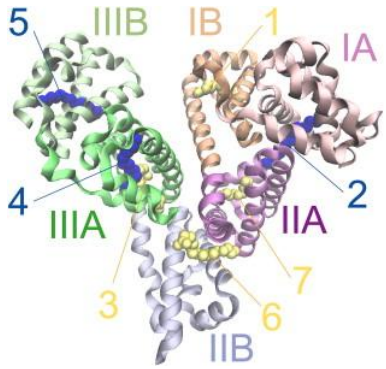

Figure 1.1 Human serum albumin (HSA) coordinated with seven palmitate molecules described by X-ray crystallography. The seven fatty acid binding sites are depicted on the structure (Fujiwara & Amisaki 2013).

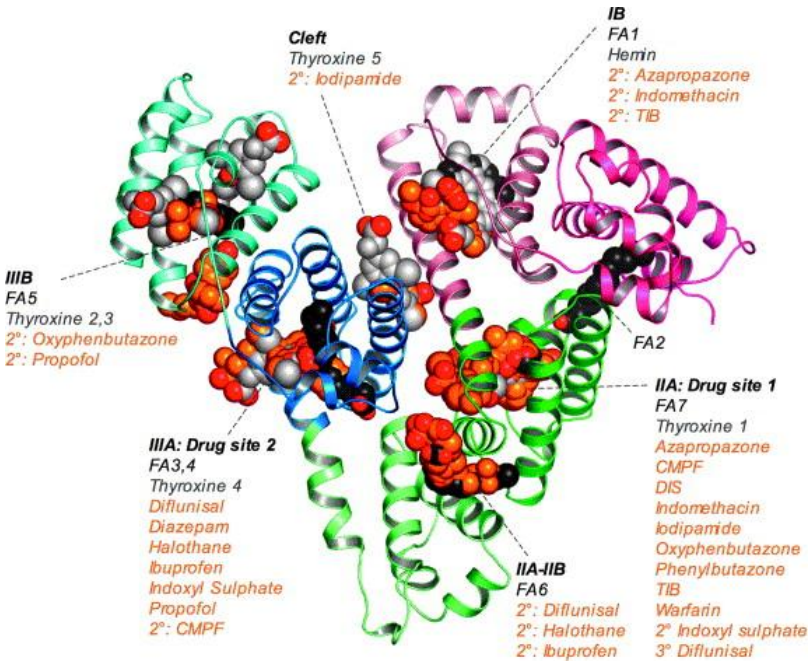

Figure 1.2 Map of human serum albumin (HSA) ligand binding sites as determined by X-ray crystallography (Ghuman et al. 2005).

1.8.1 Drug binding site 1 in defatted HSA

Drug binding site 1 is a binding pocket within subdomain IIA, containing six helices of the subdomain IIA and a loop-helix from subdomain IB. The core of the pocket is mostly

apolar, but two clusters of polar residues contribute as well. Phenylbutazone, oxyphenbutazone and warfarin are common substrates for this binding site (Ghuman et al. 2005). All these ligands have a planar group and the apolar cavities of the pocket are occupied by them to different extents. Interactions of endogenous compounds such as fatty acids with the binding pocket are able to cause a conformational rearrangement, which can have a positive or negative influence on drug binding in situ (Ghuman et al. 2005). However, when albumin is used as a drug delivery vehicle, fatty acid-depleted albumin is generally used to avoid this problem.

1.8.2 Drug binding site 2

Drug binding site 2 has many structural similarities to drug site 1 since they are both hydrophobic pockets with hydrophilic features. Drug binding site 2 also consists of six helices of subdomain IIIA, but apart from this it is smaller, and the cavity is structurally different. Diazepam, ibuprofen and difflunisal all have high affinity for the core of drug binding site 2. Despite its relatively small size, it can host two fatty acid binding sites (sites 3 and 4) (Sudlow et al. 1975; Yamasaki et al. 1996).

1.8.3 Drug binding assessment

Spectroscopic methods are a useful tool for studying the binding of a ligand to a protein. Among these techniques, fluorescence spectroscopy has been widely applied using two main approaches. The first approach uses fluorescent probes (fluorescent fatty acids analogues or small fluorescent molecules) whose binding has already been determined using a combination of techniques (x-ray crystallography, NMR) (Kragh-Hansen 1988; Hamilton 2004). The probes tend to associate with a specific binding site on the albumin molecule and form a fluorescent complex. Subsequently, the investigated drug is added to the system. Ideally, the drug will selectively displace the probe at the binding site in question causing quenching (decrease) of the fluorescent intensity measured (Oracova et al. 1996; Sudlow et al. 1975).

The second approach involves monitoring the intrinsic protein fluorescence due to the tryptophan, tyrosine and phenylalanine residues (Oracova et al. 1996; Sudlow et al. 1976). When a ligand specifically interacts with these residues, it can cause quenching in the fluorescent intensity. Generally, fluorescence spectroscopy is a quick and readily available technique that offers high sensitivity since small amounts of samples can be measured. It is also highly selective. This is useful for expensive drug compounds. On the other hand, its high sensitivity renders it susceptible to several factors (such as sample preparation variability or temperature) that may result in poor reproducibility. Finally, it can provide information only on specific binding sites and cannot give a general overview. Despite extensive research into albumin binding, the interpretation of binding and binding competition studies with albumin can be difficult given the versatility of the protein. Binding assays are complicated when used for proteins with multiple drug or fatty acid binding sites. For example, binding competition between compounds might not only occur due to competition for exactly the same binding site, but also between two compounds that bind in distinct yet partially overlapping binding sites, as have been identified in binding site 1 (Fehske et al. 1982; Kragh-Hansen 1988). Binding to an unknown number of secondary binding sites further complicates the characterisation of the drug-protein interaction (Sudlow et al. 1976; Yamasaki et al. 1996) as drug binding to one site might affect the other due to allosteric interactions between site 1 and 2 (Fitos et al. 1999; Chen & Hage 2004).

The techniques mentioned above refer to the study of specific drug-binding site interactions. Other simple conventional techniques have been used such as affinity chromatography- an HPLC method that utilises the immobilised protein as the stationary phase (Mallik et al. 2010) and other techniques based on size-separation principles, such as equilibrium dialysis (Sagar et al. 2008). These methods provide an overall affinity

assessment of drugs for albumin and are described in more detail in this review (Oracova et al. 1996).

The identification of the binding affinity of loaded drug to the building block of the nanoparticle is important due to its influence on the drug loading efficiency, the half-life and release profile of the drug. Ideally, a loaded drug should exhibit a medium binding affinity for albumin. With increasing binding affinity, the drug loading efficiency and half-life of the nanoparticle might increase, while on the other hand it could impair the drug release from the nanoparticle and the drug elimination. This effect has been described earlier for the interaction of drugs with serum albumin (Hervé et al. 1994; Kratochwil et al. 2002; Valko et al. 2003; Colmenarejo 2003). A positive correlation between binding and loading capacity has previously been reported (Oppenheim 1981; Whitehead et al. 1984; Lin et al. 2001). This is particularly important in the case of hydrophobic drugs, as albumin may enhance the solubilisation of such compounds.

1.9 Drug loading and release

There has been much interest in albumin nanoparticles as drug delivery systems in recent years. Abraxane® was the first FDA approved formulation using an albumin-bound form of paclitaxel (size ~130 nm) as a suspension in saline for paclitaxel delivery.It improves the drug's aqueous solubility, reduces side effects and subsequently dramatically improves its therapeutic effect against tumours. Researchers have also investigated using albumin nanoparticles as a carrier for the delivery of a broad variety of drugs, including ganciclovir (Merodio et al. 2000), rose-bengal (Lin et al. 2001), Aspirin (Das et al. 2005), hydrocortisone (Zimmer et al. 1994), methotrexate (Taheri et al. 2011) and proteins (Li et al. 2018).

The loading mechanism of a particular drug into albumin nanoparticles can influence the release profile of the drug. Drugs can be loaded into albumin nanoparticles in two

different ways: entrapment/encapsulation of the drug or adsorption interaction. According to the first mechanism the drug is incorporated into the particle matrix during the preparation procedure. The second mechanism relies on the drug binding/adsorbing to the albumin due to physical interactions. Sometimes the incorporation of the drug into the particles is via a combination of both phenomena. Currently, there are very few studies that investigate in detail the mechanism of drug loading in albumin nanoparticles.

The loading efficiency and the release profile of the albumin nanoparticles are influenced by the preparation method used. In most cases, drug loaded albumin nanoparticles consist of three components; albumin, a drug and a cross-linker. To prepare the nanoparticles, these components can be mixed at different times, leading to the creation of slightly different nanoparticles.

Albumin has a structure that is predominantly alpha-helical. The additional or organic solvent (desolvating agent) in the formation of albumin nanoparticles unfolds and exposes amino groups (Mohammad-beigi et al. 2016). Chemical cross-linking is achieved most commonly with the use of glutaraldehyde. The precise mechanism of cross-linking of albumin by glutaraldehyde is unknown, however mechanisms have been proposed and reviewed by Sokoloski and Royer (Sokoloski & Royer 1984) and have indicated the coupling of amino groups in the lysine residues (Sokoloski & Royer 1984; Weber, Coester, et al. 2000). Lubig et al. suggested a mechanism involving condensation of the cyclic monohydrate of glutaraldehyde and N-alkyl-2,6_dihydroxypiperidines (lysine backbone) to yield linear polymeric cross-links (Lubig et al. 1981; Saleh et al. 1989). Sufficient stabilisation of the particles via cross-linking ensures the particles do not re-dissolve again. The combined effects of the factors involved in the manufacture of albumin nanoparticles alter the secondary structure of albumin i.e. reduce the percentage of alpha-helical structure. These points are important to consider in the development of a formulation that requires the drug to covalently bind to albumin, as the overall cross-

linking of albumin by glutaraldehyde may also be affected, hence it may be useful to add the drug to the albumin prior to cross-linking.

There are concerns about the use of glutaraldehyde as it is a cytotoxic compound (Singh et al. 2010). Furst et al. studied the toxicity of glutaraldehyde release from BioGlue- a sealant used to treat aortic dissections (Fürst & Banerjee 2005). They studied the *in vitro* toxicity in human embryo fibroblasts and mouse myoblasts with cytotoxic effects being observed in both cell lines, and the *in vivo* toxicity was studied in lung, liver and aortic tissue from rabbits. Low-grade inflammation was found in the aortic tissue however the application of BioGlue to the lung and liver tissue invoked serious high-grade inflammation, oedema and toxic necrosis- attributed to the high levels of glutaraldehyde released (Fürst & Banerjee 2005). Glutaraldehyde has also been shown to cause skin sensitivity upon exposure (Wiggins et al. 1989). It should be noted that the amount of glutaraldehyde in the above studies is a lot higher than the amount used for the cross-linking of albumin nanoparticles. It should also be noted that cross-linked glutaraldehyde is not toxic, however free (unreacted) glutaraldehyde in solution may exhibit toxicity, which is why albumin nanoparticle suspensions are purified after formation to remove the free glutaraldehyde (Weber, Coester, et al. 2000; Bronze-Uhle et al. 2017).

Merodio et al. described three different preparation methods for albumin nanoparticles loaded with ganciclovir (Merodio et al. 2000). The first method was to incubate the nanoparticles with the drug after their formation, for the second method the drug was incubated with albumin prior to the nanoparticle formation and for the last method a mixture of all compounds was incubated together followed by the formation of the nanoparticles by desolvation with ethanol. The most effective method in terms of drug loading appeared to be the incubation of albumin with the drug prior to desolvation with ethanol and the addition of the cross-linker with a loading of 169.2 ± 4.1 μg/mg. The lowest loading of 15.5 ± 2.0 μg/mg was achieved when the drug was added post particle

formation. It has been shown that the electrostatic interactions regulated by the surrounding pH can modify protein's secondary structure. Therefore, the use of a crosslinking agent in order to rigidise the nanoparticles can decrease the accessibility of the drug into the binding pockets. Consequently, the incubation of the drug/protein solution or drug/protein nanoparticles can be of major importance in the drug loading efficiency.

Drug loading post particle formation occurs solely by adsorption to the particle surface and possibly into the matrix. Adding the drug before adding the cross-linking agent to stabilise the particles can increase the drug loading for particular drugs due to the ability of some drugs to covalently bind to the albumin (Merodio et al. 2000). The loading efficiency is also highly dependent on the drug and the method used to form the nanoparticles. Das et al. report a loading efficiency of 347.14 μg/mg for their aspirin loaded albumin nanoparticles for the same preparation method as the ganciclovir nanoparticles (Das et al. 2012; Das et al. 2005). Lin et al. report no significant loading difference between incubating the drug with albumin prior to particle formation and adding the drug post particle formation to manufacture rose-bengal albumin nanoparticles (Lin et al. 2001). The ability of the drug to form covalent bonds in the presence of a cross-linker, the incubation time and concentration of the cross-linker and the affinity of the drug for albumin can all affect drug loading, particle stability and drug release (Rubino et al. 1993; Weber, Coester, et al. 2000; Oppenheim 1981; Whitehead et al. 1984; Lin et al. 2001).

Understanding the mechanism of drug loading into albumin nanoparticles is important for a good understanding of the resulting performance of the drug delivery system, i.e. drug release and pharmacokinetics. In drug diffusion systems for example, when a drug is entrapped into a matrix its release profile generally conforms to the Higuchi equation (Higuchi 1963). According to this equation, the cumulative drug release is directly

proportional to the square root of time. Additionally, when the drug release is regulated by the dissociation of the drug from the protein, a constant release rate can be assumed. In the intermediate situation where the incorporation mechanism involves a combination of the two, the release is characterized from a quick burst of the drug initially due to the drug entrapment and then a slower phase due to dissociation from the protein. Generally, it has been demonstrated the entrapment method can offer a high loading capacity (Spector 1975). Drug release from erodible systems i.e. systems where the matrix undergoes degradation could be diffusion-controlled or erosion-controlled, depending on whether the drug diffusion is faster than erosion of the matrix (diffusion-controlled) or if the drug diffusion rate is low and remains in the matrix (erosion-controlled). Erosion can occur as surface erosion or bulk erosion. Surface erosion occurs when the surface of the matrix erodes, whereas bulk erosion occurs when water penetrates the bulk of the system, resulting in homogeneous erosion of the matrix (Kamaly et al. 2016). Erosion models have been summarised in this review (Peppas & Narasimhan 2014). A build up of osmotic pressure in a non-swelling system resulting in rupture of the system can also lead to drug release (Peppas & Narasimhan 2014; Kamaly et al. 2016). Mathematical modelling of drug release from osmotic systems is based on the Kedem and Katchalsky analysis (Kedem & Katchalsky 1958). Other mechanisms of drug release have been summarised in these review papers (Son et al. 2017; Aguzzi et al. 2010).

There are studies in the literature where drug release from albumin nanoparticles formed with cross-linker was shown to be biphasic, with an initial first quick release of the drug, followed by a slow-release phase (Merodio et al. 2000; Lin et al. 2001; Das et al. 2005; Das et al. 2012). This release profile can be explained by the two locations of the drug in the nanoparticle, much like Higuchi kinetics described previously. The initial burst is made up of the portion of the drug that is adsorbed on the surface of the nanoparticle. The second location of the drug is responsible for the slow release profile observed. This portion of the drug is chemically bound to albumin with cross-linkers and can therefore only be released

slowly (Merodio et al. 2000). Supporting evidence for this theory can be found from the release profile of protein loaded albumin nanoparticles that were stabilised using chitosan instead of a cross-linker where the protein was released in a monophasic, sustained fashion for up to 8 days. The release profile and speed depended on the chitosan concentration (Li et al. 2018).

1.10 Retention and degradation of albumin in the lung

Although albumin nanoparticles have shown potential as drug carriers to the lungs, concerns regarding their toxicity, as well as a lack of information on their clearance kinetics, are barriers to their clinical use. Understanding the pharmacokinetics of nanoparticles is also required to estimate drug release and administration frequency as well as understanding of possible accumulation of the drug carrier within the lungs.

Possible mechanisms for protein clearance from the lungs include mucociliary clearance, endocytosis by alveolar macrophages, degradation in alveoli or airways and absorption across the alveolar and bronchial epithelium into circulation (Hastings et al. 2004). Degradation of proteins may occur via proteases in the alveolar space, and although for the majority of proteins this is not a major clearance mechanism in the healthy lung (Ishii et al. 1991; Nadel 1990; Hastings et al. 2004) it is important to analyse this step to further determine the pharmacokinetic profile of albumin-based formulations.

Despite the fact that different proteases and subtypes have been shown to be expressed in the healthy human lung, such as cathepsins (Koslowski et al. 2003) and dipeptidyl peptidase 4 (DPP4) (Křepela et al. 1985), the exact types and amounts of these proteases has not been fully determined. Furthermore, the protease profile has been shown to change dramatically in diseased lungs where levels of enzymes found in the healthy lung are largely elevated, whilst other proteases may also become prominent, such as metalloproteinases (MMPs) in pneumonia (Chiang et al. 2014), prolyl endopepsidase in

smoking and COPD (Braber et al. 2011), and neutrophil elastase during inflammation (Kawabata et al. 2002). The comparison of healthy and diseased lung models can hence provide information to understand the implications for designing drug treatments delivered by protein-based drug carriers for patients.

It is important to note that structural changes induced during the manufacturing process of albumin nanoparticles (i.e. crosslinking mentioned earlier in this chapter) may result in differing clearance mechanisms compared to albumin molecules. This has been taken into account in various studies that have also investigated nanoparticle degradation in the presence of various enzymes and the factors that affect the degradation kinetics. Wartlick et al. observed that increasing the amount of glutaraldehyde crosslinking in albumin nanoparticles reduced the degree of degradation using enzymes trypsin and proteinase K (Wartlick et al. 2004). Langer et al. further concluded that the degree of crosslinking affects enzyme degradation using enzymes trypsin, protease, proteinase K and pancreatin (Langer et al. 2003). Furthermore, the fastest degradation was seen with pepsin at pH 2; trypsin, proteinase K, cathepsin B and protease achieved nanoparticle degradation over 24 h.

The clearance rate of nanoparticles from the lungs also depends on the material and physicochemical properties of the nanoparticles used. Lipid nanoparticles (200 nm) were shown to rapidly clear from the lungs in rats within the first hour (Videira et al. 2002), whilst poly-acrylamide nanoparticles (20-40 nm) remained mainly in the lungs over a 24 h period (Liu et al. 2009), and albumin delivered as nanoparticles (200 nm) remained in the lungs for > 48 h (Woods et al. 2015). Furthermore, albumin remained for longer in the lungs when delivered as nanoparticles compared to a solution. This could be attributed to the difference in size and form, which prevents nanoparticulate albumin from utilising the endogenous mechanisms for protein clearance from the lungs (Woods et al. 2015).

1.11 Albumin nanoparticle manufacture

Weber et al. (Weber, Coester, et al. 2000) evaluated in great detail the well-documented "desolvation method" for the preparation of albumin nanoparticles. In brief, desolvation of an aqueous solution of albumin is achieved by dropwise addition of a solvent such as ethanol or acetone to the stirred protein solution. It is a thermodynamically driven self-assembly process that separates and coacervates the albumin molecules in the aqueous phase (Jun et al. 2011). The desolvating agent has a critical effect on the protein's conformation and the morphology of the binding sites. As investigated through Fourier-transform infrared spectroscopy (FTIR) experiments, the addition of ethanol into aqueous solutions of albumin can a) significantly alter its native structure, b) solubilise the protein and c) decrease the percentage of α-helical structure (Mohammad-beigi et al. 2016; Merodio et al. 2000). As mentioned previously, a cross-linker (usually glutaraldehyde) is used to cross-link the amino groups in the nanoparticles to stabilise them so they do not solubilise (Zhao et al. 2010). Weber et al. also studied the effect of glutaraldehyde and found that increasing glutaraldehyde concentrations reduced the number of available amino groups on the albumin surface and lowered the zeta potential but had no effect on the size of the nanoparticles. As an alternative to the use of a cross-linker, heat stabilisation has also been investigated (Weber, Coester, et al. 2000). This is where instead of the addition of a cross-linker, the particles were incubated at different temperatures. This process works by heat-induced unfolding, followed by protein-protein interactions such as hydrogen bonding, hydrophobic or electrostatic interactions and disulphide-sulphydryl reaction (Yu et al. 2006; Qi et al. 2010). Weber et al. found heating for less than 48 hours at 50°C and for less than 24 hours at 60°C did not stabilise the colloidal system, confirming that albumin can survive being heated at 60°C for ten hours. Heating for two hours at 70°C however showed particles were cross-linked, and heating for more than two hours did not affect the extent of cross-linking of the amino groups. This is consistent with findings from Chen et al. that showed increasing temperature will increase the degree of cross-linking, while also decreasing the rate of dissolution of albumin in water (Chen et al.

1994). The size of the nanoparticles formed can be controlled by adjusting albumin concentration, pH, and ion content (Jun et al. 2011). The pH of the albumin solution is a major factor in determining particle size as the electrostatic interactions regulated by the pH of the surrounding medium can modify the protein's secondary structure (Langer et al. 2003). Overall, this technique proved to be reproducible and shows ease of scale up. Despite the preference to avoid cross-linkers like glutaraldehyde in the manufacture process, it is unrivalled in producing the most stable nanoparticles compared to alternatives that have been tried.

Other methods of albumin nanoparticle manufacture have been investigated. Nanoparticle albumin bound technology (nab technology) is ideal for formulating hydrophobic drugs in a nanoparticulate system. It is based on a technique where the drug is dissolved in an organic solvent and emulsified in water under high pressure homogenisation using protein (albumin) as a stabilising agent. The organic solvent is then removed so the drug can precipitate and protein coated nanoparticles can be formed. Abraxane® (nab-paclitaxel) is the first FDA approved product utilising this technology. This approach has been utilised in studies with itraconazole (Chen et al. 2008) and curcumin (Kim et al. 2017) for intravenous administration. Despite the success of this technology, albumin is not the core or matrix of these formulations but rather the main structure of the nanoparticles is based on the drug, with albumin acting as a coating stabiliser.

The emulsification method is another popular choice for the preparation of albumin nanospheres (Elzoghby et al. 2012). In general, an aqueous albumin solution forms a water/oil emulsion with its gradual addition into a continuous oily phase under high-speed homogenisation or high shearing. Subsequently, the resulting nanoparticles are crosslinked by chemical or thermal treatment and the oily phase is removed using organic solvents (Patil 2003; Sundar et al. 2010). During chemical treatment a crosslinking agent (usually glutaraldehyde) is added after the formation of the emulsion to stabilise the

already formed nanoparticles (Sirotkin et al. 2001). Under thermal stabilisation, albumin is rendered insoluble after the application of high temperature with the formation of interchain amide bonds (Lin et al. 2004). Critical parameters to control the particle size, the polydispersity index and the yield, such as the protein concentration and the aqueous phase volume, have also been determined for the emulsification technique (Sirotkin et al. 2001). Regarding the drug loading efficiency of this method, no data was found in the literature that provide information on the effect this method's parameters have on drug loading. It can be assumed, as before, that the cross-linking agent can alter the conformation of the albumin binding sites and the application of high temperatures can also influence the structural integrity of albumin. It should also be considered that hydrophobic drugs may partition into the continuous oily phase or perhaps be extracted during oily phase removal, resulting in drug loss and subsequent reduction in drug loading.

As mentioned above, spray-drying is a well-established method in the pharmaceutical industry for producing powders from a liquid phase. The Nano Spray dryer technique utilises a vibrating mesh to form fine droplets and particles are collected using an electrostatic precipitator. Lee et al. utilised this technique to form spray-dried BSA nanoparticles and found the largest determinants in particle size and morphology were the spray mesh size and surfactant concentration- for which they used tween 80 (Lee et al. 2011).

In summary, albumin nanoparticles are considered to be a promising delivery system due to their binding capacity for a wide variety of molecular classes, benign toxicological profile and potential for controlling the release of active substances. However, it is important to extensively evaluate the interactions of a drug candidate (with poor aqueous solubility) with albumin and design optimised preparation methods that will allow for optimal loading of the drug and reproducible formation of particles. While methods have

been adopted that generate particles with reproducible characteristics (particle size diameter, size distribution and zeta potential), the drug loading characteristics (binding site interactions and solubilisation properties) have been insufficiently characterised so far. As well as drug loading, nanoparticle systems for drug delivery must also be able to release the active substance at a desired rate. The study of drug release from albumin nanoparticle systems is therefore another important area that requires more extensive understanding. When it comes to the challenges with aerosolised drug delivery, it is clear that some of the most promising advances come from applying nanotechnology to particle engineering. However, the design of such a system requires understanding of drug-nanoparticulate interaction and the many formulation and technical issues that come with the development of inhalable carriers to the lung. The studies discussed here confirm the potential of albumin as an effective nano-formulation for drug delivery to the lungs, but also highlight the need for further exploration of the development of a viable and effective albumin nanoparticulate aerosol formulation for controlled delivery of hydrophobic drugs to the lungs.

1.12 Aim and scope of thesis

The overall aim of this thesis was to develop a respirable microparticle formulation containing drug-loaded albumin nanoparticles for delivery to the lungs. Taking into consideration the factors reviewed in this introduction, the key research questions to consider when developing such a system were identified. a) Can an albumin nanoparticle formulation be developed in a way that hydrophobic drug can be satisfactorily loaded, stored and released? b) Is the hydrophobic drug delivered effectively using the albumin nanoparticle formulation? c) Is it possible to formulate the albumin nanoparticles as part of a microparticle for inhaled delivery while retaining their properties? Ideally albumin nanoparticles should be able to load drugs that are typically difficult to formulate, protect them until they are required to exert their pharmacological action and sustain drug release. The developed inhaled system should be stable and display satisfactory aerosolisation properties in order to be effective at delivering drug-loaded albumin nanoparticles to the lungs.

The following specific objectives were set in order to fulfil the aim:

- Establish methods for manufacture of albumin nanoparticles and their impact on particle physicochemical properties and stability
- Investigate the mechanisms of loading and release of model drugs in albumin nanoparticles and investigate their efficacy using bioassays
- Develop prototype formulations for the encapsulation of nanoparticles in respirable microcarriers
- Optimise nanoparticle loading into the preferred respirable formulation and evaluate the viability as an inhaled medicine in terms of respirable dose, particle size distribution and release of nanoparticles upon wetting.

Chapter 2 Manufacture of albumin nanoparticles

2.1 Introduction

Albumin nanoparticles were investigated in this thesis as a potential carrier system for drug delivery to the lung. In this chapter, the method development for the manufacture of bovine-based albumin nanoparticles and subsequent human serum albumin nanoparticles is outlined. The characteristics of nanoparticles produced were explored, as well as the stability and digestion of the particles in a clinically relevant model. It was anticipated this work would provide the foundation for the development of a respirable formulation containing drug-loaded albumin nanocarriers for pulmonary drug delivery.

Albumin nanoparticles are no stranger to the drug delivery field. Albumin nanoparticulate formulations have been studied for intravenous and intravitreal administration and as mentioned previously one such formulation (Abraxane®) is commercially available. Abraxane® utilises "nab-technology" whereby albumin solution and a drug solution are mixed under high pressure to form nanoparticles. The albumin supposedly stabilises the drug particles at an average size of 130 nm. This method is different to other methods of albumin nanoparticle manufacture where albumin nanoparticles are formed via desolvation, emulsification, or thermal gelation and drug is typically loaded into them (Elzoghby et al. 2012).

Nanocoll® is a commercial product consisting of human albumin colloidal particles. It is sold as a powder and is reconstituted with aqueous sodium pertechnetate (^{99m}Tc) injection solution to create a technetium-99m albumin nanocolloid injection product (O'Brien et al. 2006). Although not used for drug delivery, it is essentially a radiopharmaceutical used intravenously for bone marrow scanning and locally to demonstrate integrity of the lymphatic system and for identifying the sentinel lymph node in some types of cancer (O'Brien et al. 2006). Nanocoll® has also been used for diagnostic lung imaging and its pulmonary deposition patterns have been studied in human subjects after nebulised administration (Bondesson et al. 2007).

The usefulness of albumin in nanoparticle formulations for anti-cancer applications is well documented in the literature. The development of a nanoparticle formulation containing albumin for the delivery of doxorubicin and tumour necrosis factor-related apoptosis-inducing ligand (TRAIL) to tumour cells has also been investigated (Thao et al. 2016) and another study showed folate-decorated BSA nanoparticles loaded with paclitaxel could target prostate cancer cell lines (Zhao et al. 2010). Other non-cancer therapeutic strategies have also been explored, although more of the recent work with albumin in this respect is focused on cancer therapy or tumour imaging (Dong et al. 2016; Tang et al. 2016; Khandelia et al. 2015). Examples of non-cancer related studies include a study by Mishra et al. which demonstrated that modifying the surface of PEG-ylated human serum albumin nanoparticles, encapsulated with an anti-viral drug azidothymidine (AZT) by anchoring transferrin ligands to it, could target the brain (Mishra et al. 2006). Ganciclovir-loaded BSA nanoparticles have been studied for intraocular delivery by intravitreal injection (Merodio et al. 2002). Das et al. studied aspirin-bovine serum albumin nanoparticle coacervates for the purposes of intraarticular delivery for anti-inflammatory disease in arthritis or intraocular delivery for diabetic retinopathy (Das et al. 2005). Li et al. studied BSA nanoparticles loaded with sodium ferulate for hepatic targeting (Li et al. 2008).

Despite albumin nanoparticle-based pharmaceuticals being available, and the high research interest in utilising albumin nanoparticles as drug delivery vehicles, no systems are available or licensed for the inhalation route or for pulmonary drug delivery. The aim therefore of this chapter was to establish the manufacturing technique of bovine serum albumin nanoparticles, translate this to human serum albumin nanoparticles and characterise these for suitability for development as a drug carrier for delivery of pharmaceutical agents to the lung. More specifically, the following objectives were set for the work in this chapter:

- Manufacture BSA nanoparticles using a modified desolvation technique and characterise these systems
- Manufacture HSA nanoparticles for comparison with BSA nanoparticles
- Study the storage stability of both BSA and HSA nanoparticle suspensions
- Investigate the breakdown of albumin nanoparticles in a protease model relevant to the lung lining fluid.

2.2 Materials

Human serum albumin [HSA; isoelectric point 4,7. (Vlasova & Saletsky 2009)] and bovine serum albumin (BSA) of molecular weight 65,000 g/mol (fatty acid free) were purchased from Sigma-Aldrich (Buckinghamshire, UK). Trypsin (~10000 BAEE units/mg) was purchased from Sigma-Aldrich. Phosphate buffered saline (PBS) tablets came from Oxoid. Ethanol, water, sodium hydroxide and glutaraldehyde were of HPLC grade and obtained from Sigma-Aldrich.

2.3 Methods

2.3.1 Albumin nanoparticle manufacture

Bovine and human serum albumin nanoparticles were manufactured using a modified desolvation method as adapted from Weber et al. (Weber, Kreuter, et al. 2000) and from Woods, 2015 (Woods 2015). Albumin (50 mg, fatty acid free) was dissolved in 1.0 mL Tris HCl buffer (0.01M, pH 8.9). After the addition of 25 µL NaOH (1M), 4.0 mL of ethanol was added drop wise to the stirred protein solution at a rate of 1 mL/min. Nanoparticles were cross-linked by addition of 47.2 µL 5% glutaraldehyde in water and overnight stirring. Particles were purified by at least 4 cycles of spin filtration [30 kDa molecular weight cut-off (MWCO)] into PBS.

2.3.2 Nanoparticle physicochemical characterisation

Particle hydrodynamic diameter and polydispersity index (PDI) was determined by Dynamic light scattering (DLS) using the Zetasizer Nano Series ZS (Malvern Instruments, Malvern, UK). DLS enables the determination of the diffusion coefficient (D) of a particle or droplet in solution (Finsy 1994). Assuming the particles are spherical, they undergo random thermal motion called Brownian motion which is modelled by the Stokes-Einstein equation (Hassan et al. 2015). The measured D can be used to calculate the hydrodynamic diameter, *d(H)*, of the particle/droplet using the equation:

Equation 2.1

$$d(H) = \frac{kT}{3\pi\eta D}$$

where *d(H)* is the hydrodynamic diameter, *k* is the Boltzman constant, *T* is temperature, *D* is the diffusion coefficient and η is the viscosity. The analysis was performed at a scattering angle of 173° and at 25°C, unless stated otherwise. Detailed descriptions of dynamic light scattering theory are documented in the international standard for

determination of particle size distribution (ISO13321) and by Dahneke (ISO 1996; Dahneke 1983).

Zeta potential was measured in water and PBS and measured at 37°C at a concentration of 20 μg/mL. The zeta potential is used in colloid chemistry for dispersive systems in liquids (such as a nanoparticle suspension) and characterises the electrical double layer on the solid/liquid interface i.e. it is related to surface charge- a property all materials possess when suspended in a liquid (Birdi 2002; Shaw 1992). The fundamentals of zeta potential are well described in colloid chemistry texts (Shaw 1992; Hunter 1981; Lyklema 1991).

2.3.3 Physical stability

Purified nanoparticle suspensions (in PBS) were stored in different temperature conditions (4°C and 25°C). Hydrodynamic diameter and polydispersity index (PDI) were used as a measure of stability of nanoparticle suspensions and were measured at regular intervals.

2.3.4 Digestion experiments

The breakdown of albumin nanoparticles was assessed in a model representative of the physiological lung. Nanoparticle suspensions (1 mL, 10 mg/mL) were incubated in PBS (0.1M, pH 7.4) supplemented with 10.8 mg/mL albumin at 37°C. The receiver fluid was supplemented with albumin to mimic the protein concentration in lung lining fluid (Bicer 2011). Nanoparticle breakdown was determined in the presence and absence of trypsin (0.1 mg/mL; ~10 000 BAEE units/mg). This concentration was selected to match lung protease concentrations from the literature (Wilson 2005). DLS was used to measure the size, polydistribution index (PDI) and derived count rate [kilo counts per second (kcps)] of samples withdrawn at various time points from both systems with and without trypsin. The derived count rate is a function of size and concentration of scattering particles and can be used as a measure of concentration for nanoscale particles (Smeraldi et al. 2012).

2.3.5 Transmission Electron Microscopy

Samples were diluted to 1 mg/mL of albumin nanoparticles (based on initial concentration) with ultrapure water. A sample, 3 µl, of suspension was then applied to a Pioloform-coated copper grid and allowed to settle for 1 min. Excess suspension was blotted away and the grids stained in 1% w/v uranyl acetate for 1 min. The excess was blotted and the grid dried before imaging. Grids were examined using a Tecnai T20 electron microscope.

2.3.6 Statistical analysis

Statistical calculations were carried out using the software SigmaPlot 14.0 for Windows (SyStat Software Inc., CA, USA). To identify statistically significant differences between particle size measurements and zeta potential, two-tailed Student t-tests were performed. P values less than 0.05 were considered significant.

2.4 Results

2.4.1 Physical characteristics of nanoparticles

Table 2.1 shows BSA / HSA sizing data and zeta potential values in different conditions. Size was measured at a 1:10 and 1:100 dilution in water and PBS and at the temperatures 25°C and 37°C, while zeta potential was measured in water and PBS. No significant differences were observed between size measurements taken in the different conditions tested. All nanoparticle batches had yields greater than 95%, with no significant differences between BSA and HSA nanoparticles. The colour of the nanoparticle suspensions (brownish) was attributed to the cross-linking by glutaraldehyde. Ma et al. found that cross-linking BSA with glutaraldehyde has an effect on its fluorescent properties, as observed by the difference in colour between BSA solution and the BSA hydrogels formed in their studies (Ma et al. 2016). Visually no differences were observed between BSA and HSA nanoparticle suspensions (Figure 2.1).

Zeta potential is the measurement of the electrostatic potential at the electrical double layer surrounding a nanoparticle in solution. A zeta potential between -10 and +10 mV is considered neutral and values greater than +30 mV or less than -30 mV is considered strongly cationic and anionic respectively (McNeil 2011). The effect of pH on the zeta potential of BSA in saline has been studied (Salgin et al. 2012). The isoelectric point is the pH at which a particle has zero net surface charge i.e. the zeta potential of a substance is 0 (Jiang et al. 2009). For BSA this has been reported as between pH 4 and 5 in sodium chloride at concentrations between 0.001 – 0.1 M (Salgin et al. 2012). At pH values below this, the zeta potential will be more positive and at more basic pH it will be more negative (Salgin et al. 2012). Zeta potential measurements were carried out at physiological pH (in the cases of both water and PBS), with different values observed for both (-23.8 ± 11.7 and -10.4 ± 3.3 respectively),attributed to the fact that zeta potential is not only dependent on pH but also the conductivity of the dispersing medium (McNeil 2011; Shaw 1992; Hunter 1981).

Table 2.1 Hydrodynamic diameter, polydispersity index (PDI) and zeta potential of BSA and HSA nanoparticle suspensions. Data marked with * represent a 1 in 10 dilution, data marked with ** represent 1 in 100 dilution. Data represent the mean and standard deviation of n = 3 nanoparticle batches.

Nanoparticle diluent	BSA			HSA		
	Size 25°C and PDI [units]	Size 37°C and PDI [units]	Zeta potential 37°C (mV)	Size 25°C and PDI [units]	Size 37°C and PDI [units]	Zeta potential 37°C
Water	*100.8 ± 6.5 [0.122 ± 0.001]	*104.4 ± 5.8 [0.125 ± 0.016]	-23.8 ± 11.7	*112.6 ± 10.7 [0.01 ± 0.001]	*114.4 ± 10.5 [0.060 ± 0.016]	-25.6 ± 8.7
	**102.6 ± 4.7 [0.155 ± 0.017]	**114.3 ± 11.2 [0.190 ± 0.063]		**110.8 ± 7.5 [0.050 ± 0.010]	**115.3 ± 11.2 [0.100 ± 0.050]	
PBS	*100.7 ± 3.3 [0.109 ± 0.011]	*108.3 ± 3.0 [0.135 ± 0.016]	-10.4 ± 3.3	*110.7 ± 8.3 [0.009 ± 0.001]	*111.3 ± 7.0 [0.011 ± 0.001]	-10.6 ± 2.7
	**104.1 ± 6.7 [0.157 ± 0.038]	**115.3 ± 10.3 [0.182 ± 0.025]		**114.1 ± 10.5 [0.070 ± 0.038]	**115.3 ± 10.3 [0.102 ± 0.025]	

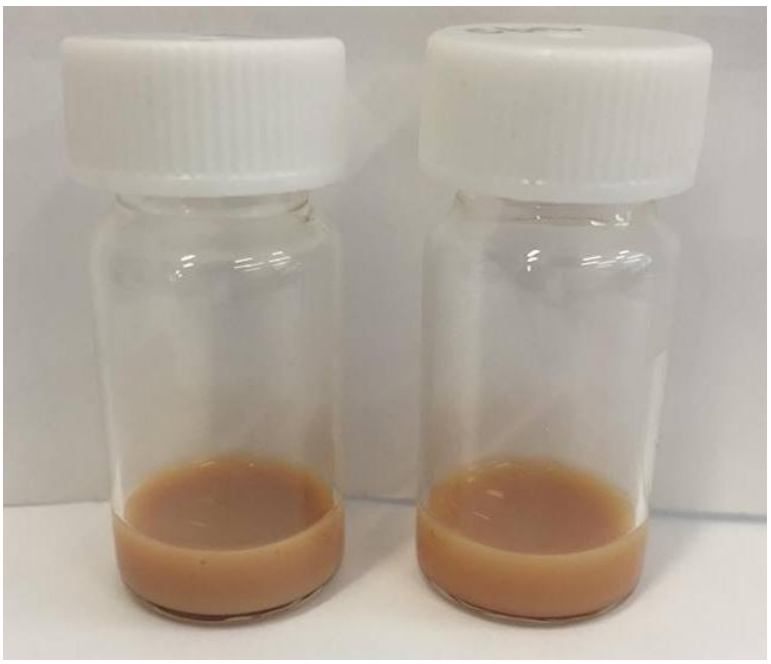

Figure 2.1 Bovine serum albumin (BSA) nanoparticles (left) and human serum albumin nanoparticle (HSA) suspensions (right).

2.4.2 Stability

Both BSA and HSA nanoparticle suspensions remained stable at 25°C for three months, while at 4°C they remained stable for six months. Nanoparticle suspensions were deemed as unstable when visual signs of aggregation were observed. Table 2.2 shows the original size and PDI for nanoparticle suspensions tested and after three or six months for storage at 25°C and 4°C respectively. No significant differences were observed for the stability of BSA vs HSA.

The storage stability of both BSA and HSA nanoparticle suspensions at room temperature and 4°C was investigated (Figure 2.2). The stability was assessed by measuring the size and PDI of nanoparticle suspensions as well as observing the physical nature of the suspensions. No differences were observed visually between BSA and HSA suspensions, however for BSA nanoparticles, a significant increase in particle size was observed after three months of storage at room temperature, an increase in size was also observed for HSA nanoparticles under the same storage conditions however this was not found to be statistically significant. Nanoparticles remained of an acceptable size and dispersity for up

to one month for nanoparticles stored at room temperature, whereas they remained stable for six months upon storage at 4°C. After these time points, suspensions showed visible signs of aggregation and sedimentation.

Table 2.2 Size and PDI data for nanoparticle suspensions after storage at either 25°C or 4°C for both bovine serum albumin (BSA) and human serum albumin (HSA) nanoparticle suspensions. Data represent the mean and standard deviation of n = 3 nanoparticle batches.

	25°C		4°C	
	T = 0	Three months	T = 0	Six months
BSA	109 ± 1 [0.07 ± 0.01]	122 ± 2 [0.28 ± 0.03]	112 ± 1 [0.09 ± 0.01]	132 ± 6 [0.25 ± 0.04]
HSA	130 ± 3 [0.08 ± 0.01]	140.5 ± 5 [0.24 ± 0.06]	130 ± 8 [0.09 ± 0.01]	144 ± 5 [0.25 ± 0.04]

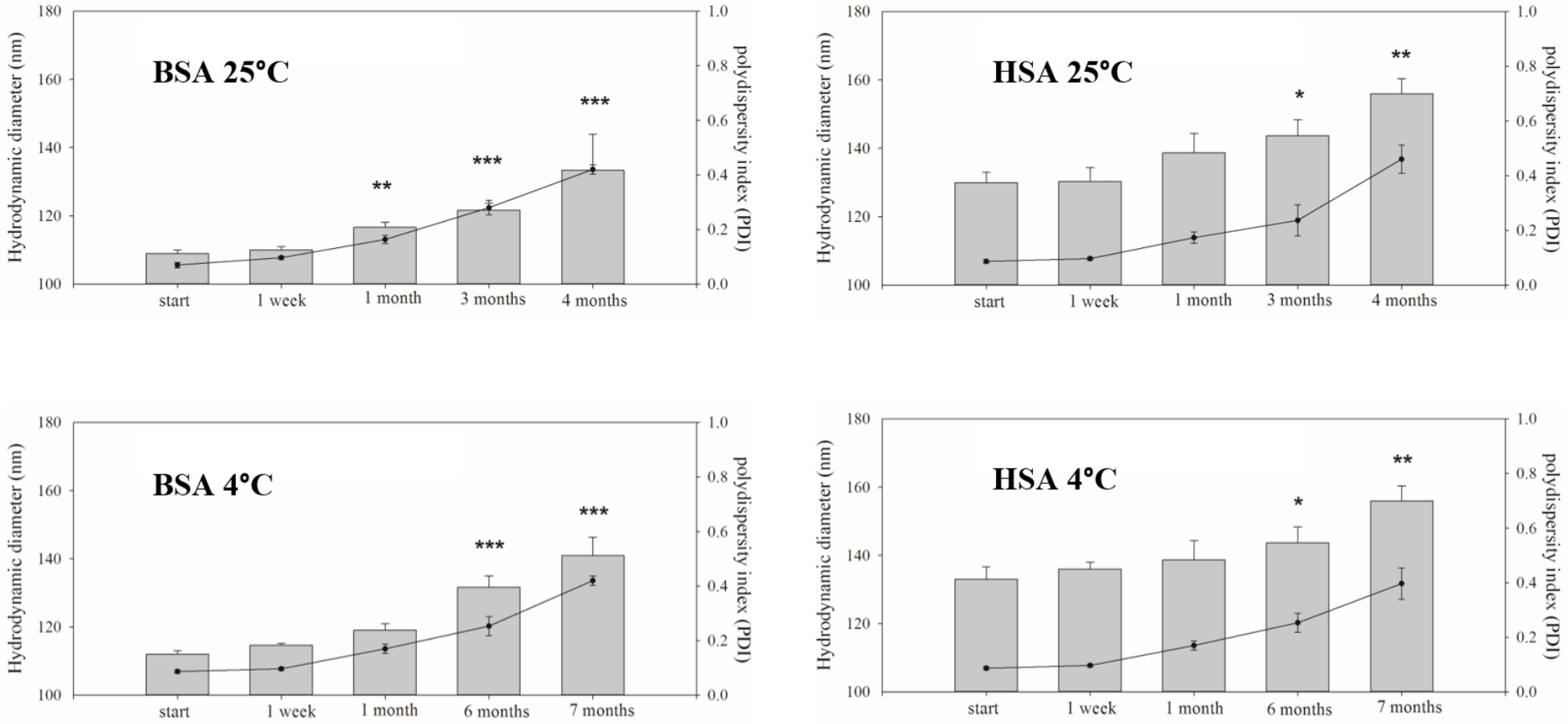

Figure 2.2 Influence of storage time on particle size and polydispersity of bovine serum albumin and human serum albumin nanoparticles At 25°C and 4°C. The bars depict the hydrodynamic diameter (nm, left side axis) of particles and the lines depict the polydispersity index (PDI, right-side axis). Data represent the mean and standard deviation of n = 3 measurements. An asterisk (*, or **, or ***) depicts a statistically significant difference in particle size compared to the initial size ($p < 0.05$, 0.01 and 0.001, respectively).

2.4.3 HSA nanoparticle digestion

Preliminary digestion experiments with BSA nanoparticles were carried out where TEM images were taken of nanoparticles treated with trypsin at different time points., in order to assess visual evidence of digestion. TEM images of untreated BSA nanoparticles are shown in Figure 2.3. Particles appear round and smooth with fairly monodisperse size populations. Figure 2.4 shows TEM images at different time points after the addition of trypsin to the nanoparticle suspensions.

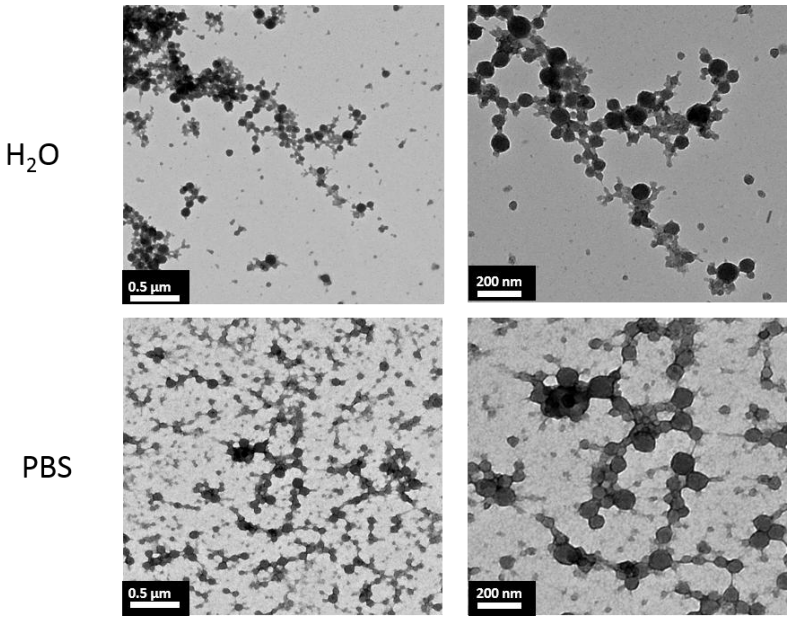

Figure 2.3 Representative TEM images of BSA nanoparticles suspended in water (top) and PBS (bottom) at two different magnifications.

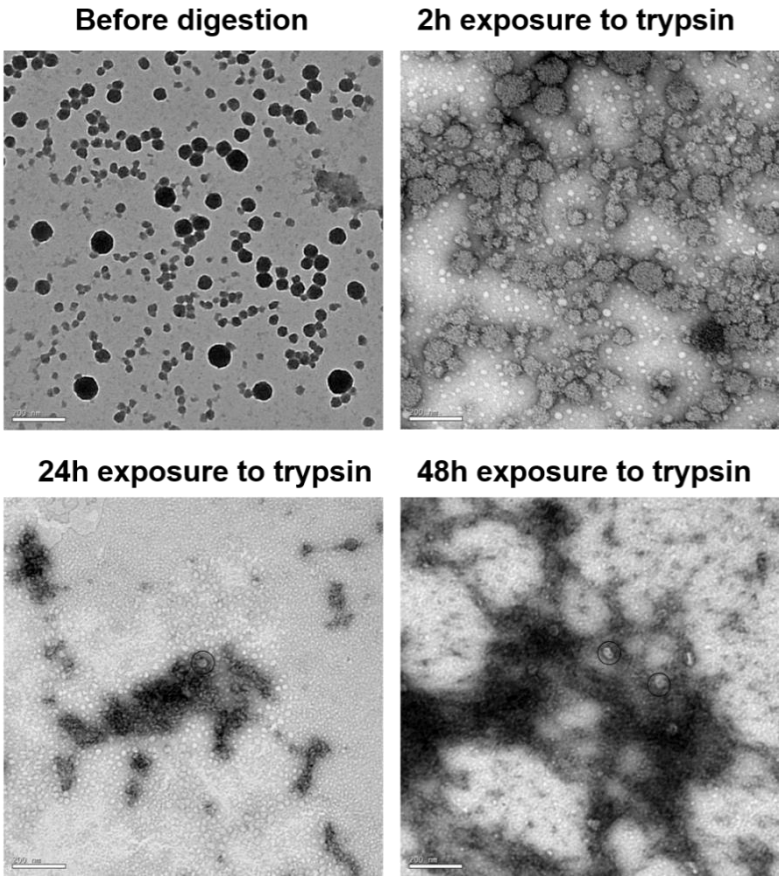

Figure 2.4 Representative TEM images showing BSA nanoparticles before and after exposure to trypsin at time points (hours): 0, 4, 24 and 48.

Digestion studies were subsequently carried out with human serum albumin nanoparticles in release medium representative of the lung lining fluid. DLS and PDI data were used to evaluate the change in concentration of the nanoparticles. DLS data only gave limited information with regard to particle breakdown, as it could not be ascertained if whole particles were being detected from the count rate or if larger particles obscured the detection of smaller fragments. Nevertheless, a trend was observed where decreasing particle count rates (Figure 2.5) and increases in polydispersity (Figure 2.6) were noted for samples retrieved from the trypsin system. Albumin nanoparticle breakdown in the trypsin system showed an initial rapid decrease in the count rate (concentration dropped to 50% after 4 hours) followed by a slower digestion rate for the remainder of the experimental period (20% concentration at 48 hours). Nanoparticles remained stable in PBS without trypsin with no changes in concentration or polydispersity noted.

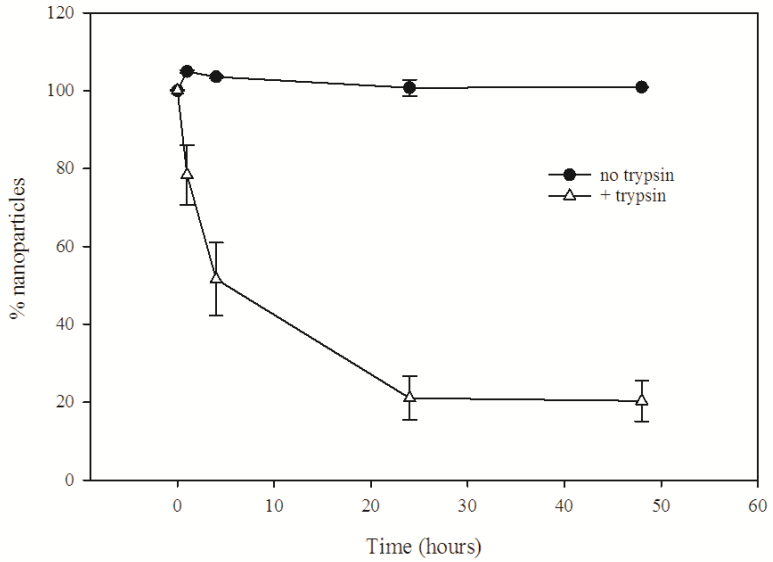

Figure 2.5 Digestion of HSA nanoparticles in PBS supplemented with albumin with and without trypsin as a model lung protease. Graph represents the count rate at each time point as a percentage of the initial count rate. Data represent the mean and standard deviation of n = 3 nanoparticle batches.

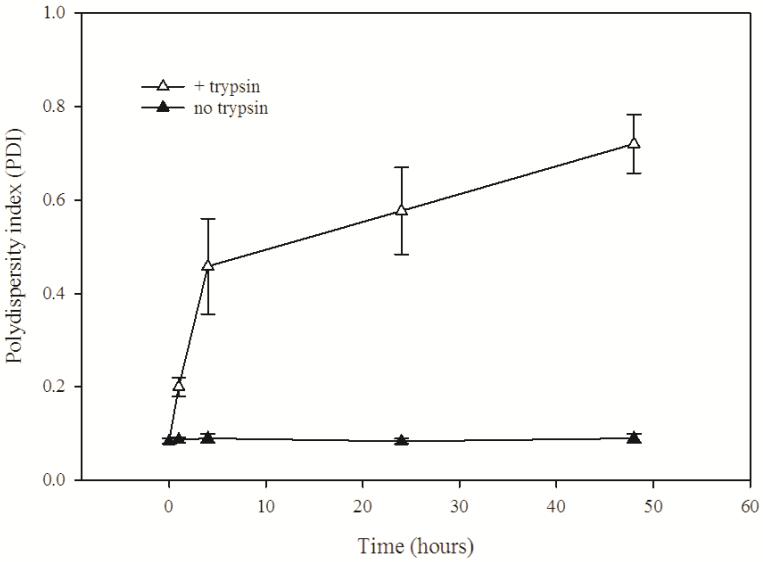

Figure 2.6 Polydispersity (PDI) of HSA nanoparticle suspensions in PBS supplemented with albumin with and without trypsin as a model lung proteaseat time points (hours): 0, 1, 4, 24 and 48. Data represent the mean and standard deviation of n = 3 nanoparticle batches.

2.5 Discussion

The characteristics of the BSA nanoparticles manufactured here are in good agreement with results from previous studies using similar conditions to form BSA nanoparticles, with sizes of 100-200 nm and narrow size distributions (Li et al. 2008; Zhao et al. 2010; Bronze-Uhle et al. 2017). Similarly, the data obtained from HSA nanoparticles are also comparable to previous studies (Wartlick et al. 2004; Von Storp et al. 2012; Kim et al. 2009). This size range was chosen because it is within this range the retention and potential controlled release properties of the nanoparticles are apparently best and this would be beneficial for exploration after incorporation of a hydrophobic drug into the formulation (Elzoghby et al. 2012). Initially, experiments were carried out with BSA in order to become familiar with the manufacturing of albumin nanoparticles using less expensive material. However, the translation from BSA to HSA is important for the future development of albumin nanoparticles as a viable formulation strategy for delivery of drugs to the lung so it was important to establish any differences between the two albumin types in terms of nanoparticle characteristics. HSA is approved by the FDA and exists as an endogenous protein, so it is usually substituted for other sources of albumin e.g. bovine serum albumin or ovalbumin to minimise the risk of a possible immunological response in *in vivo* experiments for example. HSA was therefore employed for all further experiments.

The desolvation method is a well-established methodology for the formation of albumin nanoparticles. The effects of pH, rate of addition of desolvation agent and HSA concentration have been studies previously (Langer et al. 2003). The pH was found to be the most important factor influencing the size of nanoparticles produced, as exemplified in an earlier study by Lin et al. where it was found that increasing pH leads to a reduction in size of nanoparticles- owing to the isoelectric point of HSA [4.7,(Vlasova & Saletsky 2009)]. As the HSA molecules become increasingly ionised, increased electrostatic repulsion occurs between particles (Lin et al. 1993). In this thesis, pH 8.9 was used and this was

found to be optimal for the target size range of particles (100-200nm) as determined by preliminary studies. Other factors affecting the desolvation technique (i.e. rate of addition of ethanol and HSA concentration) have previously been reported to have very little effect on the properties of nanoparticles produced, thus the current method was found to be suitable for future work.

Nanoparticle suspensions showed stability comparable to a previous study by Dreis et al. (Dreis et al. 2007). In terms of long term storage (i.e. a year or longer), freezing or freeze drying may be a suitable method for obtaining a dry powder, as displayed in a study by Zhao et al where BSA-paclitaxel nanoparticle conjugates were spray-dried with mannitol as a cryoprotectant (Zhao et al. 2010). Anhorn et al. studied the effects of different cryoprotectants on the stability of freeze-dried HSA nanoparticles and found mannitol, trehalose and sucrose as suitable cryoprotectants that prevented aggregation as opposed to no cryoprotectant being used (Anhorn et al. 2008).

DLS as a method for detecting albumin nanoparticle breakdown in trypsin digestion experiments had its limitations, however, trends could be noted in the data. The TEM images from the preliminary experiments with BSA show good agreement with the findings from this study as particles appear to undergo rapid digestion at the 4-hour timepoint, with continued digestion at the 24-hour and 48-hour time points, with a few visible in-tact particles. The trends agree with the findings in a previous study where the digestion of BSA nanoparticles was studied in the same release media (Woods et al. 2013) where release kinetics showed an initial burst effect followed by a slower rate of digestion where particles were also largely degraded within 48 h.

In summary, BSA nanoparticles were manufactured successfully, followed by the manufacture of HSA nanoparticles whose properties were similar to BSA. HSA is the more viable carrier in terms of the development of a pharmaceutical formulation as it is more

pharmaceutically acceptable as an excipient. Nanoparticles were produced with reproducible size, low polydispersity, and good stability. The breakdown of albumin nanoparticles in a mediumphysiologically relevant to the lung was also investigated. This will be investigated further when a drug is involved in the albumin nanoparticle formulation.

2.6 Conclusion

In this chapter the methodology and characterisation of albumin nanoparticle manufacture was explored. The translation from preliminary studies with BSA to HSA was successfully carried out. The physico-chemical characteristics and stability of the nanoparticles was also investigated. The work in this chapter will be used to aid future assessment of the feasibility of albumin nanoparticles as a drug delivery carrier. More specifically, the potential of HSA nanoparticles as drug carriers for drug delivery to the lung will be investigated. Therefore, the encapsulation of model drugs will be investigated. The loading, release and subsequent activity of the drug-albumin systems will also be evaluated. As the intended purpose of the albumin nanoparticle carriers is for drug delivery to the lung, the development of a respirable formulation containing these systems will also be investigated.

Chapter 3 Loading, release and activity of benzothiazinone-loaded human albumin nanoparticles

3.1 Introduction

Tuberculosis (TB) is a disease caused by *Mycobacterium tuberculosis* and it remains a global health problem. It principally affects the lungs although it can spread to other parts of the body. In 2016 it was estimated that 10.4 million people developed the disease globally while 1.7 million people died from it (World Health Organisation 2017). Rifampicin and isoniazid are current treatments for TB, however there is an increasing number of cases of multidrug-resistant TB that fail to respond to rifampicin and isoniazid (Gandhi et al. 2010). This urges the development of new anti-tuberculosis medicines.

8-Nitro-benzothiazinones (BTZs) are a relatively new class of antitubercular agents that have been shown to be effective against drug-susceptible, multidrug-resistant and extensively drug-resistant strains of *Mycobacterium tuberculosis* (Christophe et al. 2009). Lv et al. report an MIC of < 0.02 μg/mL for one of their investigated BTZ compounds (Lv et al. 2018) while Richter et al. report an MiC value of < 0.5nM for one of their synthesised BTZ compounds (Richter et al. 2018). They work by inhibiting the mycobacterial enzyme decaprenylphosphoryl-beta-D-ribose 2-epimerase (DprE1)- an essential enzyme for the biosynthesis of D-arabinose, a precursor involved in the biosynthesis of cell wall components. DprE1 is one of the enzymes involved in catalysing the conversion of decaprenylphosphoryl-β-D-ribose (DPR) to decaprenylphosphoryl-β-D-arabinose (DPA) (Mikusova et al. 2005). The formation of DPA appears to be the only source of D-arabinofuranosyl residues in *Mycobacterium tuberculosis* and therefore the irreversible inhibition of this enzyme by BTZs is responsible for their bactericidal action via mechanism-based inhibition of the target enzyme (Mikusova et al. 2014). In the first step of the inhibition reaction the BTZ binds non-covalently at the catalytic centre of DprE1, which reduces the nitro-group under formation of the nitroso-BTZ resulting in covalent inhibition of DprE1 (Trefzer et al. 2010; Trefzer et al. 2012).

BTZs have relatively poor oral bioavailability compared to the current standard TB regimen drug compounds which all have oral bioavailabilities >90% while the most promising BTZ candidates currently being studies have shown to have bioavailability of about 20% (Xiong et al. 2018; Makarov et al. 2014). This has been attributed to their low solubility and absorption and metabolism by bacteria in the gut by the reduction of the nitro-group to an amine (Makarov et al. 2014; Richter et al. 2018). This is their main metabolic pathway though a recent study has shown they are also metabolised by reduction of the aromatic benzothiazinone core by erythrocytes through formation of a Meisenheimer complex (Kloss et al. 2017). These issues collectively provide a strong rationale for exploring alternative formulation strategies and routes of administration to improve BTZ bioavailability. An example of this being implemented is shown in a Phase Ia clinical trial which is currently underway, in which the oral bioavailability of a spray-dried amorphous dispersion of a BTZ compound (PBTZ169) in comparison with the native crystalline substance is being studied (Innovative Medicines for Tuberculosis & Foundation 2018). Aside from this, little is being done to investigate alternative formulations or routes of administration to advance BTZs as viable novel treatments for TB.

Taking all the above into consideration, it was suggested that soluble albumin or albumin nanoparticles are potential vehicles for the delivery of BTZs to their primary site of action, i.e. the lungs. BTZs represent the typical model drug candidate for an albumin nanoparticle formulation strategy. In addition to the above advantages of using albumin, the potential enhanced retention of albumin nanoparticles provides additional incentive as illustrated in this study of the biocompatibility, clearance, and biodistribution profiles of albumin (Woods et al. 2015) showing that albumin delivered as nanoparticles (~180 nm) remained in the lungs of mice for longer compared to albumin delivered in solution with lung retention of 64% vs 40.6%, respectively, at 48 hours. In terms of TB therapy, delivery

of sufficient localised concentrations of the highly-potent BTZ has the potential to provide effective antimicrobial activity, which minimises the possibility of resistance developing and offers a reduced duration of treatment; all major tenets in strategies for new TB therapeutics (Gawad & Bonde 2018).

Therefore, the aim of the work in this chapter was to investigate the potential of human serum albumin (HSA) nanoparticles and HSA solution as a carrier for delivering antimycobacterial benzothiazinone (BTZ) compounds to the lungs.

The following specific objectives were set to achieve the aim:

- Investigate interactions between albumin and model BTZ compounds (Table 3.1) using solubilisation and binding studies
- Manufacture BTZ-loaded albumin nanoparticles and study their characteristics
- Investigate the drug loading, release and antimycobacterial activity of the developed formulations in relevant models.

It was hypothesised that albumin would solubilise the BTZ compounds, thereby enabling their formulation, however uncertainty around the release of the drug within a therapeutically relevant time period was addressed with *in vitro* release and antimycobacterial activity assays.

Table 3.1 Structure and physicochemical properties of the four BTZ compounds used in this study. This data was kindly provided by Adrian Richter from University of Halle, Germany.

IR 20	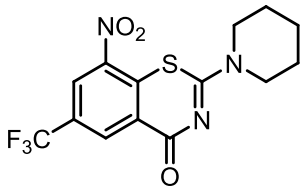	MW* 359.32 g/mol Solubility (aq) 373 µM (134 µg/ml) MIC** 3.3 µM (1.2 µg/ml)
IF 274	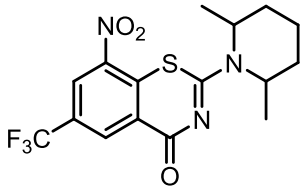	MW* 387.38 g/mol Solubility (aq) 88µM (34 µg/ml) MIC** 0.8 µM (0.3 µg/ml)
FG 2	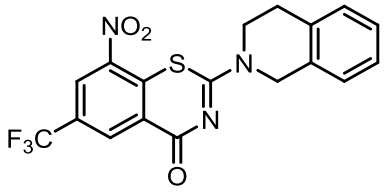	MW* 407.37 g/mol Solubility (aq) 2.3 µM (0.9 µg/ml) MIC** 0.2 µM (0.07 µg/ml)
AR 112	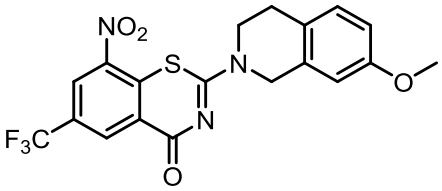	MW* 439.39 g/mol Solubility (aq) 0.9 µM (0.4 µg/ml) MIC** 0.07 µM (0.07 µg/ml)
*MW = molecular weight **MIC = minimum inhibitory concentration for *Mycobacterium tuberculosis*		

3.2 Materials

Human serum albumin (HSA) (low endotoxin, fatty acid free) was purchased from Sigma-Aldrich (Dorset, UK). Sodium chloride was obtained from Scientific Laboratory Supplies Ltd (Nottingham, UK). Phosphate buffered saline (PBS) tablets were obtained from Oxoid Ltd (UK). Ethanol, sodium hydroxide, glutaraldehyde, dichloromethane and dimethyl sulfoxide (DMSO) were obtained from Sigma-Aldrich (Dorset, UK). Benzothiazinone compounds (IR 20, IF 274, FG 2, and AR 112) were synthesised by Adrian Richter and Peter Imming (University of Halle, Germany).

3.3 Methods

3.3.1 UV analysis of benzothiazinone compounds

UV calibration curves were prepared for all four BTZ compounds and establishment of the limit of detection and quantification of compounds were carried out in DMSO using UV spectrophotometry. To determine the absorbance maximum of each compound, a solution of each drug in DMSO (22 µg/mL, 7.5 µg/mL, 6 µg/mL and 2 µg/mL for IR 20, IF 274, FG 2 and AR 112 respectively) was prepared and scanned over wavelengths from 200-800 nm using the Perkin Elmer Lambda 2 UV/Vis spectrophotometer and a quartz cuvette (High precision cell, Hellma Analytics). A peak at 347 nm was determined as a suitable wavelength for detection of all four drugs. A calibration curve of each compound in DMSO was prepared by using a serial dilution (1 in 2 dilutions) within the range 100-0.78125 µg/mL and taking a single absorbance value at 347 nm until readings within the range 1.0 to 0.1 were obtained. The linearity of the calibration plots were evaluated using least square regression analysis. LOD was calculated using the following formula:

Equation 3.1: $$LOD = 3.3\frac{\sigma}{S}$$

while LOQ was calculated using the formula:

Equation 3.2: $$LOQ = 10\frac{\sigma}{S}$$

Where σ = standard deviation and S = slope.

Three calibration curves were run on a single day to determine the intra-day sample variance. Inter-day sample variance was determined using data from three different days. Precision was calculated according to the following equation:

Equation 3.3: $$Precision = \left(\frac{SD}{mean}\right) x\ 100$$

3.3.2 Determination of Benzothiazinone-albumin interactions by solubilisation

Stock solutions of HSA (fatty acid-free, Sigma-Aldrich, Germany) in water and Tris buffer respectively (50 mg/mL) were prepared. Negative controls consisted of water and Tris buffer without HSA. HSA solutions and negative controls (1 mL) were added to separate vials containing 0.5 mg BTZ compound and incubated at 37°C for a total of six days. Samples of the supernatant (i.e. the wash product obtained upon purification of nanoparticles) were removed at pre-determined time points and UV absorbance readings were taken at 347 nm. The amount of drug dissolved by each solution was determined from the calibration curve and calculated as a percentage of the original drug content.

A further experiment was carried out with a modified design, which involved dissolving the BTZ (0.5mg) first in a volatile solvent (dichloromethane), adding the BTZ solution to a glass vial and evaporating the solvent to form a thin film of drug prior to incubation with HSA. This was implemented as a means of increasing the rate of solubilisation by increasing the surface area of drug available. This theory is characterised by the Noyes-Whitney equation:

Equation 3.4

$$\frac{dM}{dt} = \frac{DS}{h}(Cs - Cb)$$

Where M is the amount of drug dissolved in time t, D is the diffusion coefficient of the drug, S is the surface area of drug, h is the thickness of the diffusion layer, C_s is the saturation solubility of the drug and C_b is the concentration of drug in the bulk medium. Inspection of the equation reveals an increase in surface area increases dissolution rate. Although the aim here is not strictly dissolution as such, the principles still apply to the solubilisation of drug by albumin as is trying to be achieved here. The same experiment was carried out by incubating the BTZs in Tris buffer without HSA.

3.3.3 Drug-binding studies to Sudlow's site I via tryptophan quenching

BTZ binding to the albumin drug binding site I (or Sudlow's site I), i.e. the hydrophobic pocket, was assessed through tryptophan quenching studies (Abou-Zied & Al-Lawatia

2011). HSA solution (1 mL, 1 μM) was prepared in 1:1 saline (25 mM) and Tris buffer (25 mM, pH 7.4). Stock solutions (1 mL, 500 μM) of BTZ compounds, ibuprofen (negative control) and bilirubin (positive control) were prepared in DMSO. The emission spectrum of HSA tryptophan fluorescence was measured between 300 nm to 400 nm with an excitation wavelength of 285 nm and an emission slit of 10 nm using a Perkin Elmer LS 50B Fluorescence spectrometer and a quartz cuvette (Hellma Analytics). Initial fluorescence readings were taken for the HSA solution, followed by subsequent readings after sequential additions of 1 μL of drug in DMSO. The maximum emission value (arbitrary units) of tryptophan fluorescence for each titration was divided by the emission value of HSA solution and results were presented as the percentage of tryptophan quenching versus drug concentration.

3.3.4 Benzothiazinone-loaded albumin nanoparticle manufacture via pre-loading method

BTZ-loaded albumin nanoparticles were manufactured using a modified desolvation method (Weber, Kreuter, et al. 2000). HSA solution (1 mL, 50 mg/mL) was incubated with 0.5 mg of BTZ compound for 24 hours at room temperature in a glass vial (vial I). Following incubation, the BTZ-saturated HSA solution (1 mL) was removed from vial I and placed in a clean vial (vial II). After the addition of 25 μL NaOH (1M), 4.0 mL of ethanol was added drop wise to the stirred protein solution. Nanoparticles were cross-linked by addition of 47.2 μL 5% glutaraldehyde in water, stirred overnight to remove ethanol, and then purified using at least 4 cycles of spin-filtration (30 kDa MWCO) into saline (0.9%) solution. The washing fluid was collected for BTZ quantification (vial III). HSA nanoparticles without drug were prepared as controls.

The BTZ content in vials I-III was quantified by UV spectroscopy and expressed as a percentage of the original drug content (~0.5 mg). The mass balance of the drug was calculated from the process to determine the drug recovery from the experiment.

Encapsulation efficiency (EE) and drug recovery were calculated according to Equation 3.5 and Equation 3.6:

Equation 3.5:

$$EE\ (\%) = \frac{w_1}{w_0} x\ 100$$

Equation 3.6

$$Drug\ recovery\ (\%) = \frac{w_1 + w_2 + w_3}{w_0} x\ 100$$

Where W_0 is the mass of initial drug introduced in the nanoparticle manufacture process, w_1 is mass of drug in purified nanoparticles, w_2 is mass of drug in washing fluid and w_3 is mass of residual drug.

3.3.5 Benzothiazinone-loaded albumin nanoparticle manufacture via *in-situ* loading

BTZ compound (0.5 mg) was weighed in a glass vial (vial I) and dissolved in dichloromethane and ethanol (1:10, 4.4 mL). HSA solution in Tris buffer (1 mL, 50 mg/mL) was prepared in a glass vial (vial II). After the addition of 25 µL NaOH (1M) to the HSA solution, the BTZ mixture was added drop wise to the stirred protein solution. Nanoparticles were then cross-linked and purified in the same manner as described above. The washing fluid was collected for BTZ quantification (vial III). BTZ content in vials I-III was quantified and mass balance was calculated as described above for Method I.

3.3.6 Physicochemical characterisation of nanoparticle suspensions

The size, zeta potential and physical stability of nanoparticle suspensions were determined as described in Chapter 2.

3.3.7 Benzothiazinone extraction from albumin formulations

BTZ was extracted from nanoparticle suspensions using an optimised organic phase extraction method using dichloromethane. Zinc sulphate (850 µL, 0.1M) and ammonia solution (200 µL, 10%) were added to 1mL of nanoparticle suspension (50 mg/mL). Dichloromethane (5mL) was added to the mixture and sonicated in a water bath for 20 minutes and left to stand for 60 minutes. Upon phase separation, the denser organic dichloromethane layer was carefully drip-separated from the aqueous buffer phase and

allowed to evaporate at room temperature overnight. This process was repeated two further times. The dried sample containing BTZ was dissolved in 1 mL DMSO and analysed by UV spectroscopy.

3.3.8 Benzothiazinone release studies

BTZ release profiles from selected nanoparticle systems were determined in phosphate-buffered saline (0.1 M, pH 7.4) supplemented with 10.8 mg/mL albumin at 37°C. The receiver fluid was supplemented with albumin to mimic the protein concentration in lung lining fluid (Bicer 2011). BTZ release was determined in the presence and absence of trypsin (0.1 mg/mL). This concentration was selected to match lung protease concentrations from the literature (Wilson 2005). Nanoparticle suspensions (10 mg/mL, 1 mL) were placed in dialysis tubing (Fischer, MWCO 10 kDa), and then the dialysis membranes were immersed in beakers containing 10 mL release buffer. The beakers were incubated at 37°C under gentle stirring (100 strokes/min) in a water bath (Grant Instruments, Cambridge, UK). The release buffer was withdrawn from the beaker and replaced with fresh release buffer at regular intervals to maintain sink conditions. The BTZ concentration in each collected release buffer sample was determined by UV spectroscopy. BTZs were extracted from the release buffer through organic phase partitioning. Dichloromethane (10 mL) was added to the medium, sonicated for 20 minutes and left to stand for 60 minutes. Upon phase separation, the denser organic dichloromethane layer was carefully drip-separated from the aqueous buffer phase and allowed to evaporate at room temperature overnight. This process was repeated two further times. The dried sample containing BTZ was dissolved in 1 mL DMSO and analysed by UV spectroscopy. Similarity factors (f2) comparing drug release profiles were calculated according to Equation 3.7, whereby f2 values between 50 - 100 represent less than 10% difference between released BTZ at each time point measured (i.e. similarity) and values <50 are considered dissimilar (Gómez-mantilla et al. 2013). The closer the f2-value is to 100, the more similar the curves.

Equation 3.7:

$$f2 = 50 \times \log\left\{\left[1 + \frac{1}{n}\sum_{t=1}^{n}(R_t - T_t)^2\right]^{-0.5} \times 100\right\}$$

R_t = BTZ concentration (%) in release buffer at time point *t*, Method I systems; T_t = BTZ concentration (%) in release buffer at time point *t*, Method II systems; *n* = number of time points.

3.3.9 Antimycobacterial activity assay in infected macrophages

These experiments were performed by collaborators Natalja Redinger and Ulrich Schaible of Forschungszentrum Borstel–Leibniz Lung Centre and the German Centre for Infection Research in Borstel. Murine bone marrow derived macrophages (mouse strain C57BL/6 J) were seeded at 1×10^5 cells in 48-well plates in culture medium [Dulbecco's modified eagle medium (DMEM) plus 10 % foetal bovine serum (FBS), 100 µg L-glutamine]. The cells were incubated with *M. tuberculosis* H37Rv (at 37°C, 5% CO_2) for two hours then washed with culture medium to remove the extracellular mycobacteria. The Multiplicity of Infection (MOI) was 2:1 (mycobacteria: macrophage). Albumin nanocarrier formulations containing BTZs were incubated for 72 h with infected macrophage cells at three concentration levels (final concentration 36, 3.6, and 1.1 µg/mL for IR 20 in DMSO, albumin and albumin nanoparticles respectively; and 4.1, 1.2, and 0.1 µg/mL for FG 2 in DMSO, albumin and albumin nanoparticles respectively; n=3 independent experiments). Vehicle controls were BTZ-free equivalent concentrations of DMSO (4, 2 and 1%), HSA solution (5.8, 0.6 and 0.2 mg/mL) or unloaded HSA nanoparticles (1.3, 0.1 and 0.04 mg/mL). The number of intracellular bacteria was determined by colony counts after osmotic lysis of the macrophages after t= 24, 48 and 72 hours incubation with the BTZ formulations.

3.3.10 Statistical analysis

Statistical calculations were carried out using the software SigmaPlot 14.0 for Windows (SyStat Software Inc., CA, USA). To identify statistically significant differences between particle size measurements and zeta potential, two-tailed Student t-tests were performed. To identify statistically significant differences for all other data, a two-way ANOVA was performed with a post Tukey-Kramer test. P values less than 0.05 were considered significant.

3.4 Results

3.4.1 UV analysis of benzothiazinone (BTZ) compounds

All BTZs were scanned over the UV range of the wavelength spectrum (Figure 3.1). The wavelength 347 nm was deemed as suitable wavelength for detection of all four BTZ compounds and calibration curves were constructed accordingly. Calibration curves for all four BTZ compounds (Figure 3.2) showed excellent linearity over the concentration range measured with R^2 values > 0.999. LOD and LOQ values for the four BTZ compounds are shown in Table 3.2. The average intra and inter-day variation for all BTZ compounds complied with the acceptance criteria proposed in analytical guidelines [Relative standard deviation (RSD) must not be greater than 2.0%] (European Medicines Agency 1995) (Table 3.3).

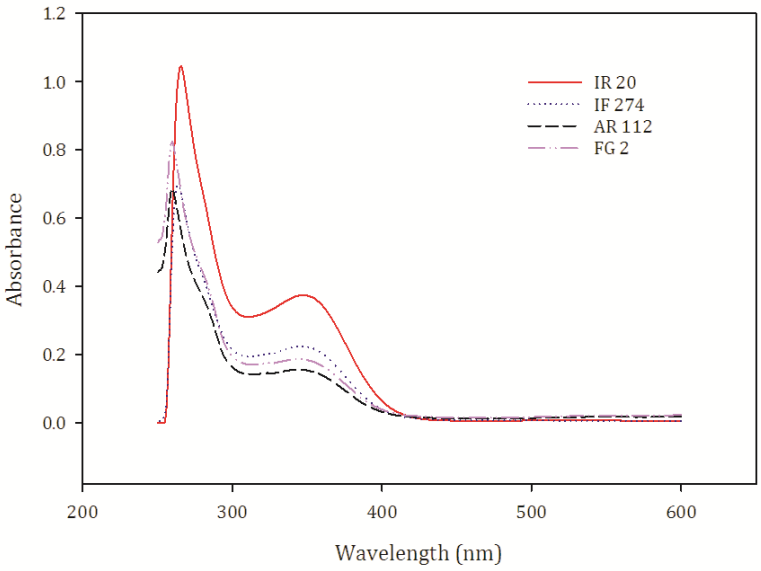

Figure 3.1 UV spectrum curves for benzothiazinone compounds in DMSO.

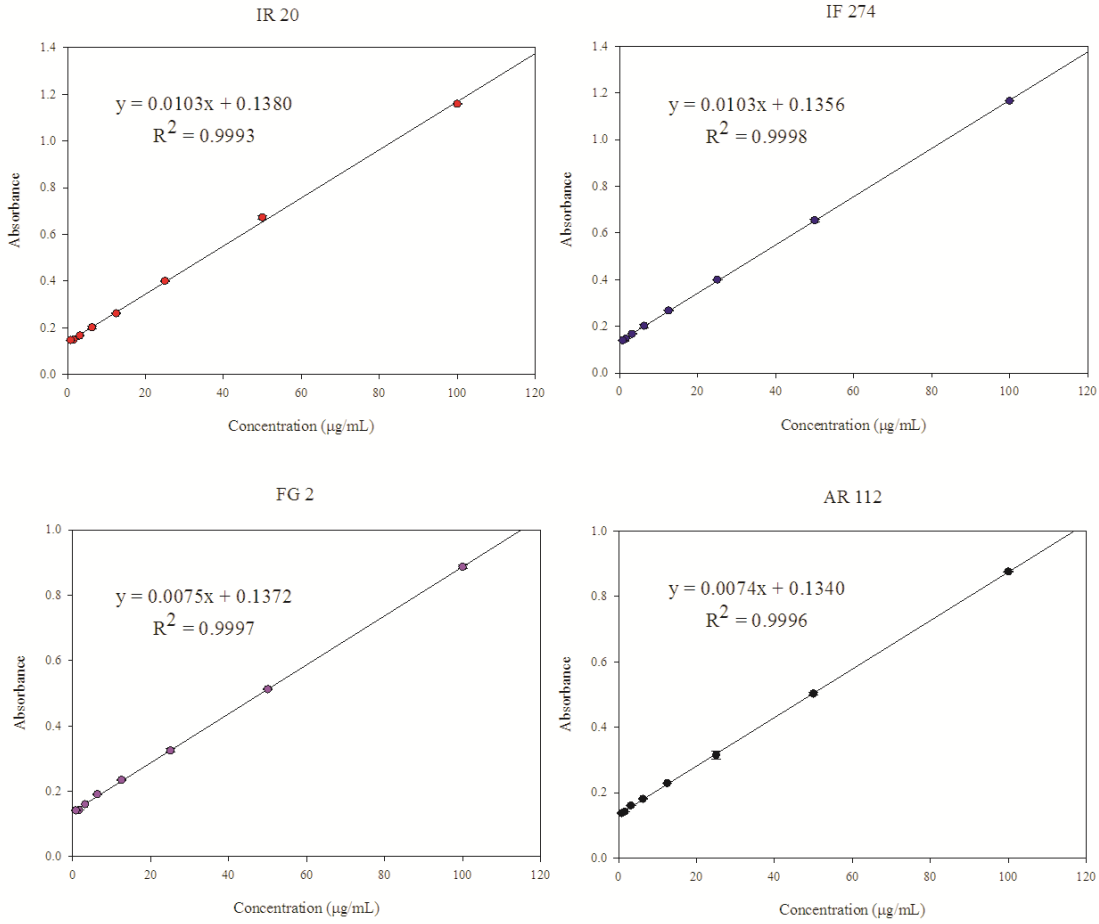

Figure 3.2 UV calibration curves for benzothiazinone (BTZ) compounds in DMSO. Results represent the mean and standard deviation of n = 3 experiments.

Table 3.2 Limits of detection (LOD) and limits of quantification (LOQ) (µg/mL) for benzothiazinone compounds.

Benzothiazinone compound	Limit of detection (LOD) (µg/mL)	Limit of quantification (LOQ) (µg/mL)
IR 20	1.37	4.16
IF 274	0.51	1.55
FG 2	2.58	7.82
AR 112	1.19	3.59

Table 3.3 Intra-day and inter-day variation in benzothiazinone (BTZ) absorbance as a function of concentration in DMSO. Intra-day variation data obtained from three days using the same standards (n=3). Inter-day variation data obtained over three days (n=9)

Concentration (µg/mL)	Coefficient of variation (%)							
	IR 20		IF 274		FG 2		AR 112	
	intraday	interday	Intraday	Interday	intraday	Interday	Intraday	interday
100	0.086281	3.190398	0.04953	0.735506	0.621388	1.123596	0.114155	0.540299
50	0.955763	4.558028	0.809098	2.268602	0.390625	2.253564	0.91886	0.9781
25	0.498753	1.589058	0.144458	1.578339	1.5822	1.714902	3.952205	3.125
12.5	0.584512	2.651141	0.749064	3.971806	0.24638	4.418861	0.252486	3.204598
6.25	2.157871	3.172254	3.569853	1.665433	0.605612	4.014687	0.319567	2.039105
3.125	0.347104	2.172019	1.197605	2.146161	0	1.547097	0.360094	2.453988
1.5625	0.388352	2.599043	0.391867	2.041236	0.405633	1.432339	0.408503	1.055893
0.78125	0.391867	2.141391	0.413377	1.428571	1.63401	1.078253	0.729927	0.724638

3.4.2 Benzothiazinone-albumin solubilisation

The temporal profile of BTZ solubilisation by HSA was initially assessed over a six-day period (Figure 3.3A). The solubility profile of the compounds in Tris and HSA solutions was assessed to determine whether drug solubilisation by albumin can occur in a buffer solution at pH 8.9, as used to generate albumin nanoparticles. Absorbance values of AR 112 were negative at all albumin concentrations tested, indicating that the amount of AR 112 dissolved in HSA was undetectable using this method.

Only one of the BTZ compounds (IR 20) was found to be soluble in tris buffer (IR 20). Originally, IR 20 was found to have a solubilisation of 2.7 ± 0.5% which corresponds to 0.25 μg drug (data not shown).

47.0 ± 1.0% IR20 was dissolved by albumin over the six-day period resulting in an approximate drug loading of 0.5% (w/w), while only 8.4 ± 0.8% and 4.5 ± 0.8% IF274 and FG2 respectively was solubilised under the same conditions, corresponding to a drug loading of 0.08% and 0.05% respectively. For IR 20, significant differences were observed between solubilisation in HSA vs Tris only from time point t = 1 day onwards. For IF 274, significant differences were observed in the extent of solubilisation in HSA vs Tris only from time point t = four days onwards. The extent of solubilisation of the most soluble BTZ compound IR 20, the poorer solubilisation of IF 274 & FG 2 and the non-detection of AR 112 suggest poor solubility needs to be overcome in order to maximise interactions between the BTZs and albumin.

To overcome the poor solubilisation profile of the BTZ compounds tested a modified approach to the experiment was carried out using a film-forming approach (Figure 3.3B). Upon using the optimised film-forming method, the solubilisation of IR 20 increased to 7.8 ± 0.1%. No solubilisation in Tris buffer was detected for the remaining three BTZ compounds. The extent of solubilisation by HSA of IR20 and IF274 increased to 55.6 ±

0.6% and 39.0 ± 4.9% respectively. FG 2 solubilisation also increased to 26.1 ± 3.8%. AR 112 solubilisation was detectable at 10.1 ± 0.4%. These values correspond to the drug loading capacities shown in Table 3.4. It also took 1-3 days to reach maximum solubilisation as opposed to the original method where it took up to six days. Statistically significant differences were observed for IR 20, IF 274 & FG 2 compared to the control for time points t = 1 day onwards. No statistically significant differences were observed for solubilisation after t = 1 for all BTZ compounds compared to further time points. Hence it was deduced incubation for 24 hours is sufficient to allow maximal BTZ solubilisation by albumin.

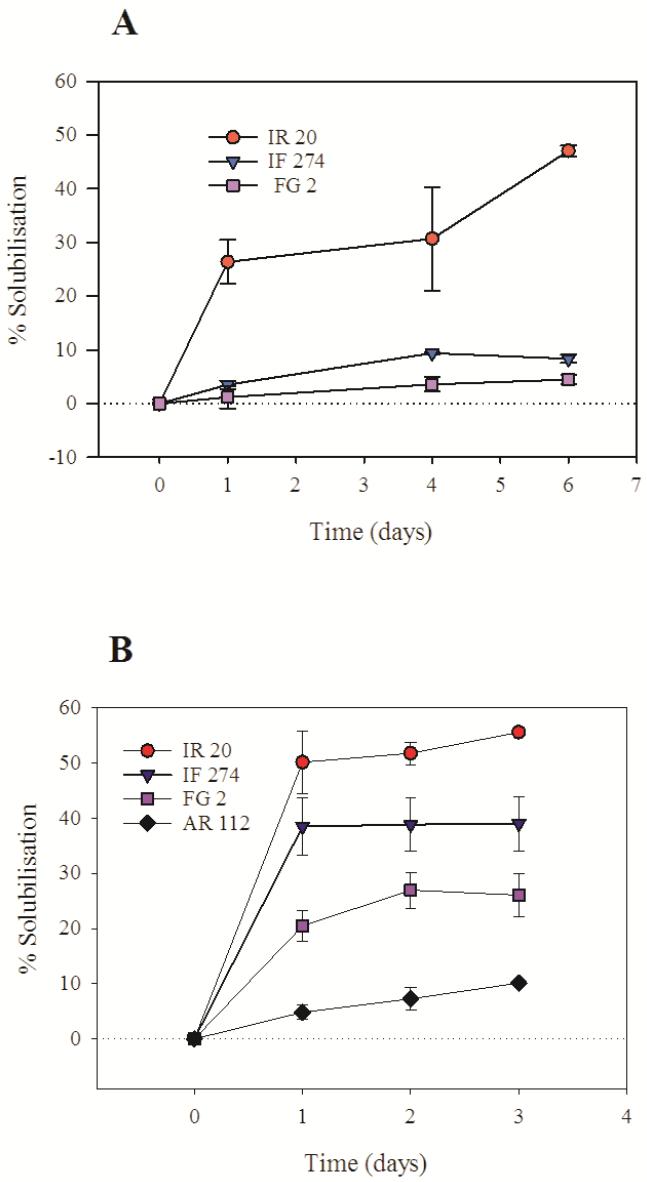

Figure 3.3 Time dependent solubilisation profiles of BTZ compounds(500 µg) in 1 mL HSA in tris buffer pH 8.9 (50 mg/mL) by (A) original method and (B) film-forming method. Results are expressed as a percentage of the original mass (500 µg) at t=0. Results reported are from n=3 experiments.

Table 3.4 Solubilisation of BTZ compounds with HSA reported as mass ratios. Values reported are the mean and standard deviation from n = 3 experiments.

Drug	**BTZ (µg) per HSA (mg)**	**Solubilisation (% w/w)**
IR 20	56 ± 0.6	5.6
IF 274	39.5 ± 4.9	4.0
FG 2	26.1 ± 3.8	2.6
AR 112	10.1 ± 0.4	1.0

A further experiment was carried out using a micronised form of IR 20 (particle size ~5-10 μm) to compare with the original non-micronized IR 20 to see whether a further increase in the extent of solubilisation by HSA would occur. In this case, there was no significant difference observed between milled and non-milled IR 20 in the degree of solubilisation by HSA (Figure 3.4).

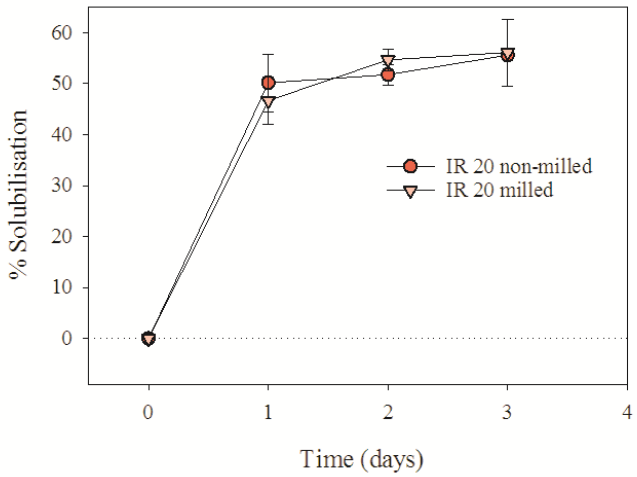

Figure 3.4 Solubilisation profiles of IR 20 Vs IR 20 (milled) using a film-forming approach in 1mL HSA in tris buffer pH 8.9 (50 mg/mL). Results are expressed as a percentage of the original mass (500 μg) at t=0. Results reported are from n=3 experiments.

3.4.3 Benzothiazinone binding to Sudlow's site I

Drug interactions with the two principal binding sites of HSA, i.e. site I in subdomain IIA and site 2 in subdomain IIIA are considered the major factors in determining the ratio of free, active drug concentration versus the protein-bound reservoir (Zsila et al. 2011). Thus, characterisation of drug binding to these sites may determine the effectiveness of HSA as a drug carrier. Sudlow's site I is a hydrophobic pocket which contains a tryptophan residue (Trp- 214), which contributes to the intrinsic fluorescence of albumin. Drug binding reduces the intrinsic fluorescence of this tryptophan and can be used to characterise drug binding to site I. Compared with ibuprofen, which does not bind to site I, and bilirubin, which shows a strong affinity to site I (Sudlow et al. 1975), the four BTZ compounds showed moderate affinity to the hydrophobic binding pocket of albumin with

a rank order of: ibuprofen < IR 20 = IF 274 < FG 2 < AR 112 << bilirubin (Figure 3.5). Based on these data, it may be inferred that all BTZ compounds studied had a weak affinity for site I.

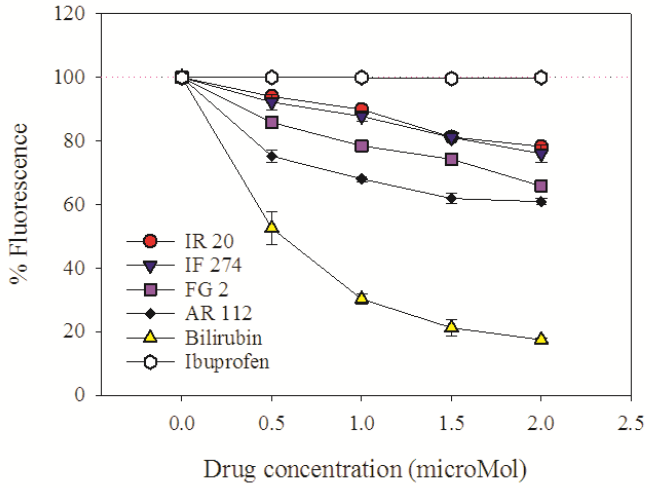

Figure 3.5 Quenching of tryptophan fluorescence indicating the affinity of BTZ binding to Sudlow's site I of HSA. Ibuprofen and bilirubin have been included as negative and positive controls, respectively. Data represent mean and standard deviation; n=3 experiments.

3.4.4 Benzothiazinone extraction optimisation

To validate the quantification method and "track" the fate of the BTZ in solubilisation and nanoparticle manufacture processes, extraction of the BTZ was carried out. IR 20 was initially extracted from Tris buffer. The solution was prepared by incubating IR 20 (0.5mg) with 1mL Tris buffer (pH 8.9) for 24 hours, centrifuging the sample for (Heraeus microfuge® pico, DJB Labcare, UK) at 2000 revolutions per minute (RPM) for two minutes and removing the supernatant. Extraction was then attempted with the sample. The residual drug left behind in glassware was also quantified. UV spectroscopy was used to calculate how much IR 20 was solubilised by Tris as described earlier. Figure 3.6 shows IR 20 recovery from Tris solution in two different conditions: initially by extraction with the addition of 2ml dichloromethane and (A) vortexing the mixture for 30 seconds, compared to (B) sonicating the mixture for 20 minutes. In both instances the extraction procedure was repeated once. By vortexing, 3.9 ± 0.9% was extracted from the sample, compared to the expected 9%. Unextracted sample was still detectable from the IR 20 in Tris solution. Upon employing sonication, the expected 9% IR 20 was extracted from the sample and IR

20 was unable to be detected from the solution. Total mass balance was 75 ± 0.9% and 79 ± 0.9% for (A) and (B) respectively. Following these findings, sonication was employed for all further extraction procedures.

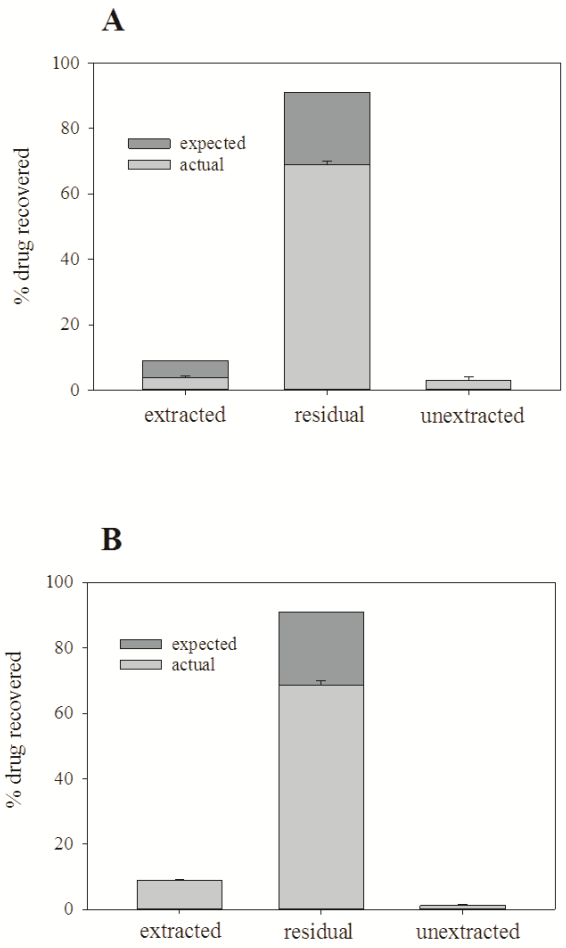

Figure 3.6 Recovery of BTZ compound IR 20 from tris buffer (1mL; pH 8.9) with dichloromethane (2mL) by (A) vortexing for 30 seconds vs (B) sonication for 20 minutes. Two rounds of extraction were carried out for both. Expected recovery (%) of IR 20 was determined as the proportion of drug solubilised by Tris (determined by UV analysis). The remaining fraction expected to be recovered was the "residual" fraction i.e. drug left behind in glassware. "unextracted" refers to drug not extracted from the solution. Data represent mean and standard deviation of n = 3-5 experiments.

Upon successful extraction of BTZ from Tris solution, extraction was carried out from IR 20 in HSA solution using the same method (Figure 3.7A). 42.0 ± 4.0% IR 20 was extracted from the solution, compared to the expected 64%. The experiment was repeated by carrying out three rounds of extraction, as opposed to the original two (Figure 3.7B). This

slightly increased the amount of IR 20 extracted from the solution to 47 ± 0.5%. Total mass balance was 61% ± 3% and 72 ± 3% for (A) and (B) respectively.

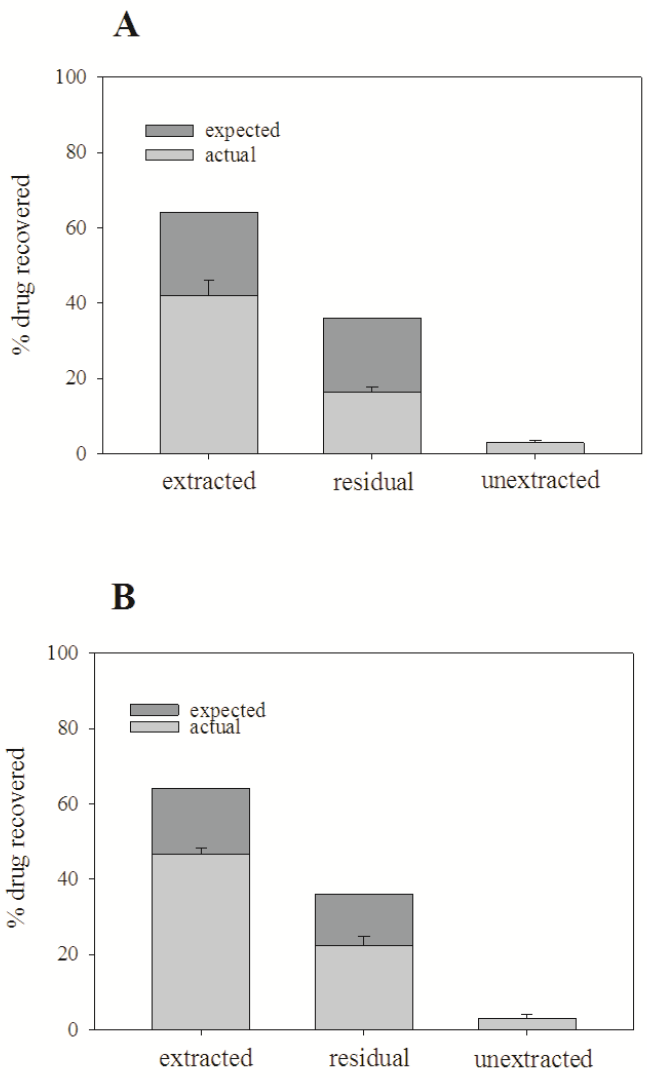

Figure 3.7 Recovery of BTZ compound IR 20 from albumin solution in tris buffer (1mL; pH 8.9) with dichloromethane (2mL) by (A) sonication for 20 minutes with two round of extraction vs (B) three rounds of extraction. Expected recovery (%) of IR 20 was determined as the proportion of drug solubilised by HSA (determined by UV analysis). The remaining fraction expected to be recovered was the "residual" fraction i.e. drug left behind in glassware. "unextracted" refers to drug not extracted from the solution. Data represent mean and standard deviation of n = 3-5 experiments.

To optimise the extraction further, zinc sulphate (0.1M) and ammonia solution (10%) was added to the IR 20 HSA solution prior to extraction with dichloromethane. This method comes from drug extraction from human serum (Bouzas et al. 2009). Upon employing this added step, 57.7% of IR 20 was extracted from the HSA solution, (from a theoretical 62%) (Figure 1.8A). This sufficiently optimised extraction procedure was carried out for the

other three BTZs (IF 274, FG 22 and AR 112) in HSA solution. Sufficient levels of BTZ (> 90% of the expected values) were extracted from these solutions with little to no BTZ being quantified as unextracted (Figure 1.8B-D). Mass balances for IF 274, FG 2 and AR 112 were 68% ± 0.6, 61% ± 1, 74% ± 1 and 97% ± 2. Residual fractions of BTZs were difficult to quantify as drug loss occurred during processing (i.e. with pipette tips, vials etc.).

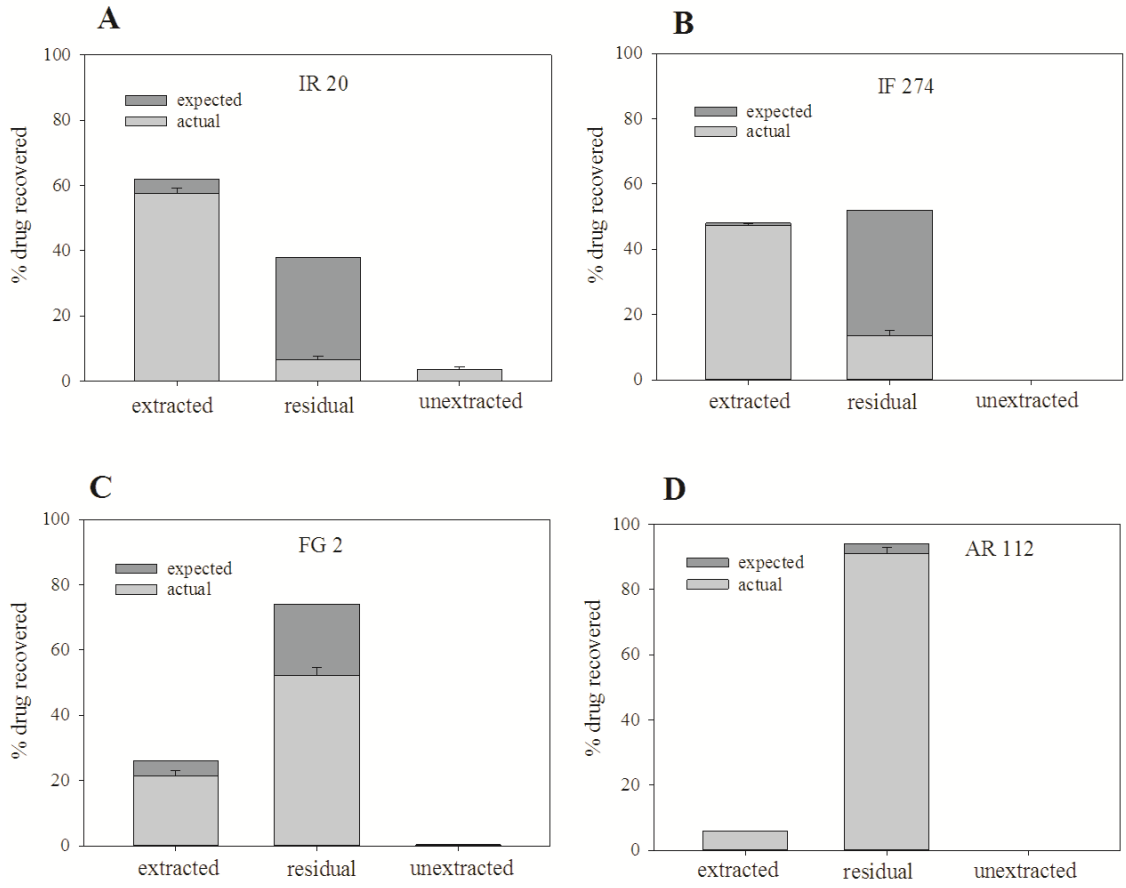

Figure 3.8 Recovery of all four BTZ compounds (A-D; IR 20, IF 274, FG 2 and AR 112 respectively) from albumin solution in tris buffer pH 8.9 with zinc sulphate (0.1M) and ammonia solution (10%) and dichloromethane (2mL), with three rounds of extraction. Expected recovery (%) of IR 20 was determined as the proportion of drug solubilised by HSA (determined by UV analysis). The remaining fraction expected to be recovered was the "residual" fraction i.e. drug left behind in glassware. "unextracted" refers to drug not extracted from the solution. Data represent mean and standard deviation of n = 3-5 experiments.

Finally, the extraction was carried out with IR 20-loaded albumin nanoparticles (Figure 3.9A). Despite 10.2% IR 20 washing off the nanoparticles with the supernatant fraction, only 36.3% of IR 20 was extracted from the nanoparticles, with 15% of drug being

unaccounted for. Thus, the amount of dichloromethane used for each round of extraction was increased from 2 to 5ml. This increased the IR 20 extraction to 45.5%, and majority of the drug was accounted for. Total mass balances for (A) and (B) were 72 ± 3% and 82 ± 1% respectively. The optimised method carried forward for all future extraction work was therefore carried out with following conditions: 3 rounds of extractions by sonication for 20 minutes with 5mL dichloromethane, zinc sulphate solution and ammonia solution.

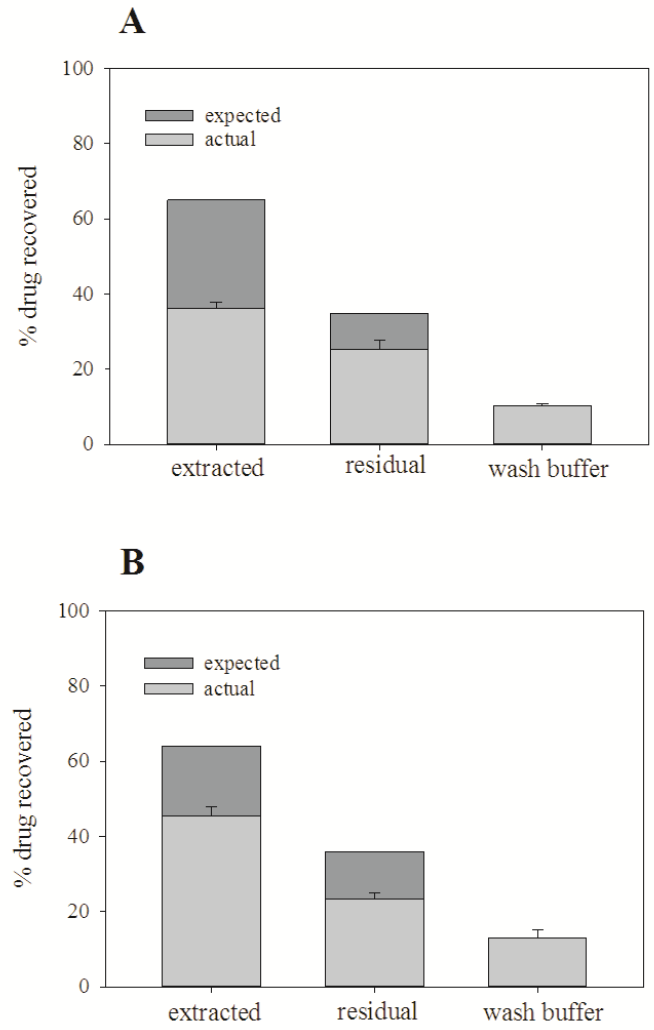

Figure 3.9 Recovery of BTZ compound IR 20 from albumin nanoparticle suspensions (1mL) by three rounds of extraction with zinc sulphate (0.1M) and ammonia solution (10%) using (A) 2mL dichloromethane vs (B) 5mL dichloromethane. Expected recovery (%) IR 20 from pre-loaded nanoparticles was determined as the proportion of drug solubilised by albumin (determined by UV analysis) and hence introduced into the manufacturing process. The remaining fraction was expected to be recovered from the "residual" fraction i.e. drug left behind in glassware. "wash buffer" refers to the wash obtained during the purification of nanoparticles. Data represent mean and standard deviation of n = 3-5 particle preparations.

3.4.5 Benzothiazinone-loaded albumin nanoparticle manufacture: pre-loading (method I) and *in-situ* loading (method II)

BTZ-loaded HSA nanoparticles were prepared using two different modifications of a reported desolvation method (Weber, Kreuter, et al. 2000): Method I (Figure 3.10), in which the HSA was incubated with BTZ compounds prior to nanoparticle formation and Method II (Figure 3.12), in which the BTZ was dissolved in dichloromethane and added to the HSA during the precipitation step. Drug encapsulation efficiencies were significantly higher with Method II (Figure 3.13) in all cases except for IR 20, which showed similar BTZ encapsulation regardless of the manufacturing method (Table 3.5). The amount of albumin was measured gravimetrically for each sample.

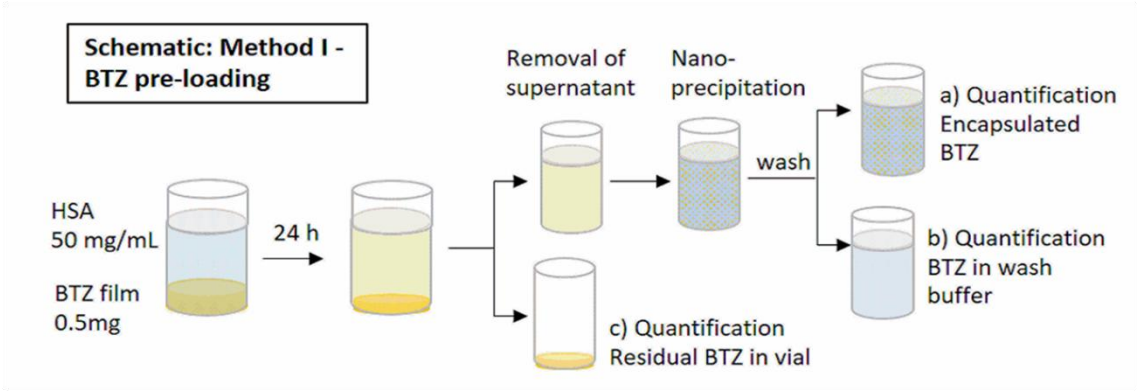

Figure 3.10 Schematic of production of BTZ-loaded albumin nanoparticles via a pre-loading method (method I)

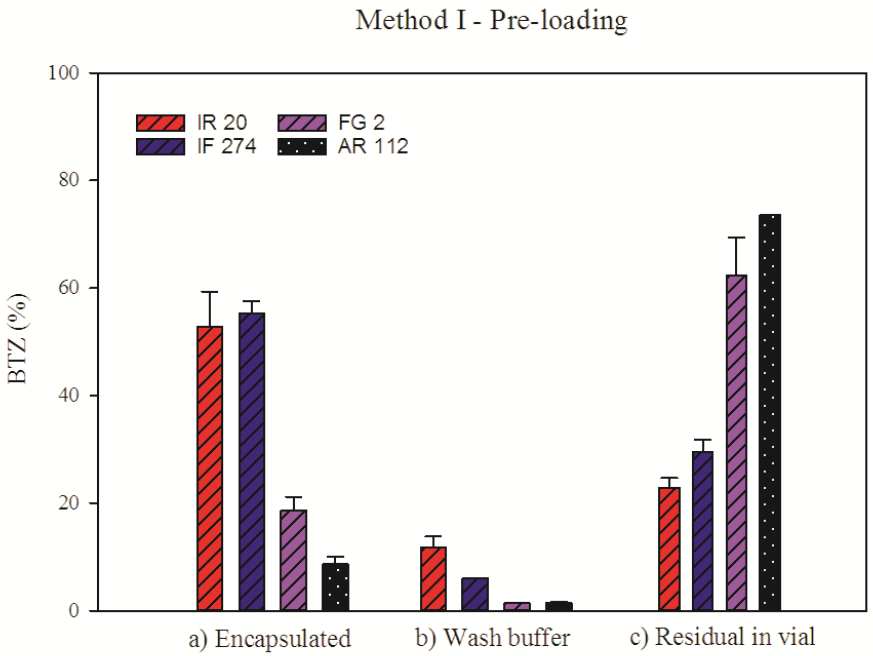

Figure 3.11 BTZ encapsulation efficiency (a) for nanoparticles manufactured via a pre-loading method (method I). BTZ encapsulation efficiency is compared to drug found in wash buffer (b) and residual drug left behind in glassware (c). Data represent the mean and standard deviation of n = 3 nanoparticle batches.

Table 3.5 Comparison of encapsulation efficiencies (%) between manufacturing methods I and II. Data represent the mean ± standard deviation of n=3 nanoparticle batches. Asterisk denotes statistically significant difference between the two method (* P<0.05, ** P<0.01, *** P<0.001).

BTZ	Encapsulation efficiency (%)		Mean BTZ:HSA (µg/mg)	
	Method I	Method II	Method I	Method II
IR 20	53 ± 7	50 ± 3	5.3 ± 1	5.0 ± 0
IF 274	55 ± 2	60 ± 2*	5.5 ± 0	6.0 ± 0
FG 2	19 ± 3	53 ± 3***	1.9 ± 0	5.3 ± 0
AR 112	9 ± 2	37 ± 5***	0.9 ± 0	3.7 ± 1

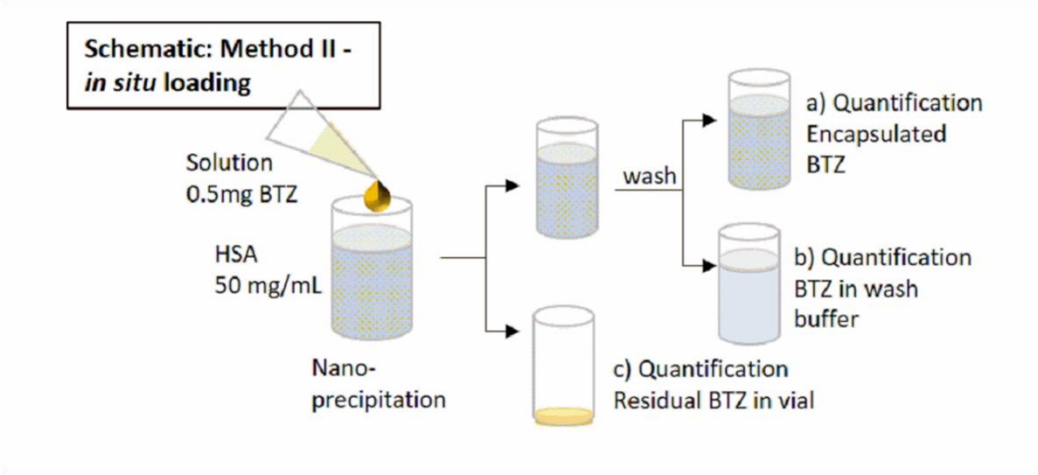

Figure 3.12 Schematic of production of BTZ-loaded albumin nanoparticles via an *in-situ*-loading method (method II)

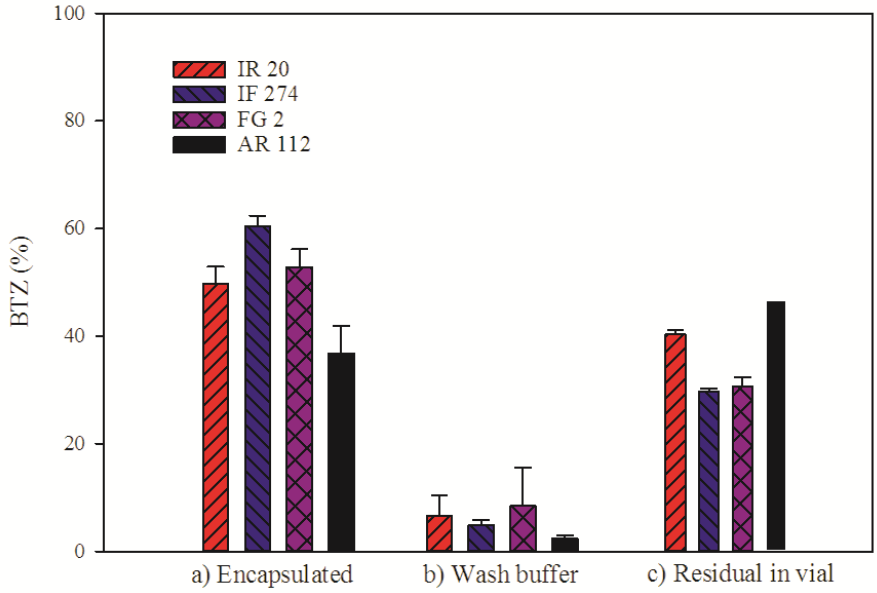

Figure 3.13 BTZ encapsulation efficiency (a) for nanoparticles manufactured via an *in-situ* method (method II). BTZ encapsulation efficiency is compared to drug found in wash buffer (b) and residual drug left behind in glassware (c). Data represent the mean and standard deviation of n = 3 nanoparticle batches.

Size distributions were unimodal with low polydispersity. Visually, nanoparticle suspensions varied slightly in colour (Figure 3.14), according to the colour of the BTZ compounds they contained. Nanoparticle size and zeta potential measurements were equivalent in nanoparticles with and without BTZ encapsulated (Table 3.6). No significant differences were observed between the particles produced by the two preparation methods.

Figure 3.14 Benzothiazinone-loaded albumin nanoparticle suspensions (from left to right): control, IR 20, IF 274, FG 2 and AR 112.

Table 3.6 Hydrodynamic diameters (nm) and zeta potential (mV) values of BTZ-loaded nanoparticles for method I and method II. Data represent the mean ± standard deviation of n=3 nanoparticle batches. These were not significantly different to blank albumin nanoparticles.

BTZ	Size (nm)		Zeta potential (mV)	
	Method I	Method II	Method I	Method II
IR 20	170 ± 11	179 ± 6	-26 ± 3	-31 ± 2
IF 274	168 ± 9	168 ± 6	-30 ± 2	-32 ± 2
FG 2	169 ± 5	178 ± 9	-31 ± 4	-29 ± 2
AR 112	175 ± 5	167 ± 9	-27 ± 2	-31 ± 3
Blank	174 ± 7	169 ± 7	-31 ± 3	-31 ± 3

3.4.6 Stability

Storage stability of BTZ-loaded albumin nanoparticle suspensions manufactured by both methods was assessed by measuring the size and polydispersity index of the suspensions at different time points after storage at 4°C and 25°C. Colloidal stability of the nanoparticle suspensions was maintained for up to six months at 4°C for both methods of manufacture (Figure 3.16 and Figure 3.18). No significant differences were observed between control

and BTZ-loaded albumin nanoparticle suspensions for all conditions tested. No differences were observed between BTZ formulations, nor between manufacturing methods. BTZ-loaded albumin nanoparticle suspensions remained stable at room temperature for up to one month, after which visual signs of aggregation were present (Figure 3.15 and Figure 3.17).

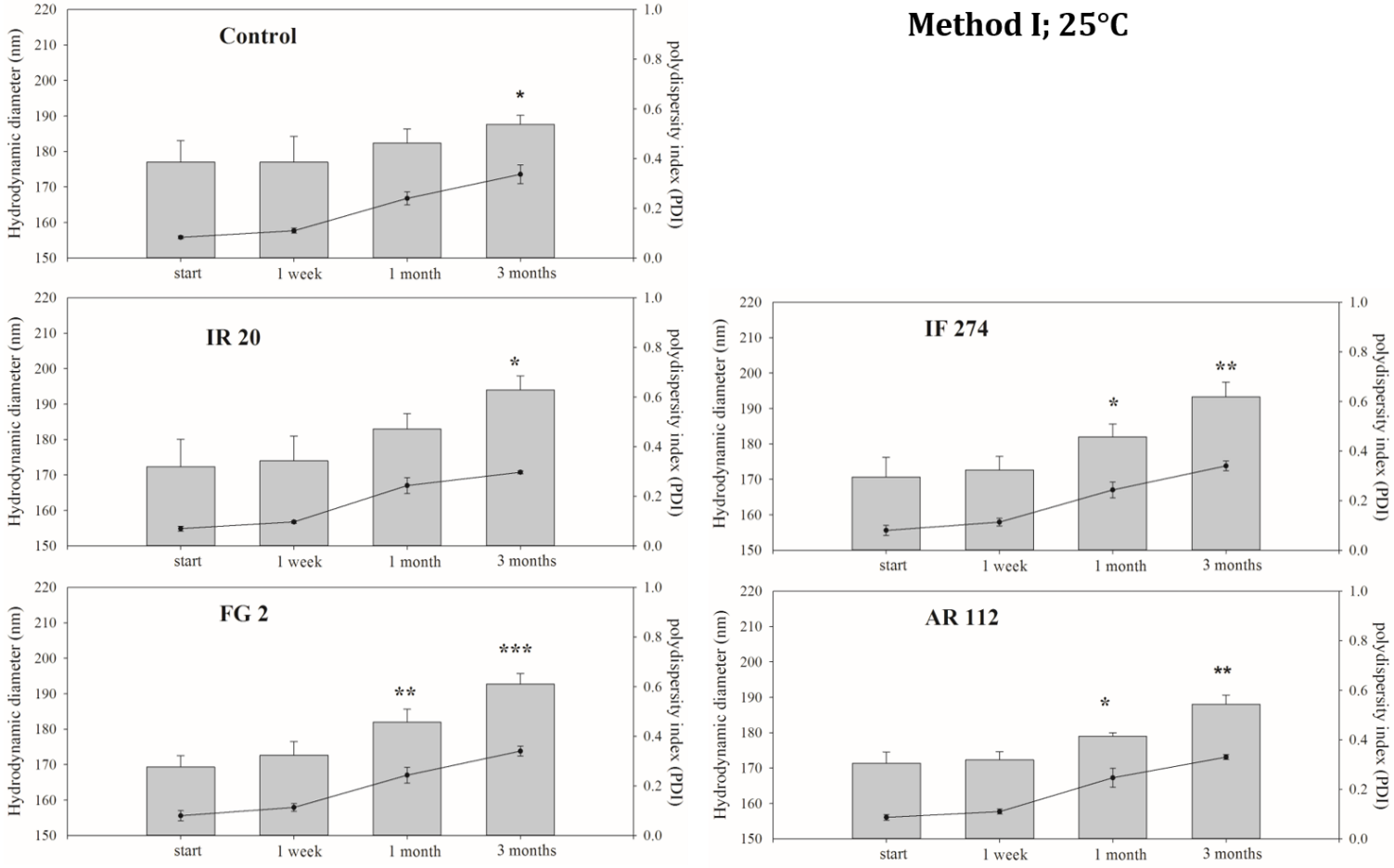

Figure 3.15 Influence of storage time at 25°C on particle size and polydispersity of benzothiazinone-loaded human serum albumin nanoparticles manufactured by method I. The bars depict the hydrodynamic diameter (nm, left side axis) of particles and the lines depict the polydispersity index (PDI, right-side axis). Error bars represent the standard deviation of 3 measurements. An asterisk (*, or **, or ***) depicts a statistically significant difference in particle size compared to the initial size ($p < 0.05$, 0.01 and 0.001, respectively).

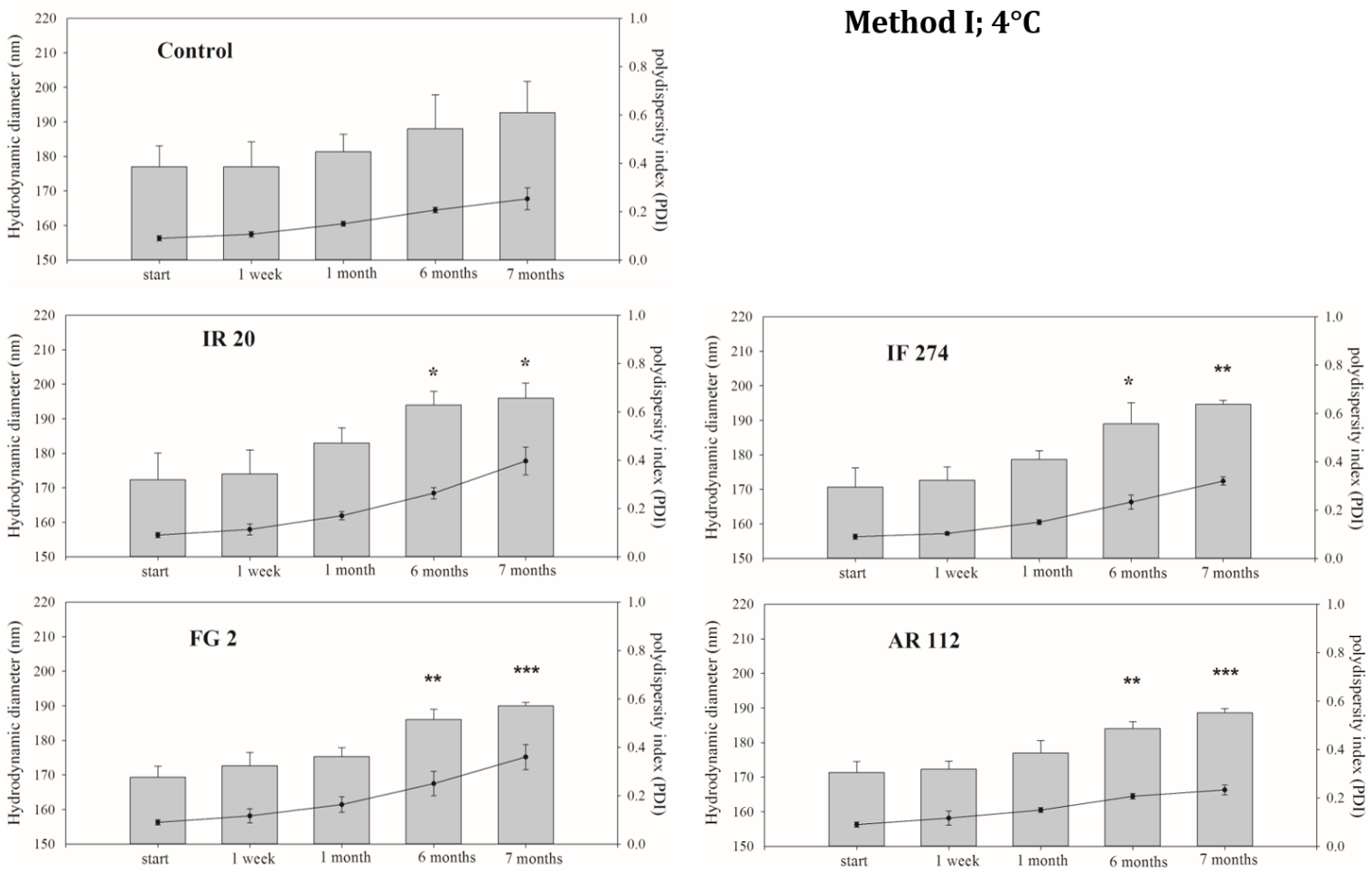

Figure 3.16 Influence of storage time at 4°C on particle size and polydispersity of benzothiazinone-loaded human serum albumin nanoparticles manufactured by method I. The bars depict the hydrodynamic diameter (nm, left side axis) of particles and the lines depict the polydispersity index (PDI, right-side axis). Error bars represent the standard deviation of 3 measurements. An asterisk (*, or **, or ***) depicts a statistically significant difference in particle size compared to the initial size ($p < 0.05$, 0.01 and 0.001, respectively).

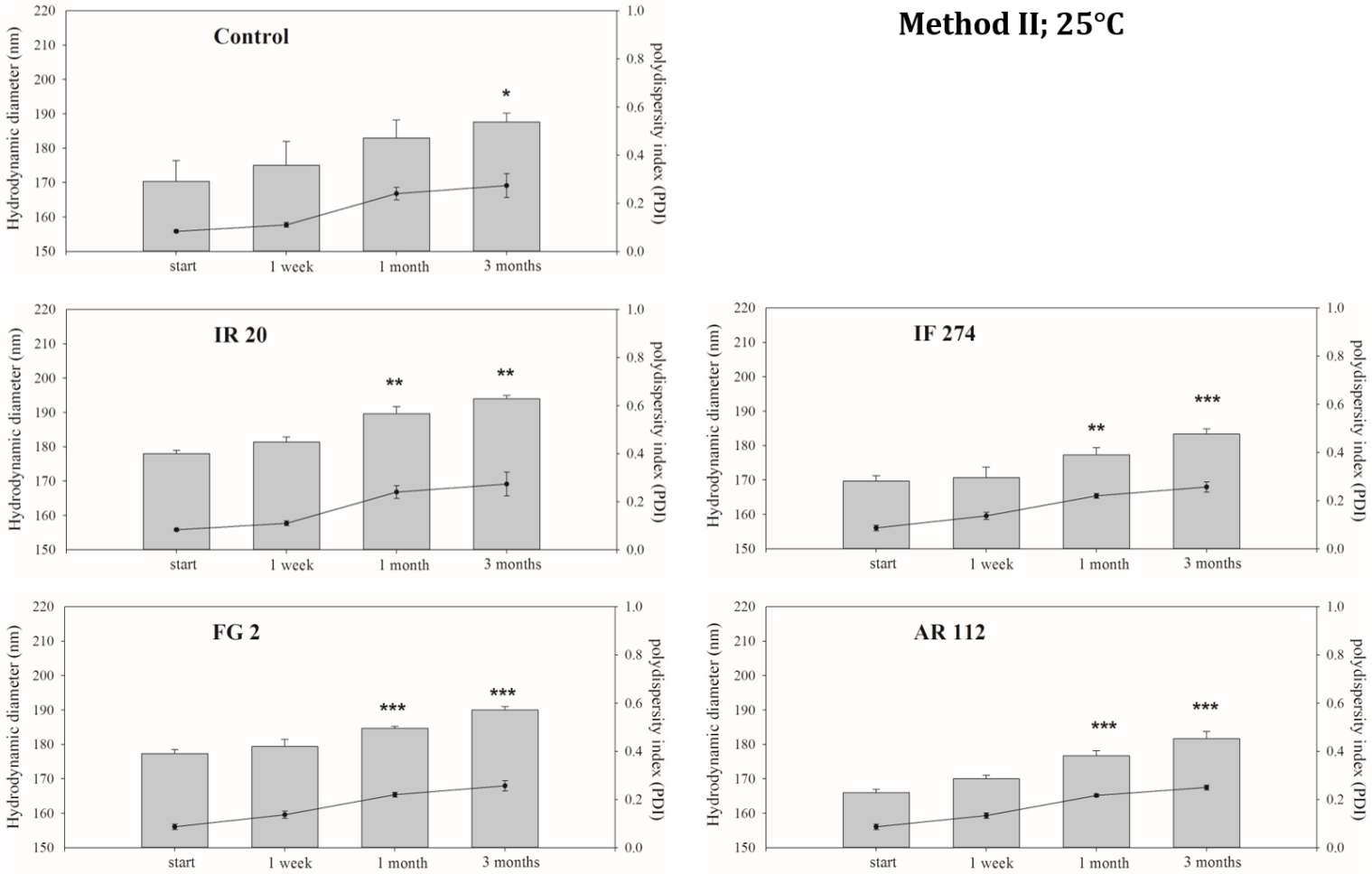

Figure 3.17 Influence of storage time at 25°C on particle size and polydispersity of benzothiazinone-loaded human serum albumin nanoparticles manufactured by method II. The bars depict the hydrodynamic diameter (nm, left side axis) of particles and the lines depict the polydispersity index (PDI, right-side axis). Error bars represent the standard deviation of 3 measurements. An asterisk (*, or **, or ***) depicts a statistically significant difference in particle size compared to the initial size ($p < 0.05$, 0.01 and 0.001, respectively).

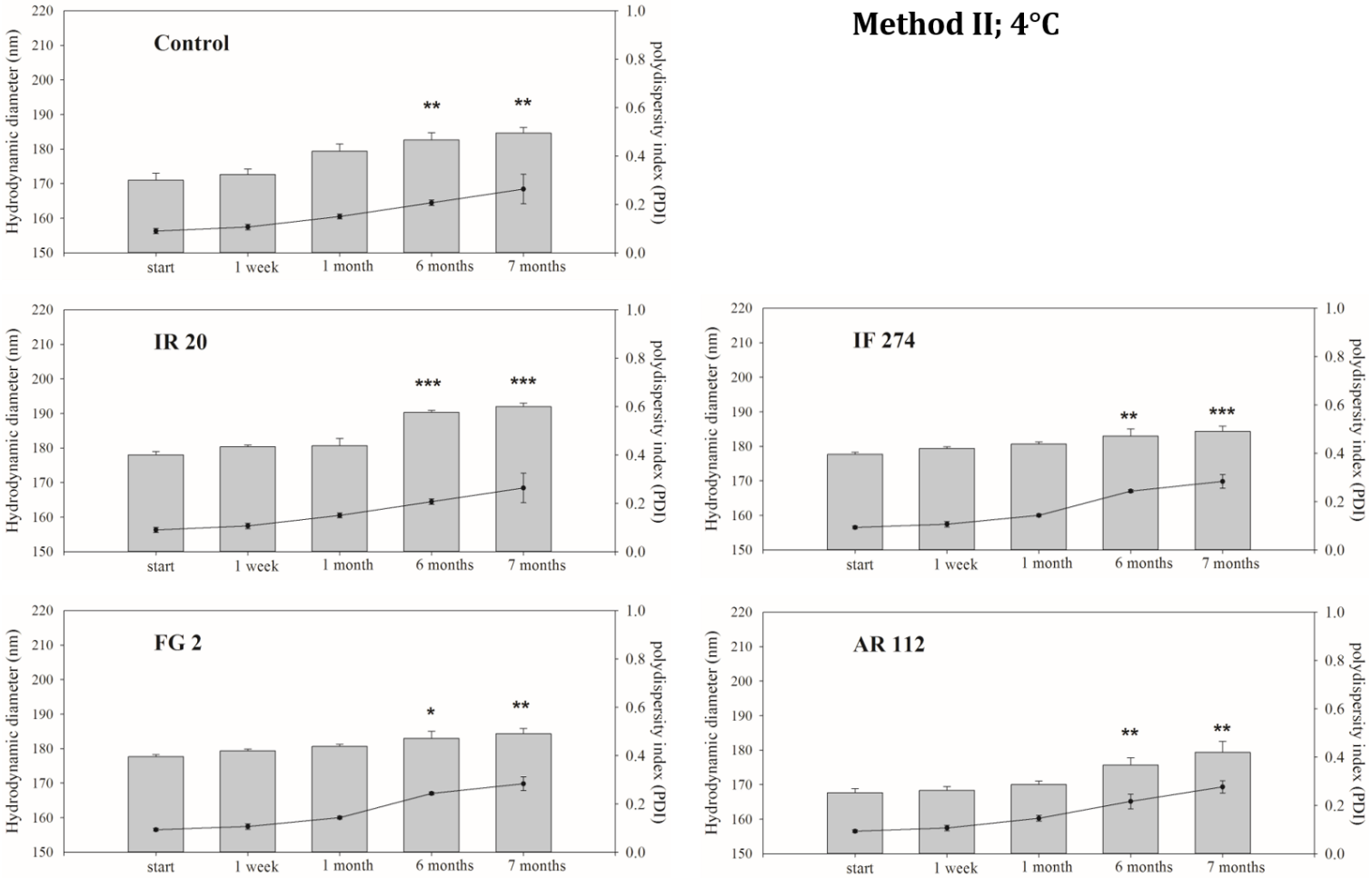

Figure 3.18 Influence of storage time at 4°C on particle size and polydispersity of benzothiazinone-loaded human serum albumin nanoparticles manufactured by method II. The bars depict the hydrodynamic diameter (nm, left side axis) of particles and the lines depict the polydispersity index (PDI, right-side axis. Error bars represent the standard deviation of 3 measurements. An asterisk (*, or **, or ***) depicts a statistically significant difference in particle size compared to the initial size ($p < 0.05$, 0.01 and 0.001, respectively).

3.4.7 Benzothiazinone release studies

BTZ release profiles from HSA nanoparticles prepared using both methods were performed over 48 h with and without the addition of 0.1 mg/mL trypsin (Figure 3.19). IR 20- and FG 2- loaded HSA nanoparticles were selected as representative BTZ formulations. In the absence of trypsin, BTZ release after 48 h was <10% and HSA nanoparticles prepared by Method I showed a marginal, but significantly higher cumulative BTZ release (%) at 48 h (Table 3.7). The presence of trypsin caused a rapid release of both BTZ compounds within the first 4 hours of incubation followed by a slower, steadier release rate over the subsequent incubation period. At the 48 h time point, ~88% and ~60% free IR 20 and FG 2 were released into the receiver medium. Due to the higher loading efficiency achieved with Method II, the mass of free FG 2 released was significantly higher for nanoparticles prepared by Method II compared to Method I (Table 3.7). Similarity factors (f2) were greater than 50 for all comparisons, indicating that the preparation method does not have a substantial influence on release rate. Dissolution modelling showed IR 20 release for both methods in the presence of trypsin followed Logistic model kinetics (R^2 = 0.988) whereas FG 2 release for both methods followed Weibull release kinetics (R^2 = 0.975).

Table 3.7 Comparison of cumulative percentage and mass of BTZ released from HSA nanoparticles prepared by Methods I and II over 48 h, both in the presence and absence of trypsin. f2 similarity factors >50 indicate that the compared release curves have on average <10% difference at each time point. Data represent the mean ± standard deviation of n=3 nanoparticle batches. * P<0.05, ** P<0.01, *** P<0.001 (comparison Method I vs II).

Trypsin (-)				Trypsin (+)			
	t = 48 h BTZ (%)	t = 48 h BTZ (µg)	f2 Similarity factor		t = 48 h BTZ (%)	t = 48 h BTZ (µg)	f2 Similarity factor
IR 20 (I)	7.5 ± 0.5***	4.0 ± 0.7***	79	IR 20 (I)	86.7 ± 3.1	45.7 ± 6.5	53
IR 20 (II)	4.0 ± 0.2	2.0 ± 0.1		IR 20 (II)	88.7 ± 5.5	44.0 ± 1.4***	
FG 2 (I)	4.1 ± 0.2***	0.8 ± 0.1	90	FG 2 (I)	60.7 ± 2.1	11.2 ± 1.2	81
FG 2 (II)	2.9 ± 0.2	1.5 ± 0.2***		FG 2 (II)	60.0 ± 5.3	31.8 ± 4.3***	

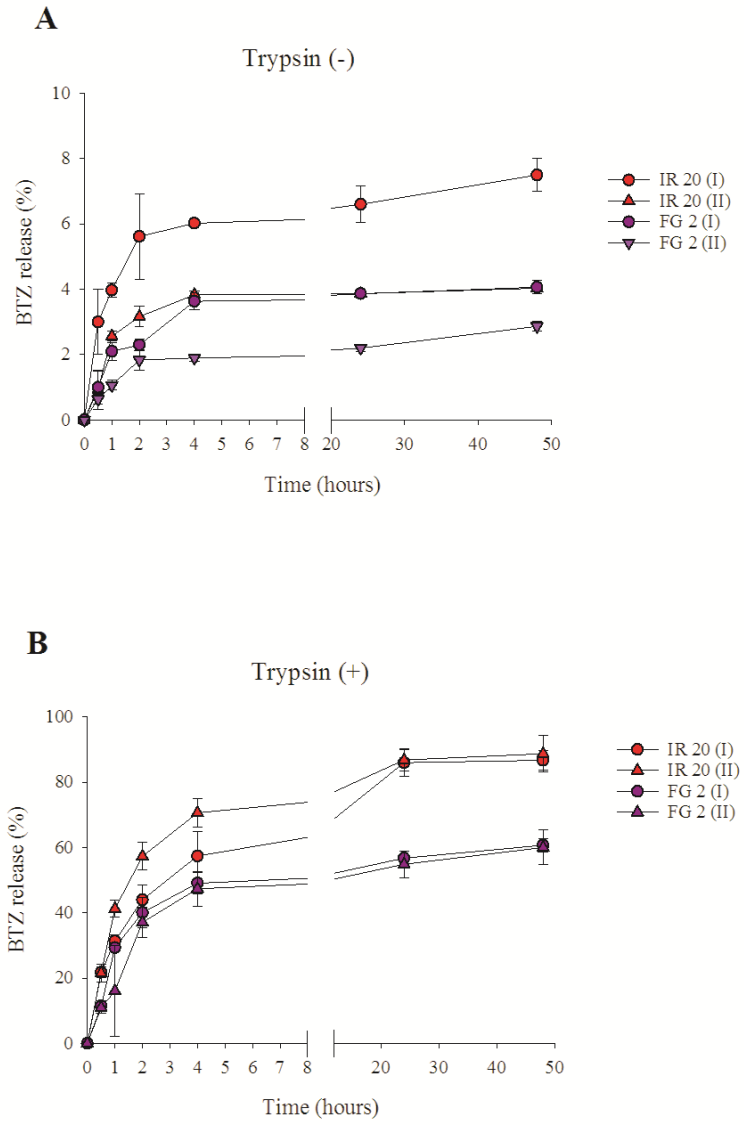

Figure 3.19 Cumulative BTZ release from HSA nanoparticles with and without the addition of 0.1 mg/mL trypsin over 24 h at 37°C. Data represent mean ± standard deviation of n=3 experiments.

3.4.8 Antimycobacterial activity of IR 20 and FG 2 formulations

The inhibition of intracellular *Mycobacterium tuberculosis* growth following macrophage infection was investigated over 72 hours of exposure to IR 20 or FG 2 formulations. IR 20 and FG 2 were dissolved in DMSO and diluted in cell culture medium (Figure 3.20 A,B), presented in an HSA solution (Figure 3.20 C,D) or-loaded into HSA nanoparticles (Figure 3.20 E,F). Different concentration ranges were used for each drug based on differences in the MIC values: 3, 10, 100 µM for IR 20 and 0.3, 3, 10 µM for FG 2. The colony forming units (CFU) per mL on days 1, 2 and 3 of incubation with the formulations or BTZ-free vehicle

controls are presented in Figure 3.20, with the lower and upper dotted lines representing the mean CFU /mL values of untreated *Mycobacterium tuberculosis*-infected macrophages on day 1 and 3, respectively.

As expected, FG 2 activity was greater than IR 20 activity for all formulations, reflecting the respective MIC values of the compounds. Interestingly, the formulation strategy had a major impact on antimycobacterial efficacy of both compounds. BTZs encapsulated in HSA nanoparticles significantly reduced *M. tuberculosis* burdens compared to corresponding formulations in DMSO and HSA solution at all concentrations and timepoints tested ($P<0.01$), thus rendering the BTZs more effective, especially at the lower drug concentrations of 3 μM. The vehicles themselves had no impact on *M. tuberculosis* growth, with the exception of the HSA solution, which unexpectedly slowed bacterial growth over the three-day period compared to untreated cells.

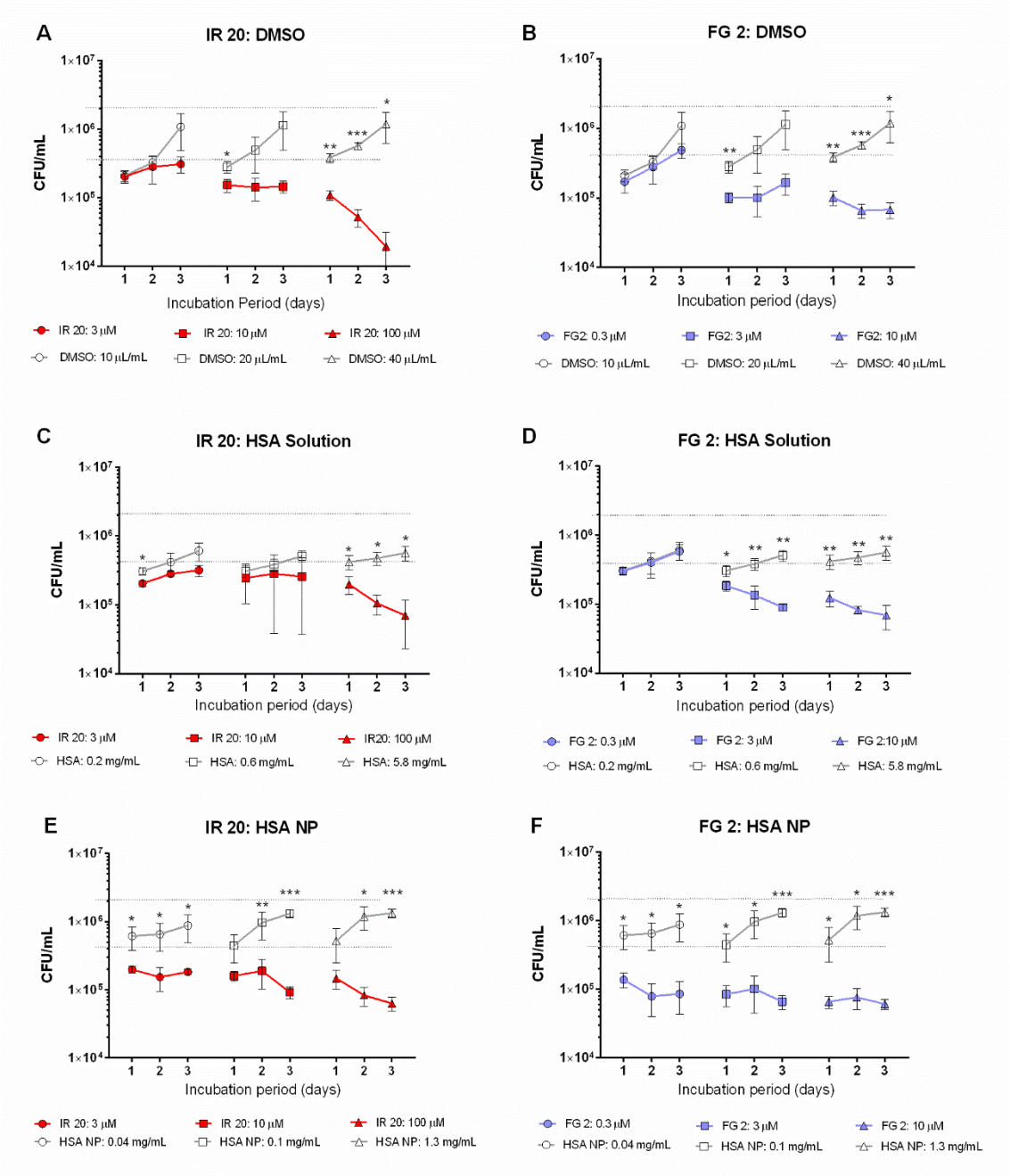

Figure 3.20 The antimycobacterial activity of three formulations of IR 20 (3, 10, 100 µM) and FG 2 (0.3, 3, 10 µM), in DMSO (A,B), HSA solution (C,D) or HSA nanoparticles (E,F). Graphs depict the total CFU/mL *M. tuberculosis* surviving drug treatment over an incubation period of three days. Bacterial survival was also measured for vehicle controls (open symbols) containing equivalent amounts of DMSO, soluble albumin or unloaded albumin nanoparticles. The dotted lines in each graph represent the mean CFU/mL M. tuberculosis counted in untreated infected macrophages on day 1 (lower line) and day 3 (upper line). The mean ± standard deviation of values from three different experiments are reported. * P<0.05, ** P<0.01, *** P<0.001 (Student t-test of vehicle vs. drug-loaded formulation at each individual time point).

3.5 Discussion

The aim of this study was to investigate the potential of human serum albumin (HSA) as a solution and as a nanocarrier for delivering antimycobacterial benzothiazinone (BTZ) compounds to the lungs. More specifically, the loading, release and antimycobacterial activity of four novel BTZ compounds were investigated. BTZs target mycobacterial-infected alveolar macrophages- a well-documented target of nanoparticulate drug carriers (Hoagland et al. 2016; Nasiruddin et al. 2017; Costa-gouveia & Brodin 2017; Kaur & Singh 2014; Costa et al. 2016; Mehanna et al. 2014; Sosnik et al. 2010; Andrade et al. 2013; Ranjita et al. 2011; Jawahar & Reddy 2012). Nanoparticles of the lipid, polymeric and inorganic variety have been investigated for TB treatment strategies however albumin-based systems have been largely overlooked. Ahmad et al. developed a bovine serum albumin-based system loaded with levofloxacin (Rather et al. 2016), however antimycobacterial efficacy was not tested. Thus, it became important to comprehensively evaluate the anti-mycobacterial efficacy of the BTZ-loaded HSA nanoparticles in this study.

To assess the suitability of albumin as a solubilising agent and carrier system for the BTZs, solubilisation studies and tryptophan quenching studies were used; the latter in particular as a rapid method for approximating BTZ binding strength to HSA. Solubilisation studies indicated HSA could increase the solubility of the BTZ compounds (2-fold for IR 20, 6-fold for IF 274 and over 100-fold for FG 2 and AR 112). However, these values were only obtained upon optimisation of the experiment via forming a BTZ film prior to incubation with HSA. This modification was carried out to determine whether an increase in drug surface area would increase the extent of BTZ solubilisation. As hypothesized solubilisation increased, particularly for the more hydrophobic FG 2 and AR 112 compounds as noted above. Hence it can be deduced that dissolving the BTZ compound and forming a film prior to exposure to HSA provides a sufficient increase in surface area for the maximum increase in solubilisation by HSA. Despite the solubilisation of AR 112 not being significantly different to the control, its low degree of solubilisation is mitigated

due to its very high potency. BTZ occupation of Sudlow's site followed the trend of compounds solubility (IR 20 > IF 274 > FG 2 > AR 112). Drug binding studies with HSA as a plasma protein are extensively carried out because the binding affects the free, active concentration of the drug and the overall pharmacological profile of the drug e.g. drug disposition, elimination and efficacy. The importance of these studies also applies to the work carried out here with the use of albumin for drug delivery as one of the major questions relating to albumin as a carrier is whether lipophilic compounds are able to dissociate from albumin binding sites within a therapeutically relevant timeframe following administration. It was established that BTZs did not bind as strongly as endogenous compounds such as bilirubin, which suggested dissociation may occur more readily for the BTZs tested.

Initially, BTZ compounds were incubated with HSA prior to manufacture of nanoparticles. Assessment of the loading of the BTZs showed good loading for IR 20 and IF 274 however poorer loading of FG 2 and AR 112 (as expected from solubilisation studies). As an attempt to improve this loading, an *in-situ* drug loading method (method II) was developed. This method particularly improved the loading for the more hydrophobic FG 2 and AR 112. This suggests method II is a suitable option for particularly hydrophobic drug compounds, whereas for less hydrophobic compounds such as IR 20 method I would still be a suitable option. The drug loading observed for the nanoparticles in these studies was comparable to other studies with albumin nanoparticles. Merodio et al. reported a loading of 14-26 μg/mg albumin for ganciclovir-loaded albumin nanoparticles (Merodio et al. 2000), while a loading of between 1 and 16 μg/mg was reported by Arnedo et al 2002 for a phosphodiester oligonucleotide (Arnedo et al. 2002).

The concerns regarding the ability of BTZs to dissociate from albumin nanoparticles in a therapeutically relevant time-frame were alleviated from the drug release studies. Diffusion of both IR 20 and FG 2 from albumin nanoparticles to albumin-containing

receiving fluid was observed over 48 h. What was interesting to note was the impact of protease on BTZ release from the nanoparticles, especially in the early time points (up to 4 hours). As these are novel compounds, it is difficult to compare the drug release to existing studies. However, the release of existing anti-TB drugs from nanoparticulate systems have been studied previously. A study by Sung et al. studied the release of rifampicin from PLGA nanoparticles *in vitro* where an initial rapid release of drug was observed. They also looked at rifampicin levels in guinea pigs after inhaled administration of the drug-loaded nanoparticle formulations compared to nanoparticle-free formulations and found rifampicin presence in the lung for up to eight hours for the nanoparticle formulations, while the nanoparticle-free formulations had very short retention for rifampicin (Sung et al. 2009). While the PLGA nanoparticles developed in this study were shown to sustain drug levels for longer, the drug-loaded albumin nanoparticles in this work appear more stable in PBS, with drug release occurring in the presence in enzyme and over a longer period. Furthermore, although PLGA is an FDA-approved excipient (Makadia & Siegel 2011), there are concerns regarding the variable cytotoxicity and inflammation in response to modified-PLGA nanoparticles (Grabowski et al. 2013). The advancement of polymeric nanoparticle-based formulations for inhalation to treat tuberculosis depends on a greater understanding of the fate of the nanoparticles i.e. their breakdown, toxicity of polymeric constituents and activity against the infection (Gelperina et al. 2005).

Regarding drug-loaded albumin nanoparticles that have been previously studied for alternative routes of administration, the drug release efficiency varies greatly. Das et al. report a drug release of 90% after 72 hours from aspirin loaded nanoparticles under physiological conditions (Das et al. 2005) and Merodio et al. found that 60% of the initially loaded drug was release from their most efficient nanoparticle for up to 5 days (Merodio et al. 2000), whereas Lin et al. only found a minimal release of less than 18% from their surface-modified albumin nanoparticles after 8 hours under physiological conditions. The drug release from those nanoparticles was increased to >90% in the presence of trypsin

(Lin et al. 2001). Interestingly, trypsin did not show an effect on the release profile in the experiments of Merodio and colleagues (Merodio et al. 2000). Furthermore, a positive correlation between drug release and increasingly acidic or basic pH was reported, likely due to the degradation of the nanoparticle (Battogtokh et al. 2018; Merodio et al. 2000; Lin et al. 2001). The different release behaviours observed for drug-loaded albumin nanoparticle systems stresses the importance of understanding drug-albumin interactions, loading mechanisms and subsequent activity of the systems.

The antimycobacterial activity of the BTZ-loaded albumin nanoparticles was assessed in a TB-infected macrophage model. These experiments demonstrated that IR 20 and FG 2 delivered by albumin vehicles within 24 hours in therapeutically relevant concentrations. Arguably the most important finding from this study was the impact the BTZ-nanoparticle formulation had on antimycobacterial activity. This can be explained by the ability of albumin nanoparticles to deliver drug to the macrophages more effectively, presumably by the preferential uptake of nanoparticles, followed by liberation of drug although this requires confirmation from mechanistic studies and the effect needs to be demonstrated *in vivo*.

3.6 Conclusion

The successful encapsulation of BTZs with both soluble albumin and albumin nanoparticles show they are effective drug carrier strategies for compounds with poor aqueous solubility such as BTZs. The nanoformulations were shown to be stable over a period of six months, with minimal drug losses via washing and other formulation processes. Drug release could be triggered by the presence of endogenous proteases, as confirmed by antimycobacterial activity studies in an *M. tuberculosis* infected macrophage model where the nanoparticle formulations not only showed retained activity despite the presence of albumin in the formulation, but demonstrated enhanced activity compared to the drug in solution.

The results of these studies indicate the suitability of albumin as a drug carrier- particularly for highly potent compounds. The development of nanoformulations for delivery by inhalation is an intricate process often limited by compound properties. Like BTZs, compounds should be highly potent and possess high affinity to the albumin carrier. In the next chapter, the ability of albumin to produce respirable powders will be evaluated. This is the next step in assessing albumin formulation strategies for inhalation therapies.

Chapter 4 Development of spray-dried powders containing albumin nanoparticles for inhalation

4.1 Introduction

In Chapter 3 it was demonstrated that albumin nanoparticles could successfully encapsulate poorly soluble anti-TB compounds (BTZs), allow drug release in a pharmaceutically relevant model and exert a pharmacological effect in a therapeutically relevant *in vitro* model. Pulmonary delivery of albumin nanoparticles provides an opportunity to deliver otherwise "difficult-to-formulate" compounds like BTZs to their site of action in a controlled and sustained manner, resulting in the use of lower doses and reduced frequency of dosing. The development of nanoformulations for inhalation therapy is a multifaceted process, requiring the formulation to exhibit excellent aerodynamic properties (such as good fine particle fraction (FPF) and emitted dose (ED) which is indicative of good powder dispersibility) to allow sufficient mass/dose of drug to deposit in the lungs.

There are currently three main types of inhaler devices used for pulmonary drug delivery: nebulisers, metered dose inhalers (MDIs) and dry powder inhalers (DPIs), each are different and require different kinds of formulations (Bailey & Berkland 2009). Nebulisers have been around historically (since the 1800s) and have been used to deliver solutions of drugs using air-jet or ultrasonic technology to generate aerosol droplets (Sung et al. 2007). There is also a variety of nebuliser that uses a vibrating mesh technology which is described in Chapter 1. Nebulisers are known to be bulky and not as portable as MDIs and DPIs, however this is now expected to change with the introduction of new "smart" nebulizer technologies (Pritchard et al. 2018). The small size of nanoparticle systems appear to make them suited for use with nebulisers, however particle agglomeration and stability is often an issue for these systems and the nanoparticle characteristics can influence particle aggregation during aerosolisation (Dailey et al. 2003). MDIs typically consist of drug dissolved or suspended in a liquid propellant such as HFA, and a metered dose is released upon actuation although these typically require co-ordination which makes them difficult to use (Bailey & Berkland 2009). MDIs containing suspensions

usually contain surface-acting agents which may impact lung performance (such as surfactants) (Siddiqui & Plosker 2005). The shortcomings of nebulisers and MDIs urged the development of an alternative delivery device, the dry powder inhaler (DPI). DPIs offer the advantage of storing drug in a dry state, conferring long-term stability (Sung et al. 2007).

Spray-drying has a wide range of applications in the pharmaceutical industry (Broadhead et al. 1992). This technique allows the modification of many parameters (such as inlet temperature, air pressure etc.) which allows optimisation of particle characteristics such as size, shape and dispersibility (Lee et al. 2011). When nanoparticles are involved in spray-drying processes, they are often prepared separately and then formulated as a dispersion where they will essentially be part of a larger microparticle, but still retain their favourable properties such as targeting or enhanced solubility (Vehring 2008; Yang, Peters, et al. 2008). These systems can become quite complex, especially when more than one solid dispersed phase is involved as is demonstrated in one example in a study where calcium salts were dispersed in an aqueous polymeric suspension and then spray dried to produce microencapsulated particles (Oneda & Ré 2003).

There are many more complex examples in which this process has been studied in order to produce nanoparticle-containing microparticles suitable for inhalation (Raffin Pohlmann et al. 2002; Beck et al. 2006; Schaffazick et al. 2006; Tewa-Tagne et al. 2006). The vast array of modified techniques and processes that have been developed (wet milling, supercritical fluid extraction, electro-spray, high-pressure homogenisation and recrystallisation via solvent displacement for example) demonstrate the ability to produce nanoparticles with a high degree of control over particle properties (Bailey & Berkland 2009). However, there are still limitations relating to drug loading, reproducibility in terms of pharmaceutical manufacture and scale up, excipient compatibility and toxicity.

The reason why nanoparticles are often formulated as part of a larger microparticle is because the optimal particle size for achieving delivery to the deep lung is 1-5 μm, while the small size of nanoparticles would likely result in exhalation (Bailey & Berkland 2009). The choice of excipient is particularly important with nanoparticle formulations as the carrier will influence the powder aerodynamic properties and subsequent activity of the drug (Pilcer & Amighi 2010). It is desirable to work with excipients that are approved as safe due to the limitations posed by working with non-approved excipients such as the likelihood of extra work and the possibility of rejection from regulatory bodies (Pilcer & Amighi 2010).

The dry powder formulations are usually preferred to the liquid counterparts (MDIs and nebulisers) because they have been shown to have the best stability properties and improved nanoparticle handling (Al-Qadi et al. 2012). This is particularly advantageous for this work with albumin nanoparticles, as particular care needs to be taken with the chemical and physical stability of protein-based formulations during processing (Maa et al. 1998).

The use of albumin nanoparticle conjugates for drug delivery is well-documented in the literature for intravenous and intravitreal routes of administration (Wartlick et al. 2004; Zhao et al. 2010; Merodio et al. 2000; Lin et al. 2001; Chen et al. 2008). The pulmonary route is less documented and although spray-drying of albumin at first thought may seem a challenge due to the high temperatures normally employed during the manufacturing process, bovine serum albumin has been spray-dried previously. Papay et al. (Pápay et al. 2017) prepared dry powders of apiginen-BSA conjugated nanoparticles in a manner similar to a study whereby high-pressure homogenisation was employed to produce nanosized drug-albumin conjugates in which albumin acts as a stabiliser for the nanosized drug particles (Chen et al. 2008). In these studies, the albumin nanoparticles are not the drug carrier themselves, rather they act as a scaffold for the drug in nanoparticulate form.

This is a different concept to the aim of this work. The purpose of this work is to utilise albumin nanoparticles as a drug carrier and preserve this in an inhalable formulation for delivery to the lung. This would allow the albumin nanoparticles themselves to dictate the drug release behaviour and subsequent pharmacological activity.

Therefore, the aim of the work in this Chapter was to develop a respirable dry powder formulation for delivery of albumin nanoparticles as an inhalable aerosol. The following were the specific objectives of this work:

- Design a formulation and manufacturing method for spray-drying based on commonly used excipients
- Characterise the powders in terms of yield, particle size distribution, redispersibility, aerosol performance and surface morphology
- Optimise the inhalable formulation in terms of nanoparticle loading and aerodynamic performance in preparation for incorporation of a model drug

A heuristic approach was employed to select a formulation platform to develop further using drug-loaded albumin nanoparticles.

4.2 Materials

Mannitol, trehalose, leucine and human serum albumin (HSA) (low endotoxin, fatty acid free) was purchased from Sigma-Aldrich (Dorset, UK). All solvents were of HPLC grade and purchased from Sigma-Aldrich (Dorset, UK).

4.3 Methods

4.3.1 Formulation strategy

Prior to spray-drying, excipients were chosen to form matrix formulations. Mannitol was selected as it is a popular excipient for spray-drying. A second system with trehalose and leucine was selected for comparison.

4.3.2 Spray-drying

Formulations were spray-dried using a laboratory scale, customised co-current spray dryer (Vectura spray dryer, Vectura Ltd.) with a two-fluid nozzle. Table 4.1 shows the operating conditions for spray-drying. The solution was pumped into the spray-dryer and the resultant powder was separated from the airstream using a cyclone separator. The powder was collected in a container.

Table 4.1 Operating conditions used for spray-drying in this study

Conditions	
Feed concentration (% w/v)	4
Inlet temperature (°C)	106
Outlet temperature (°C)	65
Feed rate (mL/min)	2.0
Atomisation flow (L/min)	17
Atomisation pressure (bar)	2.5
Drying air flow (kg/h)	17
Drying air pressure (bar)	2.5

For the preparation of albumin nanoparticle-containing microparticles, albumin nanoparticle suspensions were prepared as described in Chapter 2. For initial experiments with mannitol and trehalose/leucine matrix production, nanoparticle suspensions were purified in saline. For subsequent experiments following the selection of mannitol as an appropriate matrix for the albumin nanoparticles, nanoparticle suspensions were purified in water. All preparation mixtures contained a total solids content of 4%, and albumin nanoparticles made up 20% of the total solids. To prepare albumin nanoparticles in a mannitol matrix, albumin nanoparticles (200 mg) and mannitol (800 mg) were made up to

25 mL with water. To prepare albumin nanoparticles in trehalose/leucine matrix, albumin nanoparticles (200 mg), trehalose (600 mg) and leucine (200 mg) were made up to 25 mL with water. Controls consisted of 1g mannitol in saline/water (25 mL) and trehalose (800 mg)/leucine (200 mg) in saline (25 mL). The saline was included to mimic the saline content in the nanoparticle suspensions. The preparation mixtures were fed into the spray-dryer using a peristaltic pump. The spray-dried powders were recovered, weighed and stored at room temperature in a desiccator. Sample yields were determined by weighing the recovered powder and dividing the value by the initial mass of solids present in the feed stock.

Further spray-drying studies were carried out with albumin nanoparticles in a mannitol matrix at varying nanoparticle concentrations (20%, 30%, 40% and 50%). These nanoparticle particle suspensions were purified in water and spray-dried using the same conditions as described above.

4.3.3 Particle Size Distribution (PSD)

Powder size distribution (D_{90}, D_{50} and D_{10}) was measured using laser diffraction (Mastersizer 3000, Malvern Instruments, UK). The sample was dispersed in in 2-2-4 trimethyl pentane and sonicated at 50% intensity for 3 mins using a sonic probe [Sonopuls HD3100 (Bandelin, Germany)].

4.3.4 Reconstitution and dynamic light scattering (DLS)

Reconstitution of the spray-dried powder was carried out by dispersing 10 mg of the powder in distilled water (2 mL). After centrifugation at 2000 *g* for 10 min, 1.5 mL supernatant was removed and the presence of any nanoparticles was determined by dynamic light scattering (Zetasizer nano ZSP, Malvern Instruments, UK). The samples were measured at 25°C.

4.3.5 Nanoparticle recovery and uniformity content

Albumin nanoparticle recovery was determined by dissolving 50 mg of the spray-dried powder in water (10 mL). Nanoparticles were separated from the resulting mixture by centrifugation with centrifugal filters (MWCO 100 kDa; Amicon Ultra). Nanoparticle recovery yield (%) was determined gravimetrically.

4.3.6 Fast Screening Impactor (FSI) studies

Aerosol performance of spray dried formulations were assessed using a Fast Screening Impactor (FSI, Copley Scientific, UK) with a 5 μm cut point insert. Hand-filled sealed aluminium blisters containing 10 ± 0.5 mg spray dried powder were dispersed at 60 L/min for 4 seconds using a unit dose dry powder inhaler (Vectura Ltd, UK). Fine particle fraction (FPF % ≤ 5 μm) and blister evacuation (% fill mass) were determined gravimetrically (n=3 per formulation).

4.3.7 Scanning electron microscopy (SEM)

SEM images were kindly taken by Ursula Potter and Diana Lednitzky [Bath University (UK)]. Powder samples were sprinkled onto double sided carbon tabs and sputter coated with gold for 3 minutes. Samples were imaged using a JEOL JSM-6480LV tungsten filament scanning electron microscope in high vacuum mode. Images were taken at 100, 1,000, 3,000, 5,000 and 10,000 times magnification.

4.4 Results

4.4.1 Spray-dried microparticle characteristics

Incorporating nanoparticles into the formulations had no effect on the size of powders produced (Table 4.2). The control formulations contained saline to mimic saline content in original nanoparticle suspensions. Due to the larger D_{50} and D_{90} values for mannitol in saline (3.24 μm and 8.06 μm, respectively) saline was omitted from the matrix formulation . Henceforth mannitol was spray-dried in water only, resulting in D_{50} and D_{90} values of 2.78 μm and 4.84 μm, respectively which was comparable to the other powder batches. The recovery yields were similar for both trehalose/leucine batches with and without nanoparticles, however the incorporation of nanoparticles with mannitol resulted in a yield reduction from 73.6% to 40.8%.

Table 4.2 Particle size and yield of spray-dried formulations: mannitol in saline; trehalose (trehalose: leucine 80:20 in saline); mannitol in water only; nanoparticles suspended in saline (20% of total solids content) in a mannitol in water matrix, and finally albumin nanoparticles suspended in saline (20% of total solids content) in a trehalose/leucine in water matrix. Results are from single powder batches. Total solids content for all formulations was 4%.

Formulation matrix	**Nanoparticles?**	**D_{10}**	**D_{50}**	**D_{90}**	**Yield (%)**
Mannitol in saline	No	1.05	3.24	8.06	82.0
Trehalose and leucine in saline	No	1.12	2.43	4.65	56.2
Mannitol in water	No	0.92	2.78	4.84	73.6
Mannitol in water	Yes	0.96	2.50	4.82	40.8
Trehalose and leucine in water	Yes	0.97	2.37	4.61	58.6

4.4.2 Nanoparticle recovery from dry powders upon aqueous reconstitution

The microparticles swiftly dissolved when dispersed in aqueous solution. The size and PDI of nanoparticles recovered after dissolution as well as the size and PDI of the original nanoparticle suspensions are shown in Table 4.3. All nanoparticle sizes were similar to the original size (± 10%). Nanoparticle recovery for both the mannitol and trehalose/leucine systems was 95% & 75%, respectively.

Table 4.3 Nanoparticle size before spray-drying and after reconstitution of dry powder and nanoparticle recovery. Data is from a single powder batch.

Formulation	**Size before spray-drying (nm) & [P.D.I.]**	**Size (nm) & [P.D.I.] after reconstitution**	**Percentage (%) of nanoparticles in 50 mg powder & recovery [%]**
Mannitol	123.8 [0.059]	133.2 [0.023]	19.0 [95]
Trehalose/leucine	120.6 [0.042]	108.0 [0.060]	15.0 [75]

4.4.3 Fine Particle Fraction (FPF) evaluation of dry powders

Blister evacuation for all spray-dried powders was > 95% (Table 4.4). Trehalose/leucine systems both with and without nanoparticles had higher fine particle fractions (68.0 & 60.6% respectively) compared to mannitol systems (30.4% & 39.3%).

Table 4.4 Fine Particle Fraction (FPF) and blister evacuation (%) of dry powders screened by Fast Screening Impactor (FSI). Values reported are derived from a single powder batch with the mean and standard deviation of n = 3 blisters.

Formulation	**Blister evacuation (%)**	**FPF (%)**
Mannitol control	95.4 ± 4.4	39.3 ± 3.3
Trehalose/leucine control	100.8 ± 5.3	60.6 ± 2.9
Albumin nanoparticles in mannitol	96.5 ± 1.2	30.4 ± 5
Albumin nanoparticles in trehalose/leucine	95.4 ± 0.7	68.0 ± 5.4

4.4.4 Effect of nanoparticle concentration on dry powder characteristics

Mannitol was selected as the most appropriate excipient for formulations of the albumin nanoparticles into a dry powder. All albumin nanoparticle-containing dry powder formulations had a nanoparticle content of 20% (out of total solids). Increasing nanoparticle content would allow maximum drug content in final powders. The effect of increasing albumin nanoparticle content on the characteristics of dry powders produced was studied. Albumin nanoparticles in water embedded in a mannitol matrix were spray-dried at 20-50% content and assessed for aerodynamic properties (Table 4.5). Powders were produced with batch yields of 68-71%. There were no significant changes to nanoparticle sizes after reconstitution (Table 4.5). Laser diffraction revealed D_{50} values (geometric diameter) were in the size range 1-5 μm which is the optimum size range as it is well documented particles within this size range achieve "deep lung deposition" (Bailey & Berkland 2009; Shi et al. 2007). The D_{50} increased from 2.2 to 2.7 μm with increasing nanoparticle content. FPF (%) decreased with increasing albumin nanoparticle content, with values of 49.9% and 17.0% for powders containing 20% and 50% albumin nanoparticle content, respectively (Figure 4.1). Changes in nanoparticle content had no effect on yield or size of nanoparticles after reconstitution.

Table 4.5 Properties and aerodynamic performance of spray-dried powders composed of 20-50% (w/w) HSA nanoparticles embedded in a mannitol matrix. Values reported are derived from a single powder batch.

Formulation	**Yield (%)**	**Hydrodynamic diameter (nm)**		**PSD**			**Blister evacuation (%)**	**FPF (%)**
		Before spray-drying	**After spray-drying**	**D_{10}**	**D_{50}**	**D_{90}**		
20% (w/w)	68	120	119	0.92	2.24	5.07	94.4	49.9
30% (w/w)	71	169	167	1.01	2.42	5.42	95.8	39.6
40% (w/w)	69	165	162	1.03	2.49	6.15	98.2	34.7
50% (w/w)	78	170	164	1.02	2.70	6.84	74.7	17.0

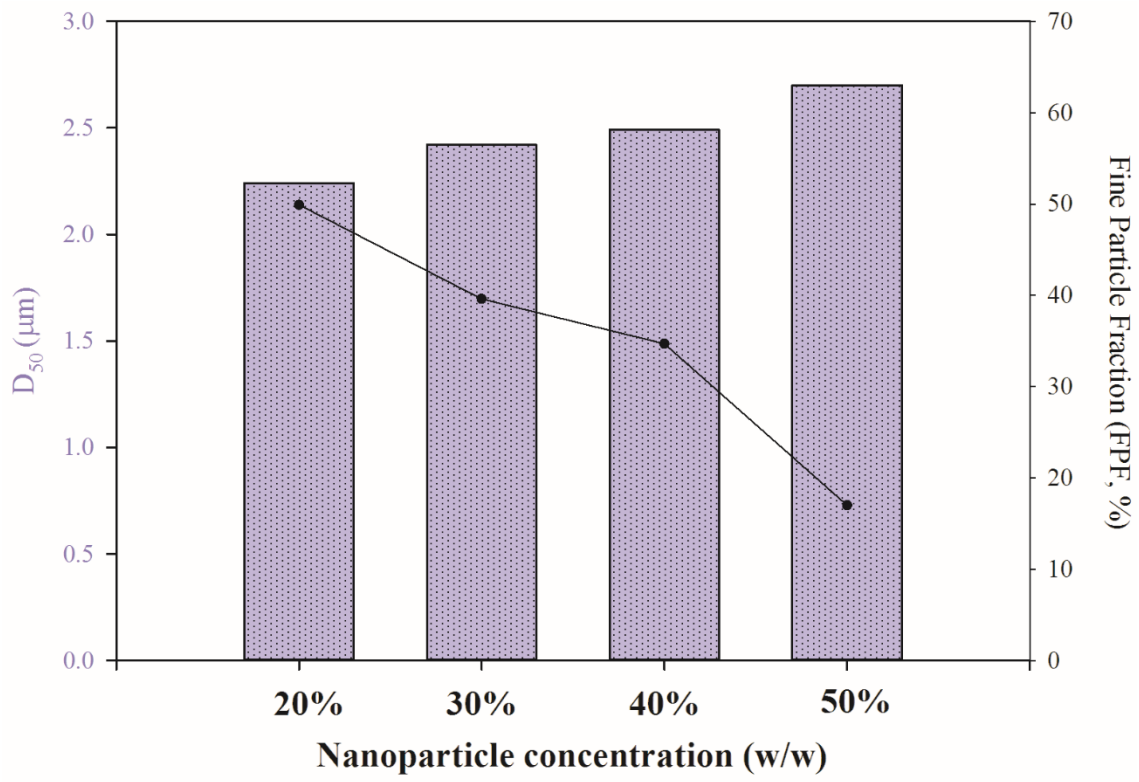

Figure 4.1 Illustration depicting the effect of albumin nanoparticle concentration in spray-dried powders embedded in a mannitol matrix on D_{50} (µm, left-side axis) and Fine Particle Fraction (%, right-side axis) as determined through Fast Screening Impactor (FSI) studies. The bars depict geometric size ($D_{50;}$ left axis), while "·" depicts fine particle fraction.

Formulation	SEM original image	Magnified image
0% (w/w)	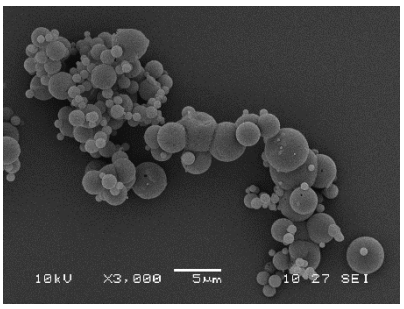	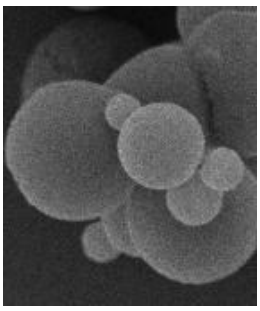
20% (w/w)	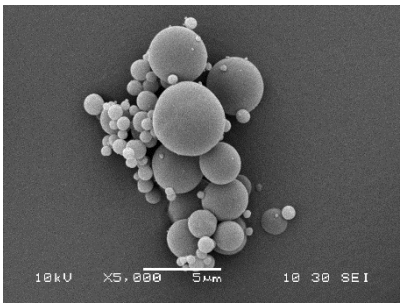	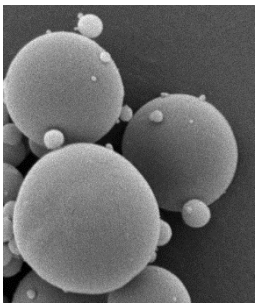
30% (w/w)	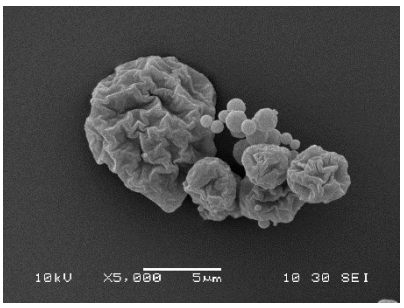	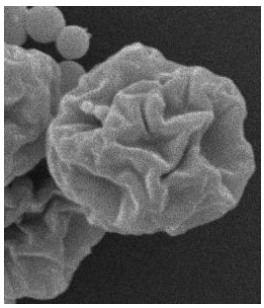
40% (w/w)	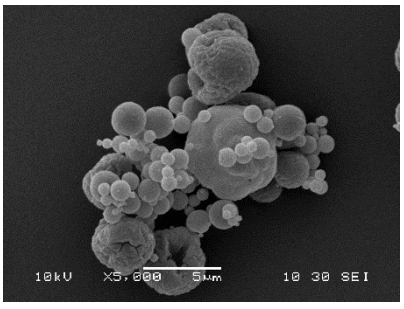	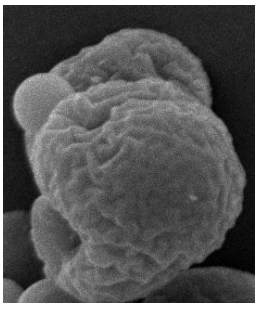
50% (w/w)	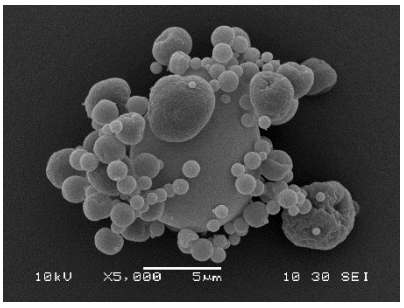	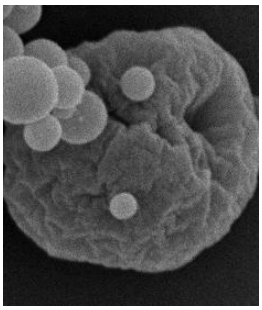

Figure 4.2 Representative scanning electron micrographs of spray-dried powders. . Images represent powders containing 0%, 20%, 30%, 40% and 50% albumin nanoparticle content with mannitol. A zoomed in image for each sample is shown for closer analysis of surface morphology.

4.5 Discussion

The suitability of albumin nanoparticles as drug carriers was previously demonstrated in Chapter 3. The natural next step for their development as an inhalable formulation is to manufacture a respirable albumin nanoparticulate formulation for delivery via inhalation. Therefore, in this chapter the development of spray-dried microparticles containing albumin nanoparticles was investigated.

The selection of appropriate spray-drying excipients is important in determining how the produced microparticles behave, particularly in terms of disintegration time and subsequent release of contents as well as stability (Grenha et al. 2005; Kho & Hadinoto 2010). A matrix-forming excipient is particularly important for nanoformulations as it forms bridges between nanoparticles during spray-drying to prevent them from agglomerating (Torge et al. 2017). The matrix in theory should dissolve in contact with liquid to release the nanoparticles. Mannitol is a popular matrix excipient for spray-drying due to its low toxicity and high aqueous solubility (Scherließ 2016; Grenha et al. 2005). Trehalose is another suitable cryoprotectant often used, its water solubility is much higher than mannitol, predicting good re-dispersibility of powders. However, it has been shown that although spray-drying with trehalose prevents aggregation and produces smaller particles, a larger fraction of these particles is left behind in the spray-drying chamber, resulting in low powder yields (Maury et al. 2005; Freitas & Müller 1998). Trehalose can sometimes also prove to be difficult to handle as a powder as it has been reported to form sticky aggregates when spray-dried at an inlet air-temperature of 90°C, suggesting it may be unsuitable on its own as an excipient for spray-drying (Adler & Lee 1999; Maa et al. 1997). To prevent this, it was suggested leucine (a hydrophobic excipient) be used in combination with trehalose as a possible means to improve aerosolisation efficiency (Kho & Hadinoto 2010; Wang et al. 2012). Leucine has been used in spray-drying with a view to improve dispersion properties of substances in microparticles and protect against moisture upon aerosolisation (Najafabadi et al. 2004; Li et al. 2016). It is among many

amino acids that have been shown to decrease hygroscopicity and improve the *in vitro* deposition profile of spray-dried powder formulations (Seville et al. 2007). In studies with various amino acids, leucine has been shown to be the best in terms of aerosolisation properties (Pilcer & Amighi 2010). Leucine, along with mannitol and trehalose is a "generally regarded as safe" (GRAS) excipient (Pilcer & Amighi 2010) and has a high glass transition temperature making it a suitable stabiliser of proteins (Adler & Lee 1999). The ratio of 1:4 leucine: trehalose was selected to ensure nanoparticle recovery from reconstitution of the powders.

The initial powders produced in this work; apart from mannitol spray-dried in saline; had diameters of ~ 4μm which was considered suitable to achieve sufficient deposition in the lower airways (Bailey & Berkland 2009). However, it should be noted that particle sizes discussed in this work are geometric particle sizes (which is measured by light diffraction). The aerodynamic diameter (d_{aer}) is related to the geometric diameter (assuming particles are spherical) by the Equation 4.1, where d is geometric diameter (nm) and p is particle density normalised by the density of water (1 g/cm^3) (Tsapis et al. 2002).

Equation 4.1

$$d_{aer} = d\sqrt{p}$$

It is widely accepted that particles of aerodynamic diameter of 1-5 μm are optimal for middle-deep lung deposition (Shekunov et al. 2007), however in reality the effective aerodynamic diameter depends on many factors such as shape, surface morphology and flow geometry (Shekunov et al. 2007). The particle density of the powders developed in this work was not evaluated, however PSD remains a major parameter that influences powder deposition in the lung and should be evaluated (Shekunov et al. 2007).

Spray-drying mannitol in saline increased the size of powders produced. However, the inclusion of saline in trehalose/leucine systems did not have this effect. It is not

understood why saline may have had this effect on the mannitol matrix system. Subsequent nanoparticle suspensions were free of saline and purified in water in a buffer exchange.

Albumin nanoparticles withstand spray-drying conditions despite concerns the high temperatures may adversely affect nanoparticle structure. Regardless of using a high inlet temperature of 106°C, a low outlet temperature of 65°C was maintained. These temperatures are favourable for the spray-drying of heat sensitive substances like proteins (Lee et al. 2011). The initial selected spray-drying conditions were kept the same throughout all the studies and were not experimentally optimised because powder characteristics were generally considered to have properties deemed within the range that was aimed for with this work (such as yield and particle size). Nanoparticle recovery and uniformity was good, with some nanoparticle loss being attributed to the spray-drying process. Redispersibility of the powders was assessed in a simplified model with a small volume of aqueous solution to mimic the small volume of fluid found in the human lung (estimated to be between 15 and 70 mL (Patton 1996). Despite this similarity, there may be other factors that need to be taken into consideration to more accurately represent *in vivo* behaviour. Ruge et al. studied the disintegration of nano-embedded microparticles on a mucus layer as an attempt to address this and found that disintegration did not occur on a static mucus layer but did occur with mechanical stirring of the mucus phase (Ruge et al. 2016). However, mucus models are limited in terms of comparability with biological mucus and are very complex, particularly for use with nanoparticle formulations (Torge et al. 2017). Some studies have used simulated lung fluid to assess the release of nanoparticles from spray-dried formulations (Debnath et al. 2017; Sinha et al. 2013; Rosière et al. 2015). It may be useful to explore other relevant models for future *in vitro* studies of disintegration behaviour of spray-dried powders.

Despite the improved FPF (%) in trehalose/leucine systems and slightly better yields, after working with both excipient systems, mannitol was selected for further experiments due to its ease of handling (lower susceptibility to moisture) and predictability. Naini et al. found mannitol to be apparently 100% crystalline upon spray-drying, with no humidity-induced changes (Naini et al. 1998). Spray-dried nanoparticle-containing microparticles with mannitol as an excipient have been produced in studies with acceptable aerodynamic properties for delivery to the lung (Grenha et al. 2007; Kho & Hadinoto 2010). Mannitol readily dissolves in water and so it was theorised after delivering spray-dried albumin nanoparticles in a mannitol matrix to the lung, the mannitol matrix would dissolve rapidly on the epithelial surface, leaving behind the nanoparticles to release drug and thereafter exert its therapeutic effect. The notion of allowing the drug-nanoparticle interactions to predominantly dictate release kinetics, as opposed to the excipient makes mannitol more favourable as leucine may potentially retard drug release in the lung due to its hydrophobicity and subsequent poor aqueous solubility (Wang et al. 2012). The trehalose/leucine systems had more favourable yields, however, when additional albumin nanoparticles in water (no saline) were spray-dried with trehalose/leucine and compared to albumin nanoparticles spray-dried with mannitol, they were found to have a yield of 60%, with the mannitol system achieving a yield of 67%. Furthermore, powders in the trehalose/leucine matrix were found to be "sticky" in nature, owing to the trehalose. It has been suggested that this stickiness can be overcome with the use of higher inlet temperatures, however for peptide/protein based products this may be counter-intuitive as thermal stress may cause protein deactivation (Adler & Lee 1999).

Therefore, mannitol was selected for further experiments investigating the effect of increasing nanoparticle content, and for other further work. Mannitol does not carry any reducing groups and so it does not cause chemical interactions with drugs or proteins, and it is highly crystalline even upon spray drying, making it seem like an ideal excipient (Maas et al. 2011). Trehalose on the other hand tends to be amorphous and deemed

inappropriate at high concentrations for aerosol applications due to its high degree of agglomeration, likely resulting in poor redispersibility (Maa et al. 1997), although it was originally considered for this work because in its amorphous state it stabilises proteins. It has been said that trehalose sorbs water and then crystallises and phase separates from the protein, acting as a dessicant (Moran & Buckton 2009). Variability in the crystalline behaviour of amorphous trehalose has also been reported, depending on the concentrations used during spray drying (Moran & Buckton 2007).

With the successful encapsulation of nanoparticles in the mannitol matrix at 20% total solids content, the next step was to investigate the effect of increasing the nanoparticle content. Maximising albumin nanoparticle content in spray-dried formulations would potentially increase the amount of drug delivered to the lung. SEM micrographs (Figure 4.2) showed spray-drying mannitol on its own and mannitol with 20% albumin nanoparticle content produced spherical particles with smooth surface. Upon increasing the nanoparticle content, the surface of the particles has ridges and appear rough although the spherical shape is retained. Having 50% albumin nanoparticle content produced powders that were sticky, as indicated by the difference in blister evacuation. It also had a remarkably lower FPF (17% compared to 35% and 40% for formulations containing 40% and 30% albumin nanoparticle content). This could be due to increased poor particle disaggregation upon aerosolisation. This could be linked to the location of the nanoparticles within the matrix. The change in size and performance suggests the nanoparticles are likely to be located at the particle surface. Confocal laser scanning microscopy (CLSM) can be used to observe the spray-dried powder particles, staining the particles with fluorescent labels would make them easier to observe under the microscope. Examination of cross-sections through the carrier particles would provide information about the distribution of nanoparticles (Sham et al. 2004). The little difference between 30% and 40% albumin nanoparticle content formulations in appearance and aerosol performance indicates 40% as the optimal nanoparticle content for spray-drying.

The 40% formulation was selected as it appears to have the most potential for delivering the highest amount of nanoparticles (through FSI testing), thus providing the most promising means for delivering therapeutically relevant doses of drug to the lungs.

4.6 Conclusion

In summary, these pilot studies demonstrate that incorporation of albumin nanoparticles into respirable carrier particles is possible. The spray-dried powders developed in this work had suitable size for lung deposition and albumin nanoparticles were recoverable after the spray-drying process with good re-dispersibility and uniformity. The spray-dried mannitol formulation with a nanoparticle content of 40% was selected as the most promising. Therefore, in the next chapter this formulation will be explored further with the incorporation of a model drug into the albumin nanoparticles that has application in the lung.

Chapter 5 Formulation and characterisation of respirable formulation containing roflumilast-loaded albumin nanoparticles

5.1 Introduction

The work carried out in chapter 4 focused on the development and optimisation of a spray-dried formulation containing albumin nanoparticles. Albumin nanoparticles were able to survive the spray-drying process and the resulting formulated powders showed promising aerosolisation properties. In order to assess the clinical viability of the aerosol formulation, a model drug must be incorporated into the formulation and investigated for suitability for aerosol delivery.

When spray-drying with nano-encapsulated drugs, carrier excipients are usually included in copious amounts which limits the amount of drug that can potentially be included in the formulation, therefore spray-drying in this case is normally suited to fairly potent drugs (Pilcer & Amighi 2010). Much like the BTZ compounds studied in chapter 3, drugs for formulation in this way i.e. encapsulated drugs, must not only be highly potent but should exhibit high encapsulation efficiencies and exhibit excellent aerodynamic properties.

The BTZs studied in Chapter 3 of this thesis were not available for spray-drying studies, therefore an alternative model drug, roflumilast, was proposed. Roflumilast is a poorly soluble phosphodiesterase-4 (PDE4) inhibitor. It is used for maintenance of severe chronic pulmonary obstructive disease (COPD) as PDE4 is the main isoenzyme in lymphocyte cells involved in COPD. It is available in tablet form and administered as 250-500 μg daily (Hohlfeld et al. 2008). Unfortunately, oral roflumilast comes with some adverse effects such as insomnia, anxiety and depression which is more common in patients with body weight < 60 kg due to higher total PDE4 inhibitory activity (Electronic medicines compendium, 2018). The pulmonary route of administration provides a potential avenue to minimise these adverse effects (Kuzmov & Minko 2015). In one study, inhaled roflumilast was administered intratracheally to Brown Norway rats and found the inhaled drug showed greater improvement in the lung function compared to oral roflumilast (Chapman et al. 2007). Roflumilast is also known to have an anti-inflammatory effect, in

one study it was found to reduce tumour necrosis factor- α (TNF-α) levels in human lung macrophages (Buenestado et al. 2012). Another study by Murad et al, 2017 showed inhaled roflumilast decreased macrophage and neutrophil levels in the BAL fluid of BALB/c mice (Murad et al. 2017). These studies report the investigation of inhaled roflumilast, however the literature lacks the application of roflumilast in a nanocarrier formulation. There is one study that investigated the use of a cyclodextrin-based microcarrier for roflumilast for inhalation (Mahmoud et al. 2018). The use of an albumin nanocarrier formulation provides the advantage of the potential for controlled release over a longer period of time and higher potency (as demonstrated in Chapter 3 with the enhanced antimycobacterial activity of the BTZ-loaded albumin nanoparticle formulations).

Dry powders can act as protectants for active compounds, protecting them from enzymatic degradation and allowing a more controlled release approach, reducing the amount and frequency of dosing (Panda et al. 2016). In the case of roflumilast, the reduction of adverse effects as well as improvement in delivery to the site of action (i.e. the lung itself) make it a suitable model drug for these studies. Direct delivery of drugs to the lungs via aerosol can enable the effective dose to be reduced up to 33-fold (Pandey et al. 2003). This means a dose of 6-12 micrograms of roflumilast in a capsule containing 10 mg powder for inhalation would be an adequate target dose (assuming a similar increase in clinical efficacy to that shown for inhaled salbutamol (200-800 micrograms vs. 4-16 mg orally) and for inhaled rifampicin (Pandey et al. 2003).

Therefore, the aim of this work was to investigate whether roflumilast can be formulated with albumin nanoparticle carriers and loaded in respirable spray-dried powders. The specific objectives to aid in achieving this were set as follows:

- study roflumilast-albumin interactions
- produce albumin nanoparticles containing roflumilast

- spray-dry these using the optimised formulation in chapter 4 and characterise their aerosolisation capabilities.

- use PreciseInhale® to study aerosol deposition in a theoretical human lung model.

5.2 Materials

Mannitol was purchased from Sigma Aldrich, UK. Roflumilast was kindly provided by Vectura Group plc. Other materials were as described in Chapter 2.

5.3 Methods

5.3.1 UV analysis of roflumilast

A UV calibration curve was prepared for roflumilast and establishment of the limit of detection and quantification in methanol using UV spectrophotometry. To determine the absorbance maximum, a solution of roflumilast (30 µg/mL) in methanol was prepared and scanned over wavelengths 200-800 nm using the Perkin Elmer Lambda 2 UV/Vis spectrophotometer and a quartz cuvette (High precision cell, Hellma Analytics). A peak at 248 nm was determined as a suitable wavelength for detection of roflumilast. A calibration curve of roflumilast in methanol was prepared using solutions within the range 100- 2 µg/mL and taking a single absorbance value at 248 nm until readings within the range 1.0 to 0.1 were obtained. LOD and LOQ was calculated using Equation 3.1 and Equation 3.2.

5.3.2 Determination of roflumilast interactions with albumin by solubilisation

Stock solutions of HSA (fatty acid-free, Sigma-Aldrich, Germany) in water and Tris buffer (50 mg/mL) were prepared. Negative controls consisted of water and Tris buffer without HSA. HSA solutions and negative controls (1 mL) were added to separate vials containing 1 mg roflumilast and incubated at 37°C for a total of three days. Samples of the supernatant were removed at pre-determined time points and UV absorbance readings in methanol were taken at 248 nm. The amount of drug dissolved by each solution was determined from the calibration curve and calculated as a percentage of the original drug content.

5.3.3 Roflumilast binding to Sudlow's site I via tryptophan quenching

Roflumilast binding to the albumin drug binding site I, i.e. the hydrophobic pocket, was assessed through tryptophan quenching studies (Abou-Zied & Al-Lawatia 2011). HSA solution (1 mL, 1 µM) was prepared in 1:1 saline (25 mM) and Tris buffer (25 mM, pH 7.4). Stock solutions (1 mL, 500 µM) of roflumilast, ibuprofen (negative control) and bilirubin (positive control) were prepared in DMSO. The emission spectrum of HSA tryptophan

fluorescence was measured between 300 nm to 400 nm with an excitation wavelength of 285 nm and an emission slit of 10 nm using a Perkin Elmer LS 50B Fluorescence spectrometer and a quartz cuvette (Hellma Analytics). Initial fluorescence readings were taken for the HSA solution, followed by subsequent readings after sequential additions of 1 µL of drug. The maximum emission value (arbitrary units) of tryptophan fluorescence for each titration was divided by the emission value of HSA solution and results were presented as the percentage of tryptophan quenching versus drug concentration.

5.3.4 Roflumilast-loaded albumin nanoparticle manufacture

Roflumilast (1 mg) was weighed in a glass vial (vial I) and dissolved in ethanol (4 mL). HSA solution in Tris buffer (1 mL, 50 mg/mL) was prepared in a glass vial (vial II). After the addition of 25 µL NaOH to the HSA solution, the roflumilast solution was added drop wise to the stirred protein solution. Nanoparticles were then cross-linked and purified in the same manner as described in Chapter 3. The washing fluid was collected for roflumilast quantification (vial III). Roflumilast content in vials I-III was quantified and mass balance was calculated as described in Chapter 3.

5.3.5 Physicochemical characterisation of nanoparticle suspensions

The nanoparticle suspensions were characterised as described in chapter 3.

5.3.6 Scaling up of nanoparticle suspensions for spray-drying studies

For spray-drying studies, roflumilast (8 mg) was dissolved in ethanol (32mL) and added drop wise to HSA solution in tris buffer (8mL, 50 mg/mL) and cross-linked and characterised in the same manner as described in chapter 2.

5.3.7 Spray-drying of roflumilast-loaded albumin nanoparticle suspensions

Roflumilast-loaded albumin nanoparticles in a mannitol matrix were produced by spray-drying at a concentration of 40% and characterised for yield and FPF as described in Chapter 4.

5.3.8 Drug content analysis of spray-dried powders

Spray-dried powder (10 mg) was reconstituted with water. Roflumilast was extracted from the suspension with dichloromethane, in the same manner as Chapter 3. Methanol was added to roflumilast extracts and quantified by UV analysis.

5.3.9 Roflumilast release studies

Roflumilast release profiles in the nanoparticle suspensions was determined in the same way as described in chapter 3. Roflumilast release from the spray-dried powder formulations were determined by reconstituting 25 mg of spray-dried powder (equating to 10 mg of nanoparticles) in 1mL water. This mixture was then analysed in the same manner as for roflumilast nanoparticle suspensions. Similarity factor (f2) was calculated using Equation 3.7 to compare drug release profiles from roflumilast-loaded albumin nanoparticles and spray-dried powders containing roflumilast-loaded albumin nanoparticles with and without the presence of trypsin. Drug release data was analysed using several mathematical models to find the best kinetic model.

5.3.10 Scanning electron microscopy (SEM)

SEM analysis was carried out as described in Chapter 4.

5.3.11 PreciseInhale®

Dry powder aerosols were generated using the PreciseInhale® system (Inhalation Sciences, Sweden) which has been described previously (Lexmond et al. 2018; Selg et al. 2013). Powder sample is loaded into the dosing chamber and then ejected by a high-

pressure air jet through a nozzle into a holding chamber, where the aerosol is collected for analysis. The aerodynamic PSD of the aerosol was determined by cascade impaction analysis using a Marple Cascade Impactor attached to the exposure outlet with gravimetric measurements (Figure 5.1).

Table 5.1 shows the cut-off diameter for each impactor stage. The Multiple Path Model of Particle Dosimetry (MPPD) software was then used to calculate theoretical aerosol composite deposition in a human lung, as well as the normalised fractional distribution between the bronchi and alveoli. The assumptions/inputs for the human lung model were as follows: breathing rate 12 breaths per minute (BPM), upright position for breathing, oral deposition only and tidal volume 625 mL. Measurements were performed in triplicate.

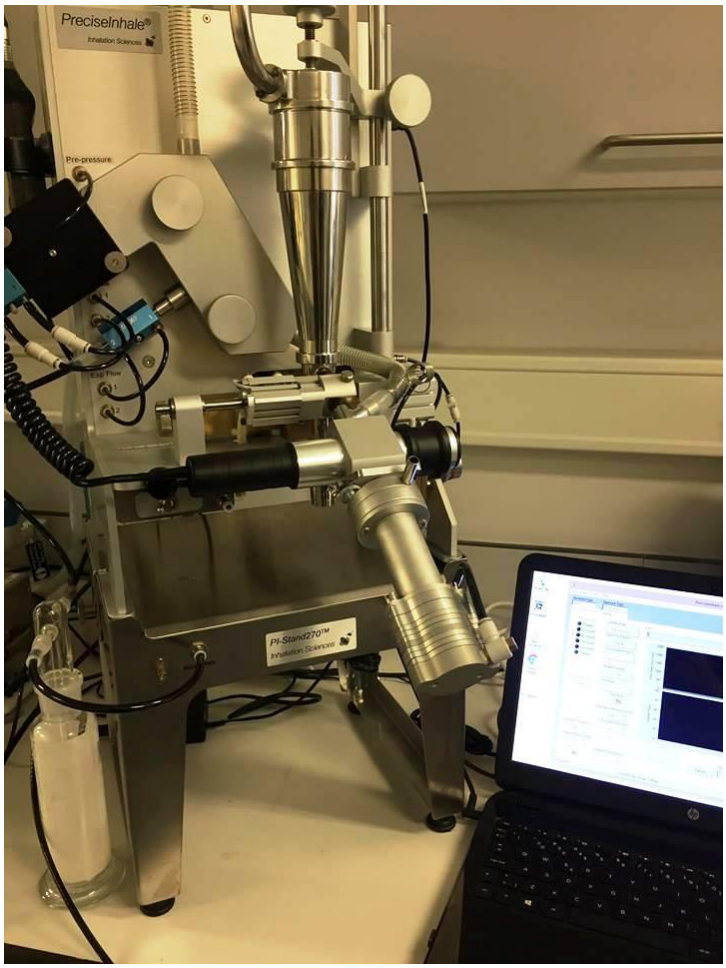

Figure 5.1 The PreciseInhale® system. Here a Marple Cascade Impactor is attached to the exposure outlet.

Table 5.1 Diameter cut-off values (μm) for Marple Cascade Impactor stages

Impactor stage	Cut-off diameter (μm)
1	21.3
2	14.8
3	9.8
4	6
5	3.5
6	1.55
7	0.93
8	0.52
End filter	0.25

5.3.12 Statistical analysis

Statistical analysis was carried out using SigmaPlot version 14.0 (SyStat software inc.). One-way ANOVA was carried out following by post-hoc tests when appropriate. P values < 0.05 were considered significant.

5.4 Results

5.4.1 UV analysis of roflumilast

Roflumilast was scanned over the UV range of the wavelength spectrum and 248 nm was deemed as a suitable wavelength. The calibration curve of roflumilast constructed in methanol showed the drug obeyed Beer-Lambert's law over the concentration range 20-100 µg/mL with a high correlation coefficient (R^2 = 0.999) and regression equation Y = 0.006x + 0.003 (Figure 5.2). The LOD was 1.56 µg/mL and the LOQ was 4.73 µg/mL. Inter-day and intraday variation is shown in Table 3.2. The average intra and inter-day variation for roflumilast complied with the acceptance criteria proposed in analytical guidelines (RSD must not be greater than 2.0%, (European Medicines Agency 1995).

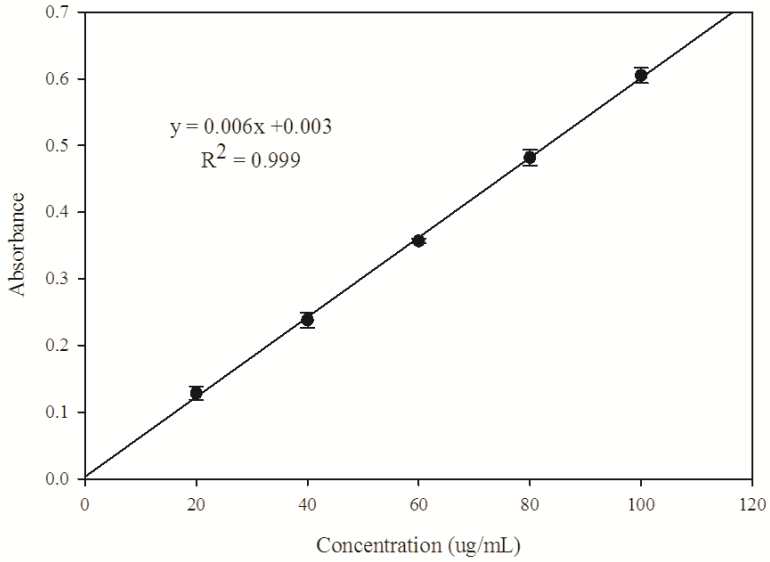

Figure 5.2 UV calibration curve for roflumilast in methanol.

Table 5.2 Inter-day and Intra-day coefficients of variation (%) for different concentrations of roflumilast solution in methanol

Concentration (µg/mL)	**Coefficient of variation (%)**	
	Intra-day	**Inter-day**
20	0.72	0.78
40	3.42	1.69
60	0.66	3.13
80	1.70	2.08
100	1.41	0.95

5.4.2 Roflumilast-albumin solubilisation

The temporal profile of roflumilast solubilisation by HSA was assessed over a three-day period (Figure 5.3). The solubility profile of roflumilast in Tris and HSA solutions was assessed to determine whether drug solubilisation by albumin can occur in a buffer solution at pH 8.9, as used to generate albumin nanoparticles. Roflumilast was not found to be soluble in tris buffer. Solubilisation in HSA was found to be ~13%, which corresponds to 2.6 µg drug per mg albumin. There was no significant increase in the degree of solubilisation after 24 hours.

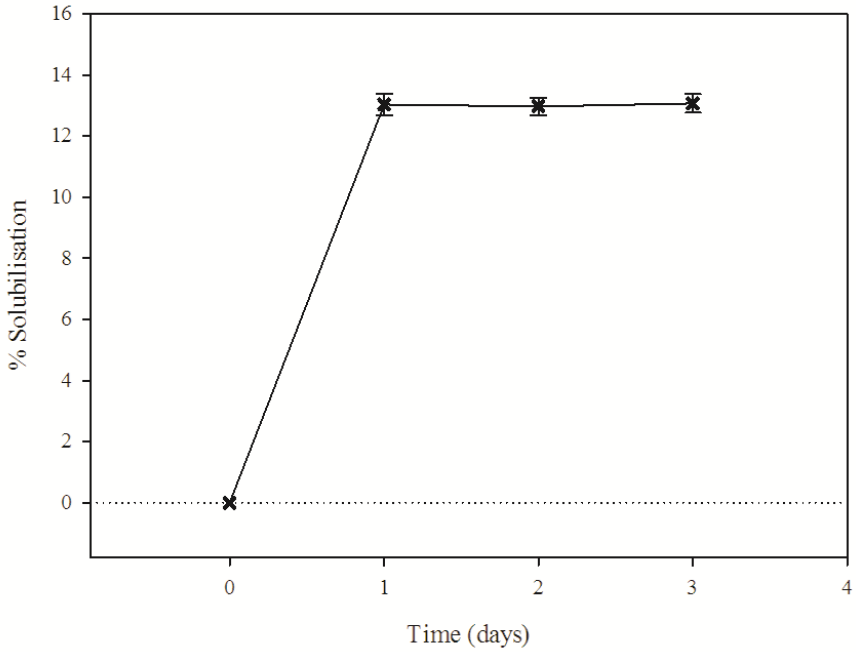

Figure 5.3 Roflumilast time dependent solubilisation profile (1 mg) in 1mL HSA in tris buffer pH 8.9. Results are expressed as a percentage of the original mass (500 µg) at t=0. Results reported are from n=3 experiments.

5.4.3 Roflumilast binding to Sudlow's site I

The importance of assessing a drug's interactions with the binding sites of albumin have been exemplified in Chapter 3. In short, characterisation of the binding of roflumilast to drug binding site I (or Sudlow's site I) of the albumin molecule may determine the effectiveness of HSA as a carrier for roflumilast, and subsequent nanoparticle and dry powder formulation.

When a drug binds to binding site I, it lowers the overall intrinsic fluorescence of the albumin molecule. Thus, characterising this change in fluorescence gives an indication of a drug's affinity for the binding site. Compared with ibuprofen, which does not bind to site I, and bilirubin, which shows a strong affinity to site I, roflumilast showed a weak affinity to the hydrophobic binding site of albumin (Figure 5.4). This affinity can be compared to the previously investigated BTZ compounds in Chapter 3. Despite the low to moderate affinity to binding site I, drug encapsulation in albumin nanoparticles appeared promising.

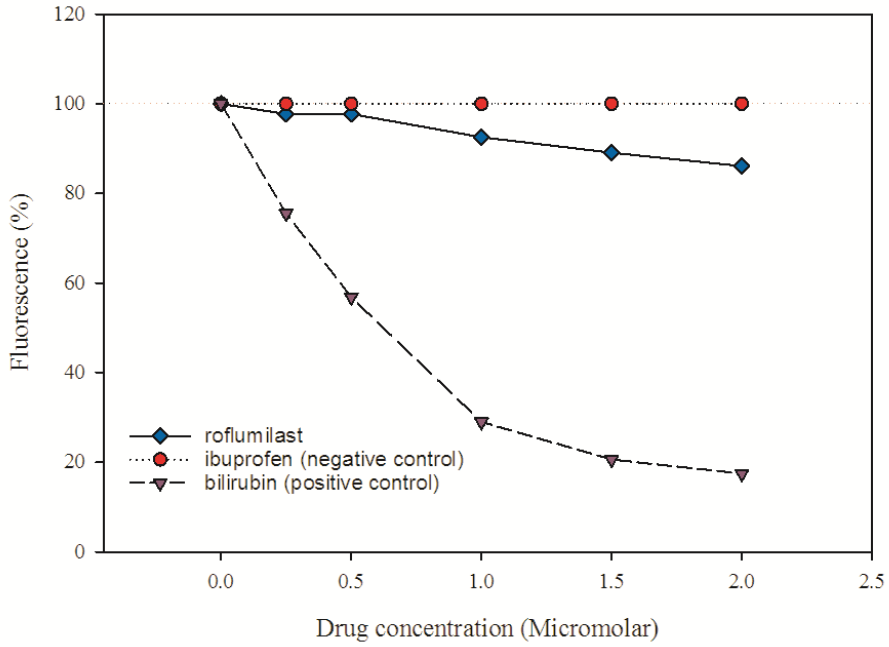

Figure 5.4 Quenching of tryptophan fluorescence indicating the strength of roflumilast binding to Sudlow's site I of HSA. Ibuprofen and bilirubin have been included as negative and positive controls, respectively. Data represent mean and standard deviation; n=3 experiments.

5.4.4 Roflumilast nanoparticle manufacture

Roflumilast-loaded albumin nanoparticles were prepared using method II (Chapter 3) or the *in-situ* loading method for albumin nanoparticle production. Roflumilast was dissolved in ethanol and added to stirred albumin solution during the precipitation step of nanoparticle manufacture. The reason this method was employed as opposed to method I (chapter 3) is because it was hypothesised drug encapsulation would be greater than that shown previously in solubilisation studies (2.6 μg per mg albumin). The encapsulation efficiency (%) was 41% (Figure 5.5) which corresponds to 4.0 μg/mg albumin. Almost the same amount of drug was washed off the particles during the purification process (43.5%) with a residual 12.4% drug quantified in remaining glassware etc. The total mass balance was 96 ± 4.0%.

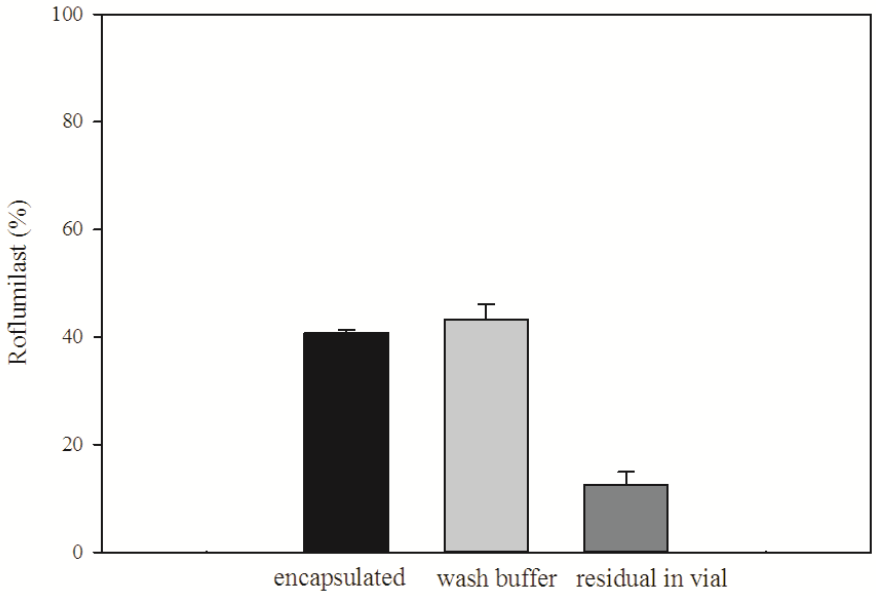

Figure 5.5 Roflumilast encapsulation efficiency (%). Roflumilast encapsulation efficiency is compared to drug recovered from the wash buffer and any residual drug left in glassware.

Nanoparticle size and zeta potential measurements were equivalent in nanoparticles with and without roflumilast encapsulated (Table 5.3). All nanoparticle suspension yields were 100%. Visually, roflumilast-loaded albumin nanoparticles looked similar to control nanoparticles (Figure 5.6).

Table 5.3 Size and zeta potential of roflumilast-loaded albumin nanoparticle suspensions and "blank" unloaded nanoparticles. Values reported are the mean and standard of n = 3 nanoparticle batches.

Formulation	**Size (nm)**	**Zeta potential (mV)**
Roflumilast	124 ± 10	-29 ± 1
Blank	133 ± 11	-31 ± 3

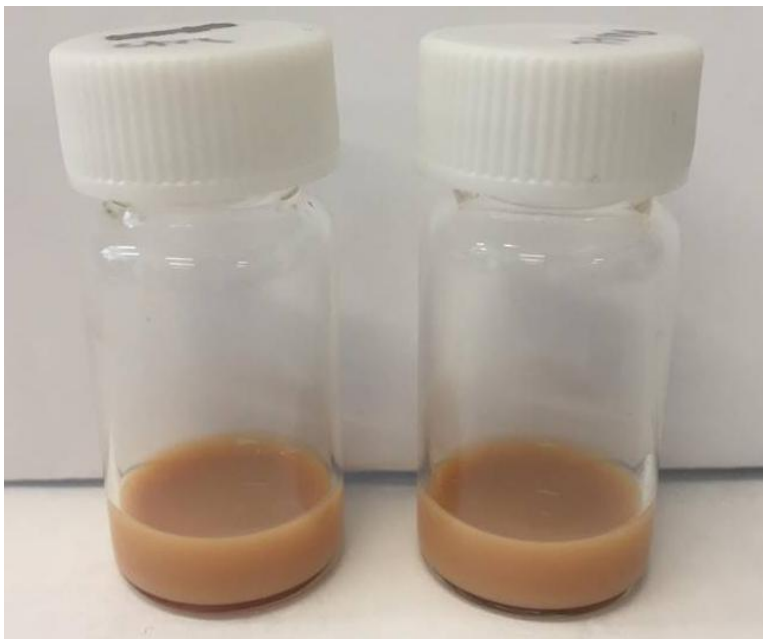

Figure 5.6 Control human serum albumin nanoparticles (left) and roflumilast-loaded human serum albumin nanoparticle suspensions (right).

5.4.5 Stability

Storage stability of roflumilast-loaded albumin nanoparticle suspensions was assessed by measuring the size and polydispersity index of the suspensions at different time points after storage at 4°C and 25°C (Figure 5.7). Colloidal stability of the nanoparticle suspensions was maintained for up to six months at 4°C and up to one month at 25°C, after which visible signs of aggregation were present. No significant differences were observed between control and BTZ-loaded albumin nanoparticle suspensions for all conditions tested.

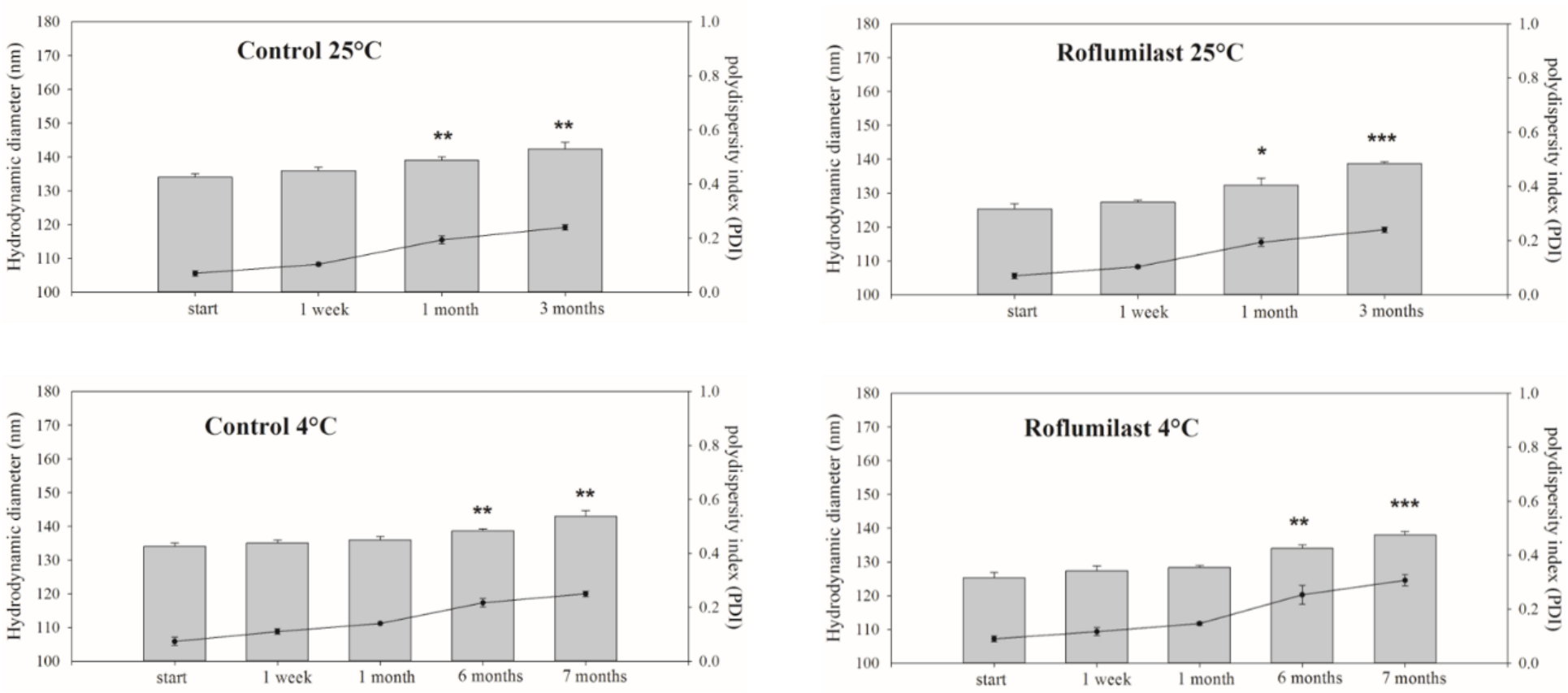

Figure 5.7 Influence of storage time at 4°C and 25°C on particle size and polydispersity of roflumilast-loaded human serum albumin nanoparticles. The bars depict the hydrodynamic diameter (nm, left side axis) of particles and the lines depict the polydispersity index (PDI, right-side axis). Error bars represent the standard deviation of 3 measurements. An asterisk (*, or **, or ***) depicts a statistically significant difference in particle size compared to the initial size ($p < 0.05$, 0.01 and 0.001, respectively)

5.4.6 Spray-dried roflumilast-albumin powders

For spray-drying studies, scaling-up of roflumilast-loaded albumin nanoparticle suspensions was attempted. Mannitol was selected as the spray-drying excipient (as per the optimised formulation selected from chapter 4). Albumin nanoparticles were to make up 40% of the total solids content of the spray-dried formulation. The physico-chemical properties of the three batches of roflumilast-loaded albumin nanoparticles prepared for spray-drying are shown in Table 5.4 along with roflumilast content. As with the original nanoparticle suspensions prior to scaling up, the mean drug loading of the suspensions was 4 μg/mg albumin. All nanoparticle batches maintained a 100% yield. No visual differences were observed between the larger scaled-up suspensions compared to the original suspensions.

Table 5.4 Physico-chemical properties of the three roflumilast-loading albumin nanoparticle suspensions used in spray-drying studies.

Roflumilast-formulation	Size (nm)	Zeta potential (mV)	Drug loading with albumin (μg/mg)
Batch 1	160	-25.6	4.0
Batch 2	201	-28.2	3.1
Batch 3	179	-26.6	4.0

The three batches of roflumilast-albumin nanoparticles were spray-dried in a mannitol matrix using a previously optimised method (chapter 4). The particle size distribution (PSD) data is shown in Table 5.5. Data from an albumin nanoparticulate control without drug is also included for comparison. No significant differences were found between roflumilast and control batches for particle size data and powder yield.

Table 5.5 PSD data for spray-dried powders

Formulation	D_{10}	D_{50}	D_{90}	Yield (%)
Roflumilast	0.99	2.46	5.6	66.5
Control	1.03	2.49	6.15	69.0

Prior to spray-drying nanoparticle suspensions were measured for size and PDI. After spray-drying, powders were reconstituted in water and the supernatant was removed and analysed for the presence of nanoparticles. Nanoparticles were found to be present for all 3 batches of roflumilast nanoparticles tested. Table 5.6 compares the original size of nanoparticles prior to spray drying with the size of nanoparticles found after reconstitution of the spray-dried powders. It also compares roflumilast content quantified from the spray-dried powders with the original drug content quantified. Sizes of all batches of roflumilast-loaded albumin nanoparticles increased after spray-drying, while control nanoparticles showed no significant difference in size. The slight increase in polydispersity index suggests some aggregation may have occurred, although this was not apparent through visual inspection of the nanoparticle suspensions. Drug content was found to be slightly lower after spray-drying the nanoparticle suspensions [prior to spray-drying drug content was found to be 3.9 μg/mg ± 0.3 (roflumilast per mg albumin) whilst after spray-drying, drug content was found to be 3.1 μg/mg ± 0.1]. This could be attributed to loss of drug during the spray-drying process.

Table 5.6 Size, PDI and drug content evaluation of spray-dried powders compared to before spray-drying.

Formulation	Original size (nm) and [PDI]	Size (nm) and [PDI] after reconstitution	Drug loading before spray-drying	Drug loading after spray-drying
Roflumilast batch 1	160 [0.08]	185 [0.14]	4.0	3.9
Roflumilast batch 2	201 [0.10]	234 [0.19]	3.1	2.4
Roflumilast batch 3	179 [0.11]	226 [0.23]	4.0	3.0
Albumin control	165 [0.10]	162 [0.10]	-	-

Aerosol performance of the powders was assessed via FSI screening for fine particle fraction (FPF). The aerosolisation properties of spray-dried roflumilast-loaded albumin nanoparticles were comparable to the control with similar FPF values.

Table 5.7 FPF and blister evacuation for spray-dried powders. Values reported are for n = 3 blisters for n = 1 batches for albumin control, and n = 3 batches for roflumilast-albumin nanoparticle formulations.

Formulation	**Blister evacuation (%)**	**FPF (%)**
Roflumilast-albumin	99.3 ± 0	30.4 ± 5
Albumin control	98.2	34.7

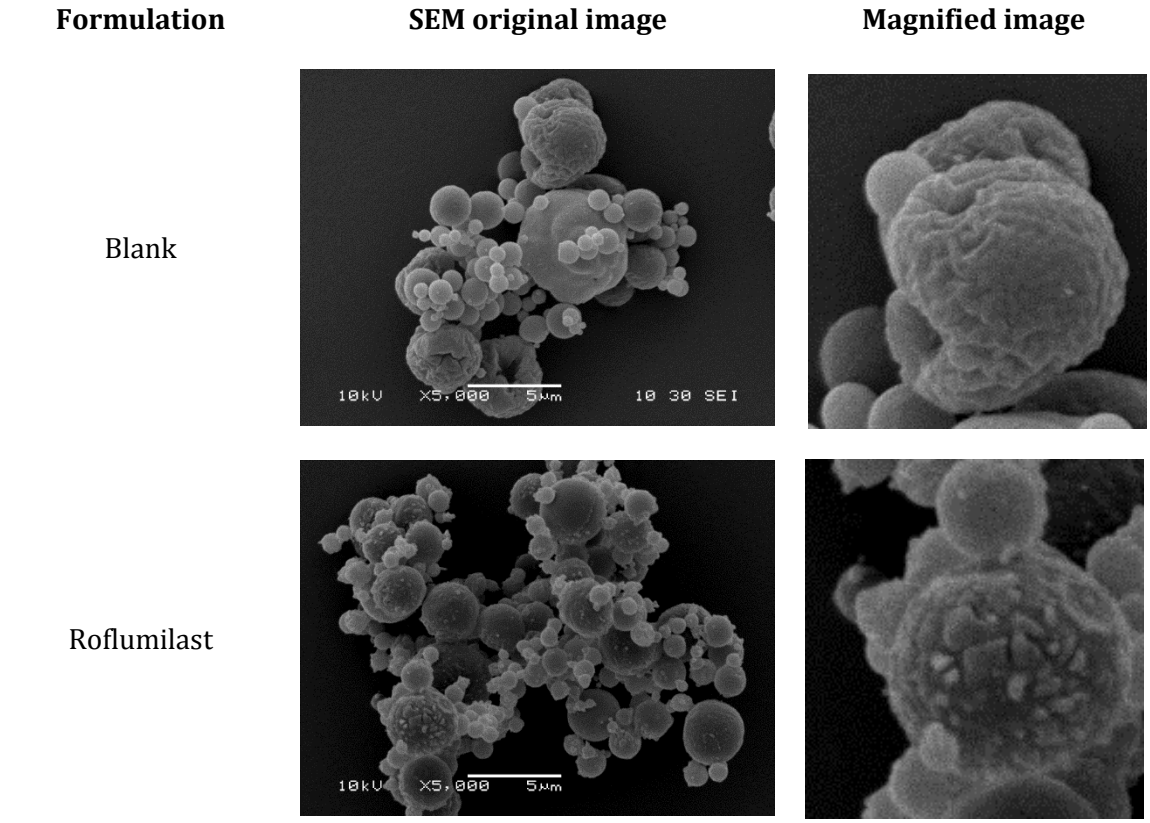

Figure 5.8 Representative scanning electron micrographs (SEM) of spray-dried mannitol microspheres containing blank albumin nanoparticles and roflumilast-loaded albumin nanoparticles.

5.4.7 Roflumilast release studies

Roflumilast release profiles were assessed over a period of 48 hours with and without the presence of trypsin (Figure 5.9). Roflumilast release was less than 20% at 48 h without the presence of trypsin (Table 5.8). The presence of trypsin caused a rapid release of drug for both nanoparticle and spray-dried systems for the first four hours of incubation, followed by a slower release rate for the remainder of the experimental period. At 48 h ~80% of roflumilast was released into the receiving medium for both nanoparticle suspensions and spray-dried powders. No significant differences were found between the two formulations at any time point for both systems with and without protease. Similarity factors (f2) were > 50 for both trypsin and non-trypsin systems which indicated that spray-drying has no significant influence on drug release rate. Dissolution modelling showed roflumilast release for both formulations (nanoparticle suspensions vs. spray-dried powders) in the presence of trypsin followed Weibull model kinetics (R^2 = 0.9883 and 0.9891, respectively). Roflumilast release for the two formulations without trypsin also followed Weibull release kinetics with R^2 = 0.9984 and 0.9975, respectively. The Weibull model is only descriptive and not deduced from any physical law (Costa & Lobo 2001).

Table 5.8 Comparison of cumulative percentage and mass of roflumilast released from HSA nanoparticles and spray-dried powders over 48 h, both in the presence and absence of trypsin. Data represent the mean and standard of n = 3 experiments.

Trypsin (-)				Trypsin (+)			
	t = 48 h roflumilast (%)	t = 48 h roflumilast (µg)	f2 Similarity factor		t = 48 h roflumilast (%)	t = 48 h roflumilast (µg)	f2 Similarity factor
Nanoparticles	16.0 ± 2.0	6.4 ± 0.8	52	Nanoparticles	80.0 ± 5.0	31.9 ± 2.0	52
Spray-dried powder	19.0 ± 1.0	7.6 ± 0.4		Spray-dried powder	82.0 ± 7.0	32.8 ± 2.8	

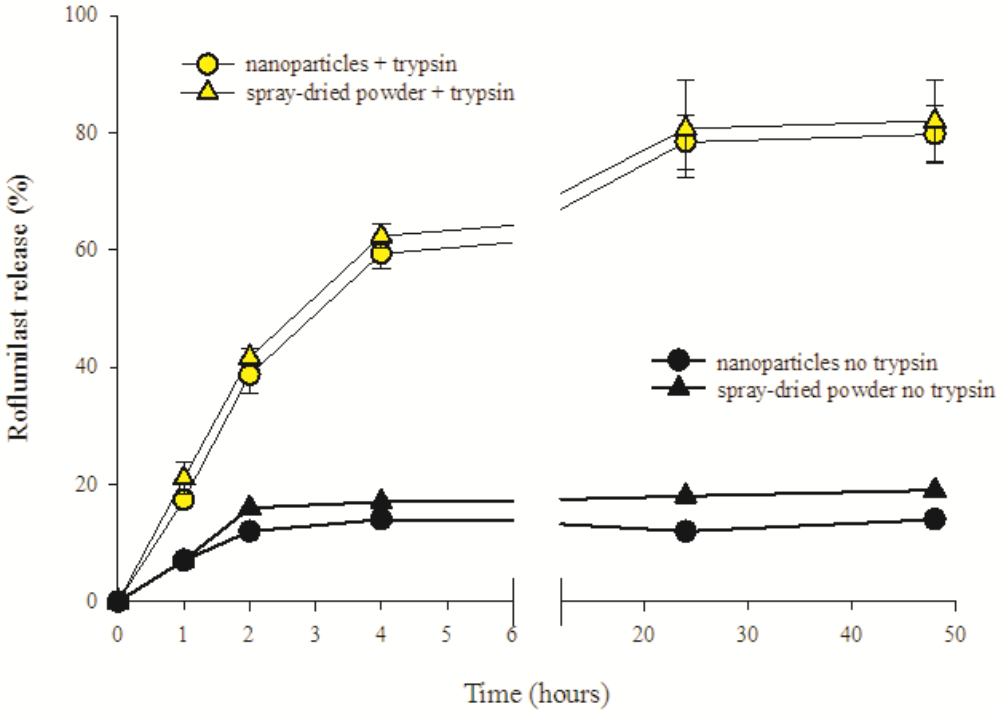

Figure 5.9 Cumulative roflumilast release from HSA nanoparticles and spray-dried powder with and without the addition of 0.1 mg/mL trypsin over 24 h at 37°C. Data represent the mean and standard deviation of n = 3 experiments.

5.4.8 PreciseInhale®

PreciseInhale® is a tool developed by Inhalation Sciences used to generate data on aerosol dosing. Customisation of the settings (i.e. tidal volume, breathing rate and route of administration) allows the generation of aerosol data for various models, such as guinea pigs, rats and the human lung model. In this work, the PreciseInhale® was used to carry out a full deposition study on the spray-dried powders generated- similar to a Next Generation Impactor (NGI) study but the dose is spread as it would in a pharmacokinetic study. Spray-dried powders were first assessed for deposition in stages 1-8 and end filter by Marple Cascade Impactor (Figure 5.10). Three systems were tested: 100% mannitol spray-dried powder, a blank albumin nanoparticulate system in a mannitol matrix, and finally roflumilast-loaded albumin nanoparticles in a mannitol matrix. This was to assess the effect (if any) of incorporating nanoparticles and a model drug into the spray-dried formulation. The mannitol formulation was found to have highest deposition in stage 6 (33.1%) followed by stage 5 (17.0%) and blank albumin nanoparticle and roflumilast-

loaded nanoparticle formulations had highest deposition in stage 5 (27.7% and 31.7% respectively). Powder deposition at stage 5 for blank albumin nanoparticles and roflumilast were found to be statistically higher than the mannitol spray-dried powder ($p < 0.05$, one way ANOVA, post Holm-Sidak test). No other statistically significant differences were noted for deposition profiles of the powders.

The theoretical composition deposition fraction of the particles and the fractional distribution between the bronchi and alveoli was calculated for the three powder formulations (Table 5.9). No sigificant differences were found in the deposition distribution patterns between the three powders tested, however the incorporation of nanoparticles in the spray-dried formulation caused a very slight increase in total deposition fraction (35% and 36% for blank and roflumilast-loaded nanoparticles respectively, compared to 33% for mannitol powder). All powders demonstrated roughly 1:1 deposition for the bronchi and alveoli i.e. of the inhaled fraction, half would target the alveoli and half would target the bronchi.

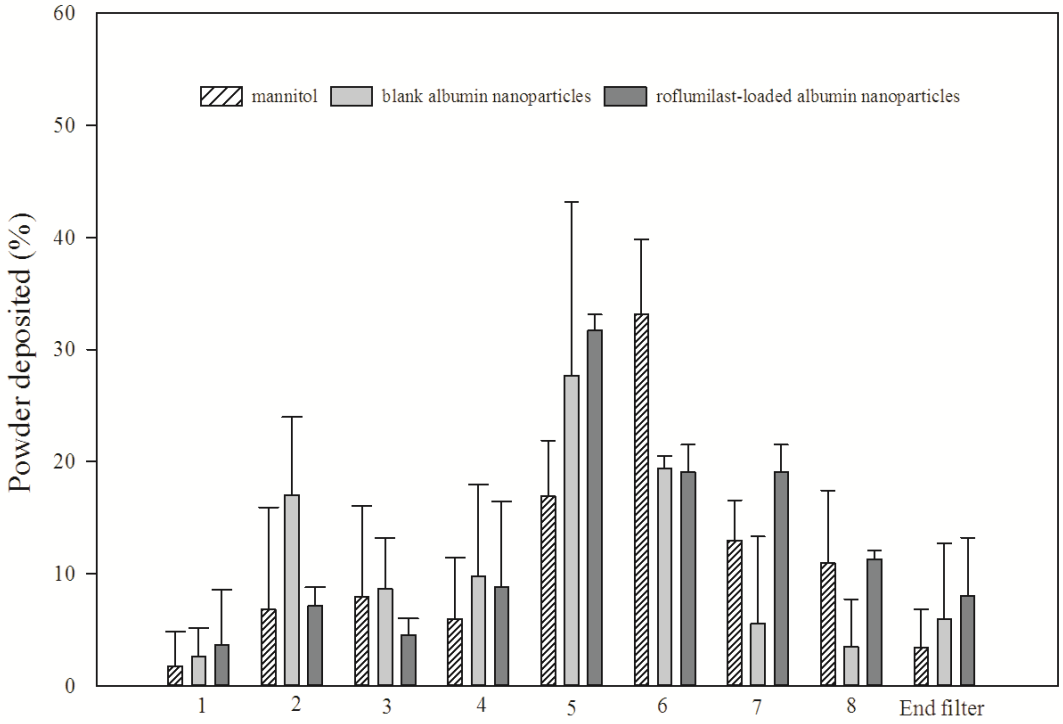

Figure 5.10 Percentage of powder deposited in different stages of the Marple Cascade Impactor for spray-dried powders containing a) 100% mannitol, b) blank albumin nanoparticles in a mannitol matrix and c) roflumilast-loaded albumin nanoparticles in a mannitol matrix. Data represent the mean and standard deviation of n = 3 replicates.

Table 5.9 Total deposition fraction and fractional deposition in bronchi and alveoli as determined by PreciseInhale experiments for spray-dried formulations a) 100% mannitol b) blank albumin nanoparticles in a mannitol matrix and c) roflumilast-loaded albumin nanoparticles in a mannitol matrix. Data represent the mean and standard deviation of n = 3 experiments.

Powder Formulation	Total Fraction of aerosol deposition (%)	Bronchial deposition (%)	Alveolar deposition (%)
Roflumilast-loaded albumin nanoparticles	36 ± 0.0	45 ± 0	55 ± 0
Unloaded nanoparticles	35 ± 0.1	49 ± 0	51 ± 0
Mannitol	33 ± 0.0	45 ± 0	55 ± 0

5.5 Discussion

It was previously demonstrated in Chapter 4 that albumin nanoparticles could be spray-dried in a mannitol matrix. To gain understanding of the clinical application of this drug delivery platform, the inclusion of an API is necessary. It is important to note the effects of the API on the physical characteristics of the formulation itself, as well as how the formulation behaves in biologically relevant models. Therefore, in this chapter the effect of the incorporation of a model drug with the albumin nanoparticles in the spray-dried powder formulation was investigated.

It is difficult to compare the release profile of roflumilast from these studies with the literature, as roflumilast and albumin nanoparticulate systems have not been investigated previously. However there have been similar drug release studies with different APIs from albumin nanoparticles and they all vary in their findings. Das et al. report a drug release of 90% after 72 hours from aspirin loaded nanoparticles under physiological conditions (Das et al. 2005) and Merodio et al. found that 60% of the initially loaded drug was release from their most efficient nanoparticle after 5 days of incubation (Merodio et al. 2000). In contrast, Lin et al. 2001 only found a release of less than 18% from their surface-modified albumin nanoparticles after 8h under physiological conditions. The drug release from those nanoparticles was increased to >90% in the presence of trypsin (Lin et al. 2001). Interestingly, trypsin did not show an effect on the release profile in the experiments of Merodio et al. (Merodio et al. 2000). This is in line with the seemingly recurring findings in this work where trypsin appears to greatly assist in the release of drug from the particles. Even without the addition of trypsin, up to 19% roflumilast was detected in the receptor medium. This could be indicative of some drug particle release from the nanoparticles having been loosely attached to their surface, while the trypsin broke down the albumin nanoparticles and released drug contained within them. This combination of different drug-albumin interactions could explain the release patterns observed.

The key finding from the drug release studies in this work is that the formulation of the nanoparticles in dry powder form had no effect on the release profiles of roflumilast- as hypothesised with the selection of mannitol as the excipient due to its excellent aqueous solubility. Kinetics modelling showed roflumilast release for all systems tested followed Weibull release kinetics. Weibull release is modelled by Equation 5.1, where m is the accumulated fraction of drug in time t, a is the time scale of the process and T_t represents the lag time before the onset of the drug release process which is usually zero. The shape parameter is b which characterises the curve as either exponential (b = 1), s-shaped with upward curvature (b > 1) or parabolic with a higher initial slope and then following the exponential (Costa & Lobo 2001). The Weibull model is only empirical and does not have any kinetic element- it can only describe the release kinetics of the drug but not adequately characterise it and therefore its uses are limited (Costa & Lobo 2001).

Equation 5.1

$$m = 1 - \exp\left[\frac{-(t - T_t)^b}{a}\right]$$

It is unclear why spray-drying seemed to cause drug loss. Roflumilast retention caused by high inlet temperature could be a possible explanation for this (Broadhead et al. 1992). SEM micrographs show spherical particles for both formulations with and without nanoparticles, with nanoparticle-containing formulations appearing to have a slight rougher surface. Powders containing roflumilast showed some bumps on the surface of the spherical particles. Further particle surface analysis would need to be carried out in order to assess whether this is an effect of the drug itself. This could be carried out using fluorescent labelling techniques [e.g. confocal laser scanning microscopy (Sham et al. 2004)]. Raman microscopy can provide structural information on a molecular level and would be able to distinguish between roflumilast and the mannitol matrix and albumin. Scanning electron microscopy with energy-dispersive X-ray analysis (SEM-EDX) may also work. This technique works by quantitative and qualitative analysis of each element in the

sample and as roflumilast contains fluorine and chlorine it would be easily distinguishable from the mannitol matrix and albumin. However, the small amount of drug present in the sample may be difficult to detect.

Dose/deposition modelling experiments with the PreciseInhale® found that the average deposition fraction for spray-dried powders containing roflumilast nanoparticles was 36%. This is also similar to the FPF calculated from FSI experiments (30%). This means the administration (aerosol delivery via inhalation) of a single capsule containing 10mg of powder would result in a roflumilast dose of roughly 6 μg. The advantages of direct pulmonary targeting have been touched upon earlier. Direct aerosol delivery enables efficacy of a drug to be achieved at a fraction of the oral dose, e.g. 200-800 μg vs 4-16 mg for salbutamol in humans (>200-fold decrease in dosage) and pre-clinical efficacy has been reported with 33-fold lower doses of inhaled rifampicin compared to oral dosing in preclinical studies (Pandey et al. 2003). This data gives a good indication for dose estimation in preparation for pharmacokinetic studies. Opportunities to deliver even higher doses to the lungs could occur with multiple dosing or larger dosing devices (carrying > 10mg powder per dose) or even further optimisation of the nanoparticle formulation to allow a higher roflumilast to albumin ratio, thereby increasing the overall drug content. As the oral dose of roflumilast in tablet form is 250 micrograms daily, the predicted dose values calculated here appear promising for achieving a therapeutic effect, however this would need to be assessed with preclinical pharmacodynamic studies to determine the therapeutic dosage for aerosol delivery of these powders.

5.6 Conclusion

In summary, the work in this chapter has culminated in the development of a formulation for pre-clinical evaluation. It could be shown from this work that the incorporation of a model drug with the developed dry powder formulation was possible, with good drug recovery from the spray-drying process and little effect on the aerodynamic properties of the powders produced. Roflumilast-albumin interactions were studied, roflumilast-loaded albumin nanoparticles were successfully manufactured and spray-dried using the optimised formulation from Chapter 4. Roflumilast was released from the spray-dried microcarriers in very much the same manner as they did in suspension form, showing the mannitol matrix in which they are formulated does not hinder drug release. Finally, deposition modelling using the PreciseInhale® system showed promise for the clinical application of dry powder albumin nanoparticle-based formulations for pulmonary drug delivery.

Chapter 6 General discussion

This chapter will recap the general advantages and state of the art in regard to inhaled nanomedicines, followed by a review of the specific aims of this thesis and how these were addressed by the development of albumin-based formulations (albumin solution and albumin nanoparticle-based formulations) for the delivery of hydrophobic model anti-tuberculosis drugs (BTZs) as well as the development of respirable microparticles containing albumin nanoparticles for the delivery of another model hydrophobic drug compound (roflumilast).

Delivery to the lungs provides an attractive route of drug administration for several reasons. As well as offering a non-invasive route for drugs normally delivered by injection, there is potential for achieving an improved pharmacokinetic profile, the prospect of reduced systemic side effects, use of lower doses and direct targeting for pulmonary diseases (Newman 2017). Unfortunately, there are some challenges with using the pulmonary route of drug delivery including the short duration of action of therapeutic agents (possibly due to the high permeability rate of the drug), the natural defence mechanisms of the lung designed to remove inhaled materials as well as difficulties in the presentation of drugs in respirable formulations. Hydrophobic APIs often present more difficulties than their hydrophilic counterparts when it comes to the design of an inhalable formulation in terms of stability, lung targeting and efficacy.

Nanoparticles offer the opportunity to assist with the delivery of hydrophobic drug compounds by increasing their solubility. They also offer the advantage of sustained drug release, thereby reducing dosing frequency (Sung et al. 2007). In terms of the treatment of respiratory diseases, nanoparticles have the potential to increase and sustain drug levels locally in the lung i.e. the site of the disease. This local targeting of disease is beneficial, particularly in combination with the potential of nanoparticles to protect APIs from degradation until they reach their target. Furthermore, their small size is thought to help reduce mucociliary clearance and clearance by macrophages (Geiser et al. 2008).

Historically, there have been safety concerns regarding inhalation of nanoparticles. It has been reported that long term exposure to nanoparticles may cause serious damage to health such as pulmonary fibrosis, granulomas, hypoxaemia and pleural effusion (Bakand et al. 2012; Song et al. 2009; Oberdörster et al. 2005). It has also been found that that inhaled nanoparticles may pass into the systemic circulation and accumulate in secondary organs such as the brain and organs of the digestive system (Balasubramanian et al. 2013; Geiser & Kreyling 2010). Several possible mechanisms of nanoparticle toxicity have been suggested, ranging from immediate reactions to long term effects (Bakand et al. 2012). Nanoparticles can penetrate cell membranes, enter different compartments of the cell and be a direct cause of cell injury owing to their small size (Song et al. 2009; Gojova et al. 2007). The complex mechanisms of nanotoxicity make it hugely important to gain a better understanding of the fate of nanoparticles in the lungs including their biological interactions and potential nanotoxicity before they may be considered as clinically acceptable for pulmonary drug delivery purposes. This means that as well as being retained in the lung for the duration required in order to deliver the therapeutic payload, it has to be demonstrated that particles (and degradation products) are also effectively cleared from the lungs and have no or little associated toxicity i.e. show that they are biodegradable and biocompatible.

There are technical challenges associated with the development of nanoformulations for delivery to the lungs. This includes a reproducible manufacturing method in which the API must be compatible with the excipients and manufacturing conditions. Nanoparticles must have the ability to interact with APIs to achieve adequate drug loading but release drug upon delivery of the nanoformulation to exert its therapeutic effect. This may prove to be difficult with particularly hydrophobic APIs. Stability of nanoparticle-based formulations can be an issue owing to their small size and high surface area which can lead to particle agglomeration. The development of a larger microparticle-containing nanoparticles can

improve the stability of the formulation as well as making it easier to deliver the nanoparticles to the lung (as smaller particles would just be exhaled back out again). The formulation must also be safe and effective at delivering therapeutic agents to the lung via inhalation.

The aim of this work therefore was to study the potential of albumin nanoparticles as drug carriers for delivery to the lung, with a focus on hydrophobic drug compounds. This included the development of respirable microparticles containing drug-loaded albumin nanoparticles for delivery to the lung by inhalation. Although albumin nanoparticles have been studied previously (Elzoghby et al. 2012), this study investigated how nanoparticle-albumin interactions affected drug-loading using different methods of manufacture and the stability of the nanoparticles on storage/release of drug after administration. There is a paradox with many nanomedicines that achieving high loading of a drug with affinity for the nanoparticle may be detrimental to the liberation of the drug after administration. The hypothesis tested for albumin nanoparticles was that proteases in the lungs will enzymatically break down the particles after administration which will release drug and prevent particle accumulation. Not only was this tested by measuring drug release using model fluids to represent lung protease concentrations, the effectiveness of anti-tuberculosis drugs when delivered in the particle formulation was investigated using an infected macrophage model.

In this thesis, albumin nanoparticles were generated initially from bovine serum albumin (BSA) using a previously reported modified desolvation technique (Weber, Kreuter, et al. 2000). This work was then translated to human serum albumin (HSA) (Chapter 2) to verify the findings using pharmaceutical grade material that has been used previously in medicinal products. No differences were found between nanoparticles manufactured with BSA and HSA. HSA was subsequently employed for all the following work. The physical characteristics of the nanoparticle suspensions (size, zeta potential) were carried out in

different conditions to explore the robustness of the measurement technique (DLS) and the reproducibility of the nanoparticle manufacturing method. Nanoparticles were formed with sizes between 100-200 nm, with low polydispersity and zeta potential (when measured in neutral medium i.e. water) of ~-25 mV, and when measured in saline, the zeta potential increased to ~-10mV due to shielding effect. This was found to be similar to the properties of previously manufactured albumin nanoparticles using the similar desolvation method (Zhao et al. 2010; Langer et al. 2003). The suspending medium had no effect on the size characterisation of nanoparticle suspensions.

Both BSA and HSA nanoparticle suspensions were found to have similar stability. Both were physically stable for up to one month at 25°C while up to six months stability was observed for nanoparticle suspensions stored at 4°C. This was consistent with preliminary studies and previously reported studies with BSA (Woods et al. 2015). Using a simple protease-digestion model to look at the breakdown of albumin nanoparticles, albumin nanoparticles were found to be stable in PBS without the presence of a protease enzyme, whereas in the presence of enzyme at concentrations similar to those found in the lung lining fluid, there was an initial fast rate of particle breakdown followed by a slower phase. TEM imaging confirmed the digestion of albumin nanoparticles. This data was promising in terms of the application of albumin nanoparticles as a controlled release formulation as it showed they are likely to be retained in the lungs for a timeframe sufficient to have a therapeutic effect but are subject to enzymatic degradation which alleviates concerns about their elimination from the body.

The loading of drug compounds in albumin nanoparticles has been carried out previously. However these studies have mostly used well-established drugs that are “easier” to formulate as they have favourable solubility e.g. aspirin and ganciclovir (Das et al. 2005; Merodio et al. 2000). As well as providing a controlled release platform for drug delivery to the lung, albumin nanoparticles were investigated as a carrier for very poorly soluble

drug compounds that have or would have poor bioavailability if formulated as a conventional oral formulation (e.g. tablets). In Chapter 3, benzothiazinones were used as model compounds for this purpose. It is important to understand how drugs interact with albumin and so BTZ-albumin interactions were studied in this chapter. Interesting insights into binding with Sudlow's binding site I on the albumin molecule were noted, namely the relationship between the binding and release of BTZ compounds, with the more hydrophobic FG 2 demonstrating stronger binding and lower drug release compared to the less hydrophobic IR 20. Despite Sudlow's site (or drug binding site I) being the most important for hydrophobic molecules (Ghuman et al. 2005), it is also important to note there are other binding sites on the albumin molecule which were not characterised in this work, namely drug binding site 2. Due to time constraints the affinity of tested compounds for drug binding site 2 was not explored. Since this site is known to largely bind polar molecules it was not considered as necessary for this work, however it would be interesting to compare binding sites and drug-albumin interactions more fully. Not least, it would be interesting to understand how binding alters as the particles degrade and albumin or albumin fragments and drug are released.

Drug loading was optimised by adopting slight differences in the manufacturing method of the nanoparticles. From the drug loading assessment, it became apparent that delivery in albumin nanoparticles is suitable only for drugs with high potency (i.e. activity in the micromolar range). For less potent compounds, the amount of albumin that would need to be delivered would be larger, and the effects of this excipient burden on delivery by inhalation and toxicity. would need to be explored. Although the loading and losses of drug were mapped during the nanoparticle manufacture process to optimise the method, in order for the drug to exert a therapeutic effect, it must be able to be released from the nanoparticles. Therefore, drug release experiments were carried out in release buffer characteristic of the lung lining fluid. A reassuring finding from these experiments were that the formulations were very stable in aqueous suspension without protease, indicating

good stability of the nanoparticles. However, upon the addition of trypsin a rapid release of drug was observed. An advantage of albumin nanoparticle systems compared to nanoparticles made from other materials (e.g. synthetic polymers, lipids) is that despite the change in albumin structure when in nanoparticle form, enzymatic clearance mechanism for endogenous albumin also play a role in their clearance, alleviating concerns about accumulation.

It was expected that the drug-loaded human serum albumin nanoparticles would be retained in the lungs when delivered *in vivo* with clearance patterns similar to the observations from previous studies with blank (unloaded) BSA nanoparticles. An *in vivo* biodistribution and clearance study comparing BSA nanoparticles with BSA solution showed that albumin delivered in nanoparticles was retained longer in the mouse lung compared to albumin solution and was distributed more highly into macrophages and lung tissue (Woods et al. 2015) . The time-frames observed fit the findings for nanoparticle degradation from experiments in this thesis. When BTZ-loaded albumin nanoparticles were evaluated in the *in vitro* infected macrophage model, the drug delivered by carrier was equally or more effective than when delivered unbound. This suggests that not only may the drug be retained in the lungs for longer, it may be delivered into cells more effectively where it can be released to affect the enhanced chemotherapeutic effect.

Formulation into larger microparticles containing albumin nanoparticles was conceived as the necessary next step for developing albumin nanoparticles for inhalation. The small size of the nanoparticles makes them prone to aggregation and if delivered in their primary particle size it means it is likely they would be exhaled back out again following inhalation, hence formulation as part of a larger microparticle would provide a respirable powder with the prospect of high lung deposition. It was hypothesised that spray drying would provide a particle engineering method to embed the nanoparticles in a readily-soluble matrix that would form respirable microparticles that would dissolve rapidly on contact

with aqueous medium and release the nanoparticles without any impairment of their form or functionality.

Heuristic developmental studies with spray-drying confirmed the exceptional robustness of the albumin nanoparticles as they were recoverable without any change to their original properties after the spray-drying process. It was anticipated that albumin as a protein may not be able to withstand the inlet and outlet temperatures of the spray drier; however, this was not the case. BSA-apiginen conjugates produced by a different technology where homogenisation is employed to produce such conjugates, were spray-dried in a study by Papay et al. (Pápay et al. 2017). Similar outlet temperatures were used in this study, with no adverse effects observed for the albumin formulation, however one should be wary about comparing these findings with the albumin systems spray-dried in this thesis as differences in Papay's include: i) albumin is utilised as a stabiliser with the drug to form conjugates, rather than active loading of drug into nanoparticles formed of albumin, ii) the study use of BSA rather than HSA iii) different excipients were used. A major difference found in the spray-dried powders produced by Papay et al. compared to the ones produced in this thesis is the drug release. Even without enzymes in the release buffer up to 80% of drug was released from the formulation. It appears the albumin played little or no part in modulating the release of the drug and its role in the formulation was to facilitate the spray-drying process to produce a respirable powder. The drug-loaded albumin nanoparticles synthesised and studied in this thesis control the release of drug over a longer time period and are stable without the presence of enzyme.

Following the approach of using pharmaceutically-acceptable materials, it was decided to utilise commonly used spray-drying excipients that fall under the category of "generally regarded as safe" excipients or gras excipients. Another consideration with regard to translation to the clinic was the importance of optimising for albumin nanoparticle content in order to achieve maximise the drug: excipient ratio and deliver the highest

payload possible of drug-loaded nanoparticles without adversely affecting the aerodynamic properties of the powder (chapter 4).

Interestingly, switching from BTZ to a new drug for further formulation studies proved unproblematic suggesting that for certain classes of API, the albumin nanoparticle may provide a platform technology. In terms of roflumilast-albumin interactions, roflumilast behaved in a similar way to the BTZ compounds (chapter 3) in its degree of binding to drug binding site I on the albumin molecule, and degree of solubilisation by albumin. However, there were differences in the drug release characteristics of both spray-dried and non-dried roflumilast nanoparticle systems compared to the BTZ release characteristics from chapter 3. BTZ release from albumin nanoparticles was very low in the absence of trypsin (<5%) however for the roflumilast-albumin formulations, drug was released to the extent of almost 20% after 48 h in aqueous suspension, even in the absence of protease. This suggests different mechanisms of binding of roflumilast to the albumin nanoparticles. Drug may attach loosely to the surface of the albumin nanoparticles, and it may be these loose interactions that cause drug release even without the breakdown of the nanoparticles with protease. The roflumilast-loaded albumin nanoparticles may contain more of these loose interactions compared to the BTZ-loaded albumin nanoparticles. Drug may also bind tightly within the core of the albumin nanoparticles upon manufacture, and these drug molecules may only be released after the digestion of the albumin nanoparticles with trypsin. It was encouraging to see the mannitol matrix of the spray-dried powder formulations had no effect on the release behaviour of roflumilast from the albumin nanoparticles as it was important for the albumin nanoparticles themselves to dictate the release of the drug.

The main findings of this work have been to advance the understanding of how to design and formulate albumin nanoparticle-based formulations for potential application in inhaled drug delivery. The robustness and ease of scale up of the manufacturing method,

versatility of albumin-drug interactions and finally the development of respirable microparticles containing albumin nanoparticles are among the key features of this work. The demonstration that delivery of BTZ using nanoparticles can enhance chemotherapeutic activity provides encouragement to develop further albumin NP formulation to test the effect on pharmacokinetics and pharmacodynamics *in vivo*.

Future work

As a follow-up to the aerosol testing carried out on the spray-dried powders containing roflumilast-loaded albumin nanoparticles, further quantitative analysis of the drug in a next generation impactor (NGI) study would be useful to evaluate the aerodynamic particle size distribution and provide an estimate of the fate of the likely regional deposition of drug in the lungs after aerosol delivery. The *in vivo* behaviour of the microparticle systems developed in this thesis needs to be investigated to augment the understanding of the clearance and biodistribution of the microparticles and their payload of nanoparticles and API. This could be coupled with imaging studies by labelling the albumin nanoparticles. In one study albumin nanoparticles were labelled with fluorescein isothiocyanate (Roser et al. 1998). Further physical assessment of the powders may also be useful, such as x-ray powder diffraction, differential scanning colorimetry (DSC), as well as the use of techniques to look at the distribution of nanoparticles within the microparticle matrix and at the surface.

Other excipients matrices could be investigated, this work evaluated trehalose/leucine, but focused on mannitol, however there are other "generally regarded as safe" excipients that could be explored, such as l-alanine (Razavi Rohani et al. 2014). Only dry powders were explored in this work as formulation options for the albumin nanoparticles. Despite previous studies investigating nebulised aerosols containing polymeric nanoparticle dispersions (Dailey et al. 2003; Yang, Tam, et al. 2008; Beck-Broichsitter et al. 2012), there are no studies looking at the delivery of albumin nanoparticle suspensions to the lung

through nebulisation, therefore nebulisation should also be explored for manufacturing and scale-up feasibility, stability and effectiveness.

Despite the BTZs being model drugs for the purpose of this thesis, the novel BTZ compounds are of great interest for tuberculosis treatment (Makarov et al. 2014; Trefzer et al. 2012; Batt et al. 2012). The infected macrophage model provides a good first step for investigating the potential benefits of an albumin nanoparticle carrier for the BTZ compounds. However, it would be a key finding to evaluate the activity of the BTZ-albumin systems *in vivo* to test whether the encouraging findings *in vitro* can be reproduced after pulmonary delivery in a pre-clinical model of tuberculosis.

As this work looked at demonstrating the potential of albumin nanoparticles as a hydrophobic drug carrier, it would be useful to assess how other similar drugs behave in these systems. The typical drug that may be of use to pursue would be hydrophobic and have relatively high potency i.e. drugs that would benefit from an improved solubility offered by albumin nanoparticles, or that otherwise have poor bioavailability as an oral formulation. Medicines that only exist as injectable formulations may benefit from a less invasive route of administration, such as pain relief medication or protein-based biologics such as monoclonal antibodies. Other anti-infective drugs for respiratory infections may also be suitable candidates for this albumin nanoparticle-based delivery platform if the enhanced lung exposure leads to greater efficacy and reduces the dose to a realistic inhaled dose. Inhaled tobramycin exists as a product in the treatment of cystic fibrosis, other antibiotics are nebulised “off-label” in the treatment of cystic fibrosis, however more work needs to focus on developing inhaled antibiotics for other respiratory conditions such as amikacin for the treatment of non-tuberculous mycobacterial disease (Quon et al. 2014).

It would be useful to assess the activity of the roflumilast-loaded albumin nanoparticle containing microparticles in an appropriate disease model. The bronchodilator and anti-inflammatory properties of roflumilast have been investigated previously in rats and guinea pigs (Bundschuh et al. 2001). Roflumilast is a drug that would benefit from a delivery system that improves lung selectivity in order to avoid systemic side effects. The formulation developed provides an opportunity to measure pharmacokinetic/pharmacodynamic relationships and use these to inform the design and development of the drug carrier system. Although a few studies have looked at the safety profile of albumin nanoparticles, this requires further investigation. Being an endogenous molecule makes albumin attractive for drug delivery purposes as does its inert nature. The toxicity and safety of the albumin nanoparticles and microcarrier systems needs to be assessed in acute and longer-term studies and an evaluation is needed regarding the potential for introducing immunogenicity as a result of the formulation steps, e.g. cross linking and aggregation of partially degraded particles. Histopathological examination of a range of organs following inhalation can be used to evaluate systemic toxicity, as well as careful histopathological evaluation of the respiratory tract as it is the site of most of the deposition of the inhaled dose (Wolff 2015).

Conclusion

The work in this thesis has demonstrated that albumin nanoparticles manufactured by a modified version of a well-documented method can be loaded with very hydrophobic drugs, release them in a therapeutically relevant timeframe and provide an enhanced chemotherapeutic effect in a relevant *in vitro* disease model. The albumin nanoparticles were formulated as respirable microparticles within a mannitol matrix with good respirable properties. The formulation was developed to deliver roflumilast - a drug with therapeutic relevance for pulmonary inflammation. Dose deposition studies using the PreciseInhale® modelling system showed good potential bronchial/alveolar deposition for the powders. In conclusion, this work has shown the potential of albumin

nanoparticles as a carrier for poorly soluble drugs, as a carrier with controlled release properties, and finally as the key component of an inhalable microcarrier formulation for the delivery of drugs to the lung via inhalation.

References

Abou-Zied, O.K. & Al-Lawatia, N., 2011. Exploring the Drug-Binding Site Sudlow i of Human Serum Albumin: The Role of Water and Trp214 in Molecular Recognition and Ligand Binding. *ChemPhysChem*, 12(2), pp.270–274.

Adler, M. & Lee, G., 1999. Stability and surface activity of lactate dehydrogenase in spray dried trehalose. *Journal of Pharamceutical Sciences*, 88(2), pp.199–208.

Aguzzi, C. et al., 2010. Mathematical models describing drug release from biopolymeric delivery systems. *Materials Technology*, 25, pp.205–211.

Al-Qadi, S. et al., 2012. Microencapsulated chitosan nanoparticles for pulmonary protein delivery: In vivo evaluation of insulin-loaded formulations. *Journal of Controlled Release*, 157(3), pp.383–390.

Andrade, F. et al., 2013. Nanotechnology and pulmonary delivery to overcome resistance in infectious diseases. *Advanced Drug Delivery Reviews*, 65(13–14), pp.1816–1827.

Anhorn, M.G., Mahler, H.C. & Langer, K., 2008. Freeze drying of human serum albumin (HSA) nanoparticles with different excipients. *International Journal of Pharmaceutics*, 363(1–2), pp.162–169.

Arnedo, A., Espuelas, S. & Irache, J.M., 2002. Albumin nanoparticles as carriers for a phosphodiester oligonucleotide. *International Journal of Pharmaceutics*, 244(1–2), pp.59–72.

Bailey, M.M. & Berkland, C.J., 2009. Nanoparticle formulations in pulmonary drug delivery. *Medicinal Research Reviews*, 29(1), pp.196–212.

Bakand, S., Hayes, A. & Dechsakulthorn, F., 2012. Nanoparticles: a review of particle toxicology following inhalation exposure. *Inhalation Toxicology*, 24(2), pp.125–135.

Balasubramanian, S.K. et al., 2013. The effect of primary particle size on biodistribution of inhaled gold nano-agglomerates. *Biomaterials*, 34(22), pp.5439–5452.

Batt, S.M. et al., 2012. Structural basis of inhibition of Mycobacterium tuberculosis DprE1 by benzothiazinone inhibitors. *Proceedings of the National Academy of Sciences*, 109(28), pp.11354–11359.

Battogtokh, G. et al., 2018. Triphenylphosphine-docetaxel conjugate-incorporated albumin nanoparticles for cancer treatment. *Nanomedicine*, 13(3), pp.325–338.

Beck-Broichsitter, M. et al., 2012. Nebulization performance of biodegradable sildenafil-loaded nanoparticles using the Aeroneb® Pro: Formulation aspects and nanoparticle stability to nebulization. *International Journal of Pharmaceutics*, 422(1–2), pp.398–408.

Beck, R.C.R. et al., 2006. NANOPARTICLE-COATED ORGANIC-INORGANIC MICROPARTICLES: EXPERIMENTAL DESIGN AND GASTROINTESTINAL TOLERANCE EVALUATION. *Quimica Nova*, 29(5), pp.990–996.

Bhushan, B. et al., 2017. Impact of albumin based approaches in nanomedicine: Imaging, targeting and drug delivery. *Advances in Colloid and Interface Science*, 246, pp.13–39.

Bicer, E., 2011. Characterising the composition of human respiratory tract lining fluids in health and disease. In *Drug Delivery to the Lungs 22*. Edinburgh.

Birdi, K., 2002. *Handbook of Surface and Colloid Chemistry* Second., Boca Raton: CRC Press.

Bondesson, E. et al., 2007. Site of deposition and absorption of an inhaled hydrophilic solute. *British Journal of Clinical Pharmacology*, 63(6), pp.722–731.

Bouzas, N.F. et al., 2009. Determination of basic drugs of abuse in human serum by online extraction and LC-MS/MS. *Analytical and Bioanalytical Chemistry*, 395(8), pp.2499–2507.

Braber, S. et al., 2011. Cigarette smoke-induced lung emphysema in mice is associated with prolyl endopeptidase, an enzyme involved in collagen breakdown. *American journal of physiology. Lung cellular and molecular physiology*, 300(2), pp.255–65.

Broadhead, J., Edmond Rouan, S.K. & Rhodes, C.T., 1992. The spray drying of pharmaceuticals. *Drug Development and Industrial Pharmacy*, 18(11–12), pp.1169–1206.

Bronze-Uhle, E.S. et al., 2017. Synthetic nanoparticles of bovine serum albumin with entrapped salicylic acid. *Nanotechnology, Science and Applications*, 10, pp.11–21.

Brown, D.M. et al., 2001. Size-dependent proinflammatory effects of ultrafine polystyrene

particles: a role for surface area and oxidative stress in the enhanced activity of ultrafines. *Toxicology and Applied Pharmacology*, 175(3), pp.191–199.

Buenestado, A. et al., 2012. Roflumilast inhibits the release of chemokines and TNF-α from human lung macrophages stimulated with lipopolysaccharide. *British Journal of Pharmacology*, 165(6), pp.1877–1890.

Bundschuh, D.S. et al., 2001. In Vivo Efficacy in Airway Disease Models of Roflumilast, a Novel Orally Active PDE4 Inhibitor. *Journal of Pharmacology and Experimental Therapeutics.*, 297(1), pp.280–290.

Byron, P.R. & Patton, J.S., 1994. Drug Delivery via the Respiratory Tract. *Journal of Aerosol Medicine*, 7(1), pp.49–75.

Chang, H., Okuyama, K. & Szymanski, W.W., 2003. Experimental Evaluation of the Optical Properties of Porous Silica/Carbon Composite Particles. *Aerosol Science and Technology*, 37(9), pp.735–751.

Chapman, R.W. et al., 2007. Effect of inhaled roflumilast on the prevention and resolution of allergen-induced late phase airflow obstruction in Brown Norway rats. *European Journal of Pharmacology*, 571(2–3), pp.215–221.

Chen, J. & Hage, D.S., 2004. Quantitative analysis of allosteric drug-protein binding by biointeraction chromatography. *Nature Biotechnology*, 22(11), pp.1445–1448.

Chen, W. et al., 2008. Development and evaluation of novel itraconazole-loaded intravenous nanoparticles. *International Journal of Pharmaceutics*, 362, pp.133–140.

Chen, Y., McCulloch, R.K. & Gray, B.N., 1994. Synthesis of albumin-dextran sulfate microspheres possessing favourable loading and release characteristics for the anticancer drug doxorubicin. *Journal of Controlled Release*, 31(1), pp.49–54.

Chiang, T.Y. et al., 2014. Matrix metalloproteinases in pneumonia. *Clinica Chimica Acta*, 433, pp.272–277.

Christophe, T. et al., 2009. High content screening identifies decaprenyl-phosphoribose 2′ epimerase as a target for intracellular antimycobacterial inhibitors. *PLOS Pathogens*, 5(10), pp.1–10.

Colmenarejo, G., 2003. In silico prediction of drug-binding strengths to human serum albumin. *Medicinal Research Reviews*, 23(3), pp.275–301.

Costa-gouveia, J. & Brodin, P., 2017. How can nanoparticles contribute to antituberculosis therapy? *Drug Discovery Today*, 22(3), pp.600–607.

Costa, A. et al., 2016. The formulation of nanomedicines for treating tuberculosis. *Advanced Drug Delivery Reviews*, 102, pp.102–115. Available at: http://dx.doi.org/10.1016/j.addr.2016.04.012.

Costa, P. & Lobo, J.M.S., 2001. Modelling and Comparison of Dissolution Profiles. *European Journal of Pharmaceutical Science*, 13, pp.123–133.

Dahneke, B.E., 1983. *Measurement of Suspended Particles by Quasi-elastic Light Scattering*, Wiley.

Dailey, L.A. et al., 2003. Nebulization of biodegradable nanoparticles: Impact of nebulizer technology and nanoparticle characteristics on aerosol features. *Journal of Controlled Release*, 86(1), pp.131–144.

Dames, P. et al., 2007. Targeted delivery of magnetic aerosol droplets to the lung. *Nature Nanotechnology*, 2(8), pp.495–499.

Das, S., Banerjee, R. & Bellare, J., 2005. Aspirin loaded albumin nanoparticles by coacervation: Implications in drug delivery. *Trends in Biomaterials and Artificial Organs*, 18(2), pp.203–212.

Das, S., Bellare, J.R. & Banerjee, R., 2012. Protein based nanoparticles as platforms for aspirin delivery for ophthalmologic applications. *Colloids and Surfaces B: Biointerfaces*, 93, pp.161–168.

Debnath, S.K., Saisivam, S. & Omri, A., 2017. PLGA Ethionamide Nanoparticles for Pulmonary Delivery: Development and in vivo evaluation of dry powder inhaler. *Journal of Pharmaceutical and Biomedical Analysis*, 145, pp.854–859.

Dong, C. et al., 2016. Dasatinib-loaded albumin nanoparticles possess diminished endothelial cell barrier disruption and retain potent anti- leukemia cell activity. *Oncotarget*, 7(31), pp.49699–49709.

Dreis, S. et al., 2007. Preparation, characterisation and maintenance of drug efficacy of doxorubicin-loaded human serum albumin (HSA) nanoparticles. *International Journal of Pharmaceutics*, 341(1–2), pp.207–214.

Electronic Medicines Compendium, 2018. Electronic Medicines Compendium (eMC). *electronic Medicines Compendium (eMC). [online] Available at: http://www.medicines.org.uk [Accessed 6 September 2018].*

Elzoghby, A.O., Samy, W.M. & Elgindy, N. a., 2012. Albumin-based nanoparticles as potential controlled release drug delivery systems. *Journal of Controlled Release*, 157(2), pp.168–182.

European Medicines Agency, 1995. *Validation of Analytical Procedures*, London.

Fader, A.N. & Rose, P.G., 2009. Abraxane for the treatment of gynecologic cancer patients with severe hypersensitivity reactions to paclitaxel. *International Journal of Gynecological Cancer*, 19(7), pp.1281–1283.

Farokhzad, O.C. & Langer, R., 2006. Nanomedicine: Developing smarter therapeutic and diagnostic modalities. *Advanced Drug Delivery Reviews*, 58(14), pp.1456–1459.

Fehske, K.J. et al., 1982. Characterization of an important drug binding area on human serum albumin including the high-affinity binding sites of warfarin and azapropazone. *Molecular Pharmacology*, 21(2), pp.387–393.

Fitos, I. et al., 1999. Stereoselective allosteric binding interaction on human serum albumin between ibuprofen and lorazepam acetate. *Chirality*, 11(2), pp.115–120.

Freitas, C. & Müller, R.H., 1998. Spray-drying of solid lipid nanoparticles (SLN). *European Journal of Pharmaceutics and Biopharmaceutics*, 46(2), pp.145–151.

Fujiwara, S. & Amisaki, T., 2013. Fatty acid binding to serum albumin: molecular simulation approaches. *Biochimica et Biophysica Acta*, 1830(12), pp.5427–34.

Fürst, W. & Banerjee, A., 2005. Release of Glutaraldehyde From an Albumin-Glutaraldehyde Tissue Adhesive Causes Significant In Vitro and In Vivo Toxicity. *The Annals of Thoracid Surgery*, 79, pp.1522–1529.

Gandhi, N.R. et al., 2010. Multidrug-resistant and extensively drug-resistant tuberculosis: a

threat to global control of tuberculosis. *The Lancet*, 375(9728), pp.1830–1843.

Gawad, J. & Bonde, C., 2018. Current Affairs, Future Perspectives of Tuberculosis and Antitubercular Agents. *Indian Journal of Tuberculosis*, 65(1), pp.15–22.

Geiser, M. et al., 2008. The role of macrophages in the clearance of inhaled ultrafine titanium dioxide particles. *American Journal of Respiratory Cell and Molecular Biology*, 38(3), pp.371–376.

Geiser, M. & Kreyling, W.G., 2010. Deposition and biokinetics of inhaled nanoparticles. *Particle and Fibre Toxicology*, 7, pp.1–17.

Gelperina, S. et al., 2005. The potential advantages of nanoparticle drug delivery systems in chemotherapy of tuberculosis. *American Journal of Respiratory and Critical Care Medicine*, 172(12), pp.1487–1490.

Ghazanfari, T. et al., 2007. The influence of fluid physicochemical properties on vibrating-mesh nebulization. *International Journal of Pharmaceutics*, 339(1–2), pp.103–111.

Ghuman, J. et al., 2005. Structural basis of the drug-binding specificity of human serum albumin. *Journal of Molecular Biology*, 353(1), pp.38–52.

Gojova, A. et al., 2007. Induction of inflammation in vascular endothelial cells by metal oxide nanoparticles: Effect of particle composition. *Environmental Health Perspectives*, 115(3), pp.403–409.

Gómez-mantilla, J. et al., 2013. Permutation Test (PT) and Tolerated Difference Test (TDT): Two new , robust and powerful nonparametric tests for statistical comparison of dissolution profiles. *International Journal of Pharmaceutics*, 441(1–2), pp.458–467.

Goszczyński, T. et al., 2013. The antileukemic activity of modified fibrinogen-methotrexate conjugate. *Biochimica et Biophysica Acta - General Subjects*, 1830(3), pp.2526–2530.

Grabowski, N. et al., 2013. Toxicity of surface-modified PLGA nanoparticles toward lung alveolar epithelial cells. *International Journal of Pharmaceutics*, 454(2), pp.686–694.

Gradishar, W.J. et al., 2005. Phase III trial of nanoparticle albumin-bound paclitaxel compared with polyethylated castor oil-based paclitaxel in women with breast cancer. *Journal of clinical oncology : official journal of the American Society of Clinical*

Oncology, 23(31), pp.7794–803.

Grenha, A. et al., 2007. Chitosan nanoparticle-loaded mannitol microspheres: Structure and surface characterization. *Biomacromolecules*, 8(7), pp.2072–2079.

Grenha, A., Seijo, B. & Remuñán-López, C., 2005. Microencapsulated chitosan nanoparticles for lung protein delivery. *European Journal of Pharmaceutical Sciences*, 25(4–5), pp.427–437.

Hamilton, J.A., 2004. Fatty acid interactions with proteins: What X-ray crystal and NMR solution structures tell us. *Progress in Lipid Research*, 43(3), pp.177–199.

Hassan, P.A., Rana, S. & Verma, G., 2015. Making sense of Brownian motion: Colloid characterization by dynamic light scattering. *Langmuir*, 31(1), pp.3–12.

Hastings, R.H., Folkesson, H.G. & Matthay, M.A., 2004. Mechanisms of alveolar protein clearance in the intact lung. *American Journal of Physiology-Lung Cellular and Molecular Physiology*, 286(4), pp.679-L689.

Hawkins, M.J., Soon-Shiong, P. & Desai, N., 2008. Protein nanoparticles as drug carriers in clinical medicine. *Advanced Drug Delivery Reviews*, 22(60), pp.876–885.

Hervé, F. et al., 1994. Drug binding in plasma. A summary of recent trends in the study of drug and hormone binding. *Clinical Pharmacokinetics*, 26(1), pp.44–58.

Higuchi, T., 1963. Mechanism of Sustained- Action Medication. Theoretical analysis of rate of release of solid drugs dispersed in solid matrices. *Journal of Pharmaceutical Sciences*, 52(12), pp.1145–1149.

Hoagland, D.T. et al., 2016. New agents for the treatment of drug-resistant Mycobacterium tuberculosis. *Advanced Drug Delivery Reviews*, 102, pp.55–72.

Hohlfeld, J.M. et al., 2008. Roflumilast attenuates pulmonary inflammation upon segmental endotoxin challenge in healthy subjects: A randomized placebo-controlled trial. *Pulmonary Pharmacology and Therapeutics*, 21(4), pp.616–623.

Hougaard, K.S. et al., 2015. A perspective on the developmental toxicity of inhaled nanoparticles. *Reproductive Toxicology*, 56, pp.118–140.

Hunter, R., 1981. *Zeta potential in Colloid Science*, London: Academic Press.

Huntosova, V. et al., 2012. Development of a new LDL-based transport system for hydrophobic/amphiphilic drug delivery to cancer cells. *International Journal of Pharmaceutics*, 436(1–2), pp.463–471.

Innovative Medicines for Tuberculosis & Foundation, 2018. Study to Evaluate the Safety, Tolerability, Pharmacokinetics and Ex-vivo Antitubercular Activity of PBTZ169 Formulation.

Ishii, Y. et al., 1991. Changes in lmmunoreactivity for Cathepsin H in Rat Type II Alveolar Epithelial Cells and Its Proteolytic Activity in Bronchoalveolar Lavage Fluid Over 24 Hours. *The Anatomical Record*, 230, pp.519–523.

ISO, 1996. International Standard ISO13321 Methods for Determination of Particle Size Distribution Part 8: Photon Correlation Spectroscopy.

Jawahar, N. & Reddy, G., 2012. Nanoparticles: A Novel Pulmonary Drug Delivery System for Tuberculosis. *Journal of Pharmaceutical Sciences and Research*, 4(8), pp.1901–1906.

Jiang, J., Oberdörster, G. & Biswas, P., 2009. Characterization of size, surface charge, and agglomeration state of nanoparticle dispersions for toxicological studies. *Journal of Nanoparticle Research*, 11(1), pp.77–89.

Jones, M.C. et al., 2014. Quantitative assessment of nanoparticle surface hydrophobicity and its influence on pulmonary biocompatibility. *Journal of Controlled Release*, 183(1), pp.94–104.

Jun, J.Y. et al., 2011. Preparation of size-controlled bovine serum albumin (BSA) nanoparticles by a modified desolvation method. *Food Chemistry*, 127(4), pp.1892–1898.

Kamaly, N. et al., 2016. Degradable Controlled-Release Polymers and Polymeric Nanoparticles : Mechanisms of Controlling Drug Release. *ACS Chemical Reviews*, 116, pp.2602–2663.

Kaur, I.P. & Singh, H., 2014. Nanostructured drug delivery for better management of tuberculosis. *Journal of Controlled Release*, 184, pp.36–50.

Kawabata, K., Hagio, T. & Matsuoka, S., 2002. The role of neutrophil elastase in acute lung

injury. *European Journal of Pharmacology*, 451(1), pp.1–10.

Kawashima, Y. et al., 1999. Pulmonary delivery of insulin with nebulized DL-lactide/glycolide copolymer (PLGA) nanospheres to prolong hypoglycemic effect. *Science*, 62, pp.279–287.

Kedem, O. & Katchalsky, A., 1958. THERMODYNAMIC ANALYSIS OF THE PERMEABILITY OF BIOLOGICAL MEMBRANES TO NON-ELECTROLYTES. *Biochimica et biophysica acta*, 27, pp.229–246.

Khandelia, R., Bhandari, S. & Pan, U.N., 2015. Gold Nanocluster Embedded Albumin Nanoparticles for Two-Photon Imaging of Cancer Cells Accompanying Drug Delivery. *Small*, 33, pp.4075–4081.

Kho, K. & Hadinoto, K., 2010. Effects of excipient formulation on the morphology and aqueous re-dispersibility of dry-powder silica nano-aggregates. *Colloids and Surfaces A: Physicochemical and Engineering Aspects*, 359(1–3), pp.71–81.

Kim, B. et al., 2017. Albumin nanoparticles with synergistic antitumor efficacy against metastatic lung cancers. *Colloids and Surfaces B: Biointerfaces*, 158, pp.157–166.

Kim, H., Robinson, S.B. & Csaky, K.G., 2009. Investigating the movement of intravitreal human serum albumin nanoparticles in the vitreous and retina. *Pharmaceutical Research*, 26(2), pp.329–337.

Kloss, F. et al., 2017. In Vivo Dearomatization of the Potent Antituberculosis Agent BTZ043 via Meisenheimer Complex Formation. *Angewandte Chemie*, 56(8), pp.2187–2191.

Koslowski, R. et al., 2003. Cathepsins in bleomycin-induced lung injury in rat. *European Respiratory Journal*, 22(3), pp.427–435.

Kragh-Hansen, U., 1988. Evidence for a large and flexible region of human serum albumin possessing high affinity binding sites for salicylate, warfarin, and other ligands. *Molecular Pharmacology*, 34(2), pp.160–71.

Kratochwil, N. a. et al., 2002. Predicting plasma protein binding of drugs: A new approach. *Biochemical Pharmacology*, 64(9), pp.1355–1374.

Kratz, F., 2008. Albumin as a drug carrier: Design of prodrugs, drug conjugates and

nanoparticles. *Journal of Controlled Release*, 132(3), pp.171–183.

Křepela, E. et al., 1985. Dipeptidyl peptidase IV in mammalian lungs. *Lung*, 163(1), pp.33–54.

Kreuter, J., 1991. Nanoparticle-based drug delivery systems. *Journal of Controlled Release*, 16, pp.169–176.

Kunda, N.K. et al., 2013. Nanocarriers targeting dendritic cells for pulmonary vaccine delivery. *Pharmaceutical Research*, 30(2), pp.325–341.

Kuzmov, A. & Minko, T., 2015. Nanotechnology approaches for inhalation treatment of lung diseases. *Journal of Controlled Release*, 219, pp.500–518.

Labiris, N.R. & Dolovich, M.B., 2003. Pulmonary drug delivery. Part I: Physiological factors affecting therapeutic effectiveness of aerosolized medications. *British Journal of Clinical Pharmacology*, 56(6), pp.588–599.

Langer, K. et al., 2003. Optimization of the preparation process for human serum albumin (HSA) nanoparticles. *International Journal of Pharmaceutics*, 257(1–2), pp.169–180.

Lee, S.H. et al., 2011. Nano spray drying: A novel method for preparing protein nanoparticles for protein therapy. *International Journal of Pharmaceutics*, 403(1–2), pp.192–200.

Lexmond, A.J. et al., 2018. A novel method for studying airway hyperresponsiveness in allergic guinea pigs in vivo using the PreciseInhale system for delivery of dry powder aerosols. *Drug Delivery and Translational Research*, pp.760–769.

Li, F.Q. et al., 2008. Preparation and characterization of sodium ferulate entrapped bovine serum albumin nanoparticles for liver targeting. *International Journal of Pharmaceutics*, 349(1–2), pp.274–282.

Li, L. et al., 2016. L-Leucine as an excipient against moisture on in vitro aerosolization performances of highly hygroscopic spray-dried powders. *European Journal of Pharmaceutics and Biopharmaceutics*, 102, pp.132–141.

Li, Y. et al., 2018. Chitosan-stablized bovine serum albumin nanoparticles having ability to control the release of NELL-1 protein. *International Journal of Biological*

Macromolecules, 109, pp.672–680.

Lin, S.Y. et al., 2004. Effect of ethanol or/and captopril on the secondary structure of human serum albumin before and after protein binding. *European Journal of Pharmaceutics and Biopharmaceutics*, 57(3), pp.457–464.

Lin, W. et al., 2001. Preparation and characterisation of rose Bengal-loaded surface-modified albumin nanoparticles. *Journal of Controlled Release*, 71(1), pp.117–26.

Lin, W. et al., 1993. Preparation of sub-100 nm human serum albumin nanospheres using a ph-coacervation method. *Journal of Drug Targeting*, 1(3), pp.237–243.

Liu, Y. et al., 2009. Impact of hydrogel nanoparticle size and functionalization on in vivo behavior for lung imaging and therapeutics. *Molecular Pharmaceutics*, 6(6), pp.1891–1902.

Lubig, R. et al., 1981. Mechanism of protein reactions with glutaraldehyde. *Monatshefte für Chemie*, 112, pp.1313–1323.

Luyts, K. et al., 2013. How physico-chemical characteristics of nanoparticles cause their toxicity: complex and unresolved interrelations. *Environmental Science: Processes & Impacts*, 15(1), p.23.

Lv, K. et al., 2018. Design , synthesis and antitubercular evaluation of benzothiazinones containing a piperidine moiety. *European Journal of Medicinal Chemistry*, 151, pp.1–8.

Lyklema, J., 1991. *Fundamentals of Interface and Colloid Science*, Amsterdam: Elsevier.

Ma, X. et al., 2016. A Biocompatible and Biodegradable Protein Hydrogel with Green and Red Autofluorescence: Preparation , Characterization and In Vivo Biodegradation Tracking and Modeling. *Scientific Reports*, 6, pp.1–12.

Maa, Y.F. et al., 1998. Effect of spray drying and subsequent processing conditions on residual moisture content and physical/biochemical stability of protein inhalation powders. *Pharmaceutical Research*, 15(5), pp.768–775.

Maa, Y.F. et al., 1997. The effect of operating and formulation variables on the morphology of spray-dried protein particles. *Pharmaceutical Development and Technology*, 2(3), pp.213–223.

Maas, S.G. et al., 2011. The impact of spray drying outlet temperature on the particle morphology of mannitol. *Powder Technology*, 213(1), pp.27–35.

Mahmoud, A.A., Elkasabgy, N.A. & Abdelkhalek, A.A., 2018. Design and characterization of emulsified spray dried alginate microparticles as a carrier for the dually acting drug roflumilast. *European Journal of Pharmaceutical Sciences*, 122, pp.64–76.

Makadia, H. & Siegel, S., 2011. Poly Lactic-co-Glycolic Acid (PLGA) as Biodegradable Controlled Drug Delivery Carrier. *Journal of Polymer Science Part B: Polymer Physics*, 3(3), pp.1377–1397.

Makarov, V. et al., 2014. Towards a new combination therapy for tuberculosis with next generation benzothiazinones. *EMBO Molecular Medicine*, 6(3), pp.372–383.

Mallik, R. et al., 2010. ANALYSIS OF DRUG-PROTEIN BINDING BY ULTRAFAST AFFINITY CHROMATOGRAPHY USING IMMOBILIZED HUMAN SERUM ALBUMIN. *Journal of Chromatography A*, 1217(17), pp.2796–2803.

Maury, M. et al., 2005. Spray-drying of proteins: Effects of sorbitol and trehalose on aggregation and FT-IR amide I spectrum of an immunoglobulin G. *European Journal of Pharmaceutics and Biopharmaceutics*, 59(2), pp.251–261.

McNeil, S., 2011. *Characterization of Nanoparticles Intended for Drug Delivery*, Springer.

Mehanna, M.M., Mohyeldin, S.M. & Elgindy, N.A., 2014. Respirable nanocarriers as a promising strategy for antitubercular drug delivery. *Journal of Controlled Release*, 187, pp.183–197.

Merodio, M. et al., 2000. Ganciclovir-loaded albumin nanoparticles: Characterization and in vitro release properties. *European Journal of Pharmaceutical Sciences*, 12(3), pp.251–259.

Merodio, M. et al., 2002. Ocular disposition and tolerance of ganciclovir-loaded albumin nanoparticles after intravitreal injection in rats. *Biomaterials*, 23(7), pp.1587–1594.

Mikusova, K. et al., 2005. Decaprenylphosphoryl Arabinofuranose, the Donor of the D-Arabinofuranosyl Residues of Mycobacterial Arabinan, Is Formed via a Two-Step Epimerization of Decaprenylphosphoryl Ribose. *Journal of Bacteriology*, 187(23),

pp.8020–8025.

Mikusova, K., Makarov, V. & Neres, J., 2014. DprE1 - from the Discovery to the Promising Tuberculosis Drug Target. *Current Pharmaceutical Design*, 20(27), pp.4379–403.

Mishra, V. et al., 2006. Targeted brain delivery of AZT via transferrin anchored pegylated albumin nanoparticles. *Journal of Drug Targeting*, 14(1), pp.45–53.

Mohammad-beigi, H. et al., 2016. The Effects of Organic Solvents on the Physicochemical Properties of Human Serum Albumin Nanoparticles. *Iranian Journal of Biotechnology*, 14(1), pp.45–50.

Moran, A. & Buckton, G., 2007. Adjusting and understanding the properties and crystallisation behaviour of amorphous trehalose as a function of spray drying feed concentration. *International Journal of Pharmaceutics*, 343(1–2), pp.12–17.

Moran, A. & Buckton, G., 2009. Studies of the Crystallization of Amorphous Trehalose Using Simultaneous Gravimetric Vapor Sorption/Near IR (GVS/NIR) and "Modulated" GVS/NIR. *AAPS PharmSciTech*, 10(1), pp.297–302.

Mühlfeld, C. et al., 2008. Interactions of nanoparticles with pulmonary structures and cellular responses. *American Journal of Physiology-Lung Cellular and Molecular Physiology*, 294(5), pp.817–829.

Muller, R.H., Jacobs, C., Kayser, O., 2001. Nanosuspensions as particulate drug formulations in therapy . Rationale for development and what we can expect for the future. *Advanced Drug Delivery Reviews*, 47, pp.2–19.

Murad, H.A. et al., 2017. Co-inhalation of roflumilast, rather than formoterol, with fluticasone more effectively improves asthma in asthmatic mice. *Experimental Biology and Medicine*, 242(5), pp.516–526.

Nadel, J.A., 1990. Decreased Neutral Endopeptidases: Possible Role in Inflammatory Diseases of Airways. *Lung*, Suppl, pp.123–127.

Naini, V., Byron, P.R. & Phillips, E.M., 1998. Physicochemical stability of crystalline sugars and their spray-dried forms: Dependence upon relative humidity and suitability for use in powder inhalers. *Drug Development and Industrial Pharmacy*, 24(10), pp.895–

909.

Najafabadi, A.R. et al., 2004. The effect of vehicle on physical properties and aerosolisation behaviour of disodium cromoglycate microparticles spray dried alone or with L-leucine. *International Journal of Pharmaceutics*, 285(1–2), pp.97–108.

Nasiruddin, M., Neyaz, K. & Das, S., 2017. Nanotechnology-Based Approach in Tuberculosis Treatment. *Tuberculosis Research and Treatment*, 2017, pp.1–12.

Newman, S.P., 2017. Drug delivery to the lungs: Challenges and opportunities. *Therapeutic Delivery*, 8(8), pp.647–661.

Nyambura, B.K., Kellaway, I.W. & Taylor, K.M.G., 2009. Insulin nanoparticles: Stability and aerosolization from pressurized metered dose inhalers. *International Journal of Pharmaceutics*, 375(1–2), pp.114–122.

Nyman, D.W. et al., 2005. Phase I and Pharmacokinetics Trial of ABI-007, a Novel Nanoparticle Formulation of Paclitaxel in Patients With Advanced Nonhematologic Malignancies. *Journal of Clinical Oncology*, 23(31), pp.7785–7793.

O'Brien, L.M., Duffin, R. & Millar, A.M., 2006. Preparation of 99mTc-Nanocoll for use in sentinel node localization: Validation of a protocol for supplying in unit-dose syringes. *Nuclear Medicine Communications*, 27(12), pp.999–1003.

Oberdörster, G., Oberdörster, E. & Oberdörster, J., 2005. Nanotoxicology: An emerging discipline evolving from studies of ultrafine particles. *Environmental Health Perspectives*, 113(7), pp.823–839.

Oneda, F. & Ré, M.I., 2003. The effect of formulation variables on the dissolution and physical properties of spray-dried microspheres containing organic salts. *Powder Technology*, 130(1–3), pp.377–384.

Oppenheim, R., 1981. Solid colloidal drug delivery systems: Nanoparticles. *International Journal of Pharmaceutics*, 8(3), pp.217–234.

Oracova, J., Bohs, B. & Lindner, W., 1996. Drug-protein binding studies new trends in analytical and experimental methodology. *Journal of Chromatography B*, 677, pp.1–28.

Panda, A. et al., 2016. Formulation and characterization of clozapine and risperidone co-entrapped spray-dried PLGA nanoparticles. *Pharmaceutical Development and Technology*, 21(1), pp.43–53.

Pandey, R. et al., 2003. Poly (DL-lactide-co-glycolide) nanoparticle-based inhalable sustained drug delivery system for experimental tuberculosis. *Journal of Antimicrobial Chemotherapy*, 52(6), pp.981–986.

Pápay, Z.E. et al., 2017. Study on the Pulmonary Delivery System of Apigenin-Loaded Albumin Nanocarriers with Antioxidant Activity. *Journal of Aerosol Medicine and Pulmonary Drug Delivery*, 30(4), pp.274–288.

Paranjpe, M. & Müller-Goymann, C., 2014. Nanoparticle-Mediated Pulmonary Drug Delivery: A Review. *International Journal of Molecular Sciences*, 15(4), pp.5852–5873.

Pastor, M. et al., 2014. Sodium colistimethate loaded lipid nanocarriers for the treatment of Pseudomonas aeruginosa infections associated with cystic fibrosis. *International Journal of Pharmaceutics*, 477(1–2), pp.485–494.

Patil, G. V., 2003. Biopolymer albumin for diagnosis and in drug delivery. *Drug Development Research*, 58(3), pp.219–247.

Patlolla, R.R. et al., 2010. Formulation, characterization and pulmonary deposition of nebulized celecoxib encapsulated nanostructured lipid carriers. *Journal of Controlled Release*, 144(2), pp.233–241.

Patton, J.S., 1996. Mechanisms of macromolecule absorption by the lungs. *Advanced Drug Delivery Reviews*, 19(1), pp.3–36.

Peppas, N.A. & Narasimhan, B., 2014. Mathematical models in drug delivery: How modeling has shaped the way we design new drug delivery systems. *Journal of Controlled Release*, 190, pp.75–81. Available at: http://dx.doi.org/10.1016/j.jconrel.2014.06.041.

Pilcer, G. & Amighi, K., 2010. Formulation strategy and use of excipients in pulmonary drug delivery. *International Journal of Pharmaceutics*, 392(1–2), pp.1–19.

Pritchard, J.N. et al., 2018. Mesh nebulizers have become the first choice for new nebulized

pharmaceutical drug developments. *Therapeutic Delivery*, 9(2), pp.121–136.

Qi, J. et al., 2010. Nanoparticles with dextran/chitosan shell and BSA/chitosan core — Doxorubicin loading and delivery. *International Journal of Pharmaceutics*, 393(1–2), pp.176–184.

Quon, B.S., Goss, C.H. & Ramsey, B.W., 2014. Inhaled antibiotics for lower airway infections. *Annals of the American Thoracic Society*, 11(3), pp.425–434.

Raffin Pohlmann, A. et al., 2002. Spray-dried indomethacin-loaded polyester nanocapsules and nanospheres: Development, stability evaluation and nanostructure models. *European Journal of Pharmaceutical Sciences*, 16(4–5), pp.305–312.

Ranjita, S., Shaal, A. & Khalil, M., 2011. Present Status Tuberculosis of Nanoparticle for Treatment of. *Journal of Pharmaceutical Sciences*, 14(1), pp.100–116.

Rather, M. et al., 2016. Preparation and In Vitro Characterization of Albumin Nanoparticles Encapsulating an Anti- Tuberculosis Drug-Levofloxacin. *Advanced Science, Engineering and Medicine*, 8, pp.912–917.

Razavi Rohani, S.S., Abnous, K. & Tafaghodi, M., 2014. Preparation and characterization of spray-dried powders intended for pulmonary delivery of Insulin with regard to the selection of excipients. *International Journal of Pharmaceutics*, 465(1–2), pp.464–478.

Rejinold, N.S. et al., 2011. 5-Fluorouracil loaded fibrinogen nanoparticles for cancer drug delivery applications. *International Journal of Biological Macromolecules*, 48(1), pp.98–105.

Richter, A. et al., 2018. Novel insight into the reaction of nitro, nitroso and hydroxylamino benzothiazinones and of benzoxacinones with Mycobacterium tuberculosis DprE1. *Scientific Reports*, (8), pp.1–12.

Roser, M., Fischer, D. & Kissel, T., 1998. Surface-modified biodegradable albumin nano- and microspheres. II: Effect of surface charges on in vitro phagocytosis and biodistribution in rats. *European Journal of Pharmaceutics and Biopharmaceutics*, 46(3), pp.255–263.

Rosière, R. et al., 2015. New dry powders for inhalation containing temozolomide-based

nanomicelles for improved lung cancer therapy. *International Journal of Oncology*, 47(3), pp.1131–1142.

Rubino, O.P., Kowalsky, R. & Swarbrick, J., 1993. Albumin Microspheres as a Drug Delivery System: Relation Among Turbidity Ratio, Degree of Cross-linking, and Drug Release. *Pharmaceutical Research*, 10(7), pp.1059–1065.

Ruge, C.A. et al., 2016. Disintegration of nano-embedded microparticles after deposition on mucus: A mechanistic study. *Colloids and Surfaces B: Biointerfaces*, 139, pp.219–227.

Sagar, J.V. et al., 2008. Protein Binding Studies of Gossypin by Equilibrium Dialysis. *Current Trends in Biotechnology and Pharmacy*, 2(3), pp.396–401.

Saleh, A.M. et al., 1989. Effect of some drugs and additives on the cross-linking of bovine serum albumin by glutaraldehyde. *International Journal of Pharmaceutics*, 51, pp.205–210.

Salgin, S., Salgin, U. & Bahadir, S., 2012. Zeta potentials and isoelectric points of biomolecules: The effects of ion types and ionic strengths. *International Journal of Electrochemical Science*, 7(12), pp.12404–12414.

Schaffazick, S.R. et al., 2006. Development of nanocapsule suspensions and nanocapsule spray-dried powders containing melatonin. *Journal of the Brazilian Chemical Society*, 17(3), pp.562–569.

Scherließ, R., 2016. Exploring the potential of mannitol as an alternative to lactose in dry powder inhalation. *Inhalation*.

Scheuch, G. et al., 2006. Clinical perspectives on pulmonary systemic and macromolecular delivery. *Advanced Drug Delivery Reviews*, 58(9–10), pp.996–1008.

Selg, E. et al., 2013. Dry Powder Inhalation Exposures of the Endotracheally Intubated Rat Lung, Ex Vivo and In Vivo: The Pulmonary Pharmacokinetics of Fluticasone Furoate. *Journal of Aerosol Medicine and Pulmonary Drug Delivery*, 26(4), pp.181–189.

Seville, P.C. et al., 2007. Amino acid-modified spray-dried powders with enhanced aerosolisation properties for pulmonary drug delivery. *Powder Technology*, 178(1), pp.40–50.

Sham, J.O.H. et al., 2004. Formulation and characterization of spray-dried powders containing nanoparticles for aerosol delivery to the lung. *International Journal of Pharmaceutics*, 269(2), pp.457–467.

Sharma, K. et al., 2012. Crosslinked chitosan nanoparticle formulations for delivery from pressurized metered dose inhalers. *European Journal of Pharmaceutics and Biopharmaceutics*, 81(1), pp.74–81.

Shaw, D., 1992. *Introduction to Colloid and Surface Chemistry* Fourth., Elsevier Science Ltd.

Shekunov, B.Y. et al., 2007. Particle size analysis in pharmaceutics: Principles, methods and applications. *Pharmaceutical Research*, 24(2), pp.203–227.

Shi, L., Plumley, C.J. & Berkland, C., 2007. Biodegradable nanoparticle flocculates for dry powder aerosol formulation. *Langmuir*, 23(22), pp.10897–10901.

Shoyele, S. & Cawthorne, S., 2006. Particle engineering techniques for inhaled biopharmaceuticals. *Advanced Drug Delivery Reviews*, 58(9–10), pp.1009–1029.

Siddiqui, M. & Plosker, G., 2005. The Novolizer: a multidose dry powder inhaler. *Treatments in Respiratory Medicine*, 4(1), pp.63–69.

Singh, H. et al., 2010. Acta Biomaterialia Poly- L -lysine-coated albumin nanoparticles : Stability , mechanism for increasing in vitro enzymatic resilience , and siRNA release characteristics. *Acta Biomaterialia*, 6, pp.4277–4284.

Sinha, B., Mukherjee, B. & Pattnaik, G., 2013. Poly-lactide-co-glycolide nanoparticles containing voriconazole for pulmonary delivery: In vitro and in vivo study. *Nanomedicine: Nanotechnology, Biology, and Medicine*, 9(1), pp.94–104.

Sirotkin, V. et al., 2001. Calorimetric and Fourier transform infrared spectroscopic study of solid proteins immersed in low water organic solvents. *Biochimica et Biophysica Acta*, 1547(2), pp.359–69.

Smeraldi, J. et al., 2012. Statistical evaluation of photon count rate data for nanoscale particle measurement in wastewaters. *Journal of Environmental Monitoring*, 14(1), pp.79–84.

Smola, M., Vandamme, T. & Sokolowski, A., 2008. Nanocarriers as pulmonary drug delivery

systems to treat and to diagnose respiratory and non respiratory diseases. *International Journal of Nanomedicine*, 3(1), pp.1–19.

Smyth, H. & Hickey, A.J., 2011. *Controlled Pulmonary Drug Delivery* 1st ed. H. Smyth & A. J. Hickey, eds., New York: Springer-Verlag New York.

Sokoloski, T.D. & Royer, G.P., 1984. Drug entrapment within native albumin beads. In E. Tomlinson, ed. *MIcrospheres and Drug Therapy. Pharmaceutical, Immunological and Medical Aspects*. Amsterdam: Elsevier, pp. 295–307.

Son, G.-H., Lee, B.-J. & Cho, C.-W., 2017. Mechanisms of drug release from advanced drug formulations such as polymeric-based drug-delivery systems and lipid nanoparticles. *Journal of Pharmaceutical Investigation*, 47(4), pp.287–296.

Song, Y., Li, X. & Du, X., 2009. Exposure to nanoparticles is related to pleural effusion, pulmonary fibrosis and granuloma. *European Respiratory Journal*, 34(3), pp.559–567.

Sosnik, A. et al., 2010. New old challenges in tuberculosis: Potentially effective nanotechnologies in drug delivery. *Advanced Drug Delivery Reviews*, 62(4–5), pp.547–559.

Spector, A., 1975. Fatty acid binding to plasma albumin. *Journal of Lipid Research*, 16(3), pp.165–179.

Stern, S.T., Adiseshaiah, P.P. & Crist, R.M., 2012. Autophagy and lysosomal dysfunction as emerging mechanisms of nanomaterial toxicity. *Particle and Fibre Toxicology*, 9, pp.20–37.

Von Storp, B. et al., 2012. Albumin nanoparticles with predictable size by desolvation procedure. *Journal of Microencapsulation*, 29(2), pp.138–146.

Sudlow, G., Birkett, D.J. & Wade, D.N., 1975. Characterization of two specific drug binding sites on human serum albumin. *Molecular Pharmacology*, 11(6), pp.824–832.

Sudlow, G., Birkett, D.J. & Wade, D.N., 1976. Further characterization of specific drug binding sites on human serum albumin. *Molecular Pharmacology*, 12(6), pp.1052–61.

Sugiyama, Y. et al., 2006. Buckling and crumpling of drying droplets of colloid-polymer suspensions. *Langmuir*, 22(14), pp.6024–6030.

Sundar, S., Kundu, J. & Kundu, S.C., 2010. Biopolymeric nanoparticles. *Science and Technology of Advanced Materials*, 11(1), pp.1–13.

Sung, J.C. et al., 2009. Formulation and pharmacokinetics of self-assembled rifampicin nanoparticle systems for pulmonary delivery. *Pharmaceutical Research*, 26(8), pp.1847–1855.

Sung, J.C., Pulliam, B.L. & Edwards, D.A., 2007. Nanoparticles for drug delivery to the lungs. *Trends in Biotechnology*, 25(12), pp.563–570.

Taheri, A. et al., 2011. Nanoparticles of Conjugated Methotrexate-Human Serum Albumin: Preparation and Cytotoxicity Evaluations. *Journal of Nanomaterials*, 2011, pp.1–7.

Tang, X. et al., 2016. RSC Advances nanoparticles as drug delivery vehicles by self-assembly. *RSC Advances*, 6, pp.43284–43292.

Tewa-Tagne, P., Briançon, S. & Fessi, H., 2006. Spray-dried microparticles containing polymeric nanocapsules: Formulation aspects, liquid phase interactions and particles characteristics. *International Journal of Pharmaceutics*, 325(1–2), pp.63–74.

Tezcaner, A., Baran, E.T. & Keskin, D., 2016. Nanoparticles Based on Plasma Proteins for Drug Delivery Applications. *Current Pharmaceutical Design*, 22(22), pp.3445–3454.

Thao, L.Q. et al., 2016. Doxorubicin-Bound Albumin Nanoparticles Containing a TRAIL Protein for Targeted Treatment of Colon Cancer. *Pharmaceutical Research*, 33, pp.615–626.

Tiano, S.L. & Dalby, R.N., 1996. Comparison of a respiratory suspension aerosolized by an air-jet and an ultrasonic nebulizer. *Pharmaceutical Development and Technology*, 1(3), pp.261–268.

Torge, A. et al., 2017. The influence of mannitol on morphology and disintegration of spray-dried nano-embedded microparticles. *European Journal of Pharmaceutical Sciences*, 104, pp.171–179.

Tran, C.L. et al., 2011. A hypothetical model for predicting the toxicity of high aspect ratio nanoparticles (HARN). *Journal of Nanoparticle Research*, 13(12), pp.6683–6698.

Trefzer, C. et al., 2010. Benzothiazinones : Prodrugs That Covalently Modify the

Decaprenylphosphoryl-D-ribose 2′epimerase DprE1 of Mycobacterium tuberculosis. *Journal of the American Chemical Society*, 132, pp.13663–13665.

Trefzer, C. et al., 2012. Benzothiazinones Are Suicide Inhibitors of Mycobacterial Decaprenylphosphoryl-β-D-ribofuranose 2′-Oxidase DprE1. *Journal of the American Chemical Society*, 134, pp.912–915.

Tsapis, N. et al., 2005. Onset of buckling in drying droplets of colloidal suspensions. *Physical Review Letters*, 94(1), pp.1–4.

Tsapis, N. et al., 2002. Trojan particles: large porous carriers of nanoparticles for drug delivery. *Proceedings of the National Academy of Sciences of the United States of America*, 99(19), pp.12001–12005.

Valavanidis, A., Fiotakis, K. & Vlachogianni, T., 2008. Airborne particulate matter and human health: toxicological assessment and importance of size and composition of particles for oxidative damage and carcinogenic mechanisms. *Journal of Environmental Ccience and hHealth. Part C, Environmental Crcinogenesis & Ecotoxicology Reviews*, 26(4), pp.339–362.

Valko, K. et al., 2003. Fast gradient HPLC method to determine compounds binding to human serum albumin. Relationships with octanol/water and immobilized artificial membrane lipophilicity. *Journal of Pharmaceutical Sciences*, 92(11), pp.2236–2248.

Vedakumari, W.S. et al., 2013. Fibrin nanoparticles as Possible vehicles for drug delivery. *Biochimica et Biophysica Acta*, 1830(8), pp.4244–4253.

Vehring, R., 2008. Pharmaceutical particle engineering via spray drying. *Pharmaceutical Research*, 25(5), pp.999–1022.

Videira, M.A. et al., 2002. Lymphatic uptake of pulmonary delivered radiolabelled solid lipid nanoparticles. *Journal of Drug Targeting*, 10(8), pp.607–613.

Vlasova, I.M. & Saletsky, A.M., 2009. STUDY OF THE DENATURATION OF HUMAN SERUM ALBUMIN BY SODIUM DODECYL SULFATE USING THE INTRINSIC FLUORESCENCE OF ALBUMIN. *Journal of Applied Spectroscopy*, 76(4), pp.536–541.

Wang, Y. et al., 2012. A comparison between spray drying and spray freeze drying for dry

powder inhaler formulation of drug-loaded lipid-polymer hybrid nanoparticles. *International Journal of Pharmaceutics*, 424(1–2), pp.98–106.

Warheit, D.B., Reed, K.L. & Sayes, C.M., 2009. A role for nanoparticle surface reactivity in facilitating pulmonary toxicity and development of a base set of hazard assays as a component of nanoparticle risk management. *Inhalation Toxicology*, 21, pp.61–67.

Wartlick, H. et al., 2004. Tumour cell delivery of antisense oligonuclceotides by human serum albumin nanoparticles. *Journal of Controlled Release*, 96(3), pp.483–495.

Weber, C., Coester, C., et al., 2000. Desolvation process and surface characterisation of protein nanoparticles. *International Journal of Pharmaceutics*, 194(1), pp.91–102.

Weber, C., Kreuter, J. & Langer, K., 2000. Desolvation process and surface characteristics of HSA-nanoparticles. *International Journal of Pharmaceutics*, 196(2), pp.197–200.

Whitehead, R.H. et al., 1984. Development and testing of proteinaceous nanoparticles containing cytotoxics. In *Microspheres and Drug Therapy, Pharmaceutical, Immunological and Medical Aspects*. Amsterdam: Elsevier Science, pp. 117–128.

Wiggins, P., McCurdy, S. & Zeidenberg, W., 1989. Epistaxis Due to Glutaraldehyde Exposure. *Journal of Occupational Medicine*, 31(10), pp.845–856.

Wilson, W., 2005. *of Humans: Their Ecology and Role in Health and Disease*, Cambridge: Cambridge University Press.

Wolff, R.K., 2015. Toxicology Studies for Inhaled and Nasal Delivery. *Molecular Pharmaceutics*, 12(8), pp.2688–2696.

Woods, A., 2015. *Albumin nanoparticles: Investigations into suitability for pulmonary application*.

Woods, A. et al., 2013. Albumin Nanoparticles for Drug Delivery to the Lungs - In Vitro Investigation of Biodegradation as a Mechanism of Clearance. In *Drug Delivery to the Lungs 24*. Edinburgh.

Woods, A. et al., 2015. In vivo biocompatibility, clearance, and biodistribution of albumin vehicles for pulmonary drug delivery. *Journal of Controlled Release*.

World Health Organisation, 2017. *Global Tuberculosis Report*, Geneva.

Xiong, L. et al., 2018. Identification of a new series of benzothiazinone derivatives with excellent antitubercular activity and improved pharmacokinetic profiles. *RSC Advances*, 8, pp.11163–11176.

Yamasaki, K. et al., 1996. Characterization of site I on human serum albumin: concept about the structure of a drug binding site. *Biochimica et Biophysica Acta*, 1295(2), pp.147–157.

Yang, W., Tam, J., et al., 2008. High bioavailability from nebulized itraconazole nanoparticle dispersions with biocompatible stabilizers. *International Journal of Pharmaceutics*, 361(1–2), pp.177–188.

Yang, W., Peters, J.I. & Williams, R.O., 2008. Inhaled nanoparticles- a current review. *International Journal of Pharmaceutics*, 356(1–2), pp.239–247.

Yu, S. et al., 2006. Nanogels Prepared by Self-Assembly of Oppositely Charged Globular Proteins. *Biopolymers*, 83(2006), pp.148–158.

Zahoor, A., Sharma, S. & Khuller, G.K., 2005. Inhalable alginate nanoparticles as antitubercular drug carriers against experimental tuberculosis. *International Journal of Antimicrobial Agents*, 26(4), pp.298–303.

Zhang, H., 2012. Use of Metal Oxide Nanoparticle Band Gap to Develop a Predictive Paradigm for Oxidative Stress and Acute Pulmonary Inflammation. *ACS Nano*, 6(5), pp.4349–4368.

Zhang, J. et al., 2011. Formation, characterization, and fate of inhaled drug nanoparticles. *Advanced Drug Delivery Reviews*, 63(6), pp.441–455.

Zhao, D. et al., 2010. Preparation, characterization, and in vitro targeted delivery of folate-decorated paclitaxel-loaded bovine serum albumin nanoparticles. *International Journal of Nanomedicine*, 5(1), pp.669–677.

Zimmer, A.K. et al., 1994. Hydrocortisone delivery to healthy and inflamed eyes using a micellar polysorbate 80 solution or albumin nanoparticles. *International Journal of Pharmaceutics*, 110(3), pp.211–222.

Zsila, F. et al., 2011. Evaluation of drug-human serum albumin binding interactions with

support vector machine aided online automated docking. *Bioinformatics*, 27(13), pp.1806–1813.